

**UNIVERSIDADE DE BRASÍLIA
FACULDADE DE TECNOLOGIA
DEPARTAMENTO DE ENGENHARIA MECÂNICA**

**PROJETO OTIMIZADO DE UM VEÍCULO
LANÇADOR DE SATÉLITES BASEADO EM
PROPELENTES HÍBRIDOS**

PEDRO LUIZ KALED DA CÁS

ORIENTADOR: CARLOS ALBERTO GURGEL VERAS

DISSERTAÇÃO DE MESTRADO EM CIÊNCIAS MECÂNICAS

BRASÍLIA/DF: MARÇO – 2013

**UNIVERSIDADE DE BRASÍLIA
FACULDADE DE TECNOLOGIA
DEPARTAMENTO DE ENGENHARIA MECÂNICA**

**OTIMIZAÇÃO E PROJETO DE UM MICRO
LANÇADOR DE SATÉLITES BASEADO EM PROPELENTES
HÍBRIDOS**

PEDRO LUIZ KALEL DACÁS

**DISSERTAÇÃO SUBMETIDA AO DEPARTAMENTO DE
ENGENHARIA MECÂNICA DA FACULDADE DE TECNOLOGIA
DA UNIVERSIDADE DE BRASÍLIA COMO PARTE DOS
REQUISITOS NECESSÁRIOS PARA A OBTENÇÃO DO GRAU DE
MESTRE EM CIÊNCIAS MECÂNICAS**

APROVADA POR:

**Prof^o Carlos Alberto Gurgel Veras
(Orientador)**

**Prof^o José Alexander Araújo, PhD (ENM-UnB)
(Examinador Interno)**

**•Luiz Eduardo Vergueiro Loures da Costa, DSc (IAE)
(Examinador Externo)**

BRASÍLIA/DF, 10 DE ABRIL DE 2013

FICHA CATALOGRÁFICA

KALED DA CÁS, PEDRO LUIZ

Otimização e Projeto de um Micro Lançador de Satélites Baseado em Propelentes Híbridos
[Distrito Federal] 2013.

xvii, 145p., 210 x 297 mm (ENM/FT/UnB, Mestre, Ciências Mecânicas, 2013).

Dissertação de Mestrado – Universidade de Brasília. Faculdade de Tecnologia.

Departamento de Engenharia Mecânica.

1. Projeto Aeroespacial

2. Otimização Genética

3. Propulsão Híbrida

4. Projeto Multidisciplinar

I. ENM/FT/UnB

II. Título (série)

REFERÊNCIA BIBLIOGRÁFICA

KALED DA CÁS, P. L. (2013). Otimização e Projeto de um Micro Lançador de Satélites Baseado em Propelentes Híbridos. Dissertação de Mestrado em Tecnologia Ciências Mecânicas, Publicação ENM.DM-206A/2013, Departamento de Engenharia Mecânica, Universidade de Brasília, Brasília, DF, 145p.

CESSÃO DE DIREITOS

AUTOR: Pedro Luiz Kaled Da Cás.

TÍTULO: Otimização e Projeto de um Micro Lançador de Satélites Baseado em Propelentes Híbridos

GRAU: Mestre

ANO: 2013

É concedida à Universidade de Brasília permissão para reproduzir cópias desta dissertação de mestrado e para emprestar tais cópias somente para propósitos acadêmicos e científicos. O autor reserva outros direitos de publicação e nenhuma parte dessa dissertação de mestrado pode ser reproduzida sem autorização por escrito do autor.

Pedro Luiz Kaled Da Cás

Super Quadra Sul 106 Bloco C Apartameto 602, Asa Sul.

70345-030 Brasília – DF – Brasil.

CONTENTS

1.1 A Launcher for Brazil.....	13
1.2 Motivation	15
1.2.1 A Simpler alternative.....	16
1.4 Objective	17
1.5 Methodology	17
1.6 Dissertation Structure	18
2-MARKET AND MISSION.....	20
2. Market Analysis	20
2.1.1 Buyers.....	20
2.1.2 New entrants.....	22
2.1.3 Suppliers.....	23
2.1.4 Competing technologies	24
2.2 Size and Behavior of the Market.....	25
2.2.1 Mass Range	25
2.2.2 Orbital Range	27
2.2.3 The market in Brazil.....	28
2.2.4 Future Forecast	29
2.3 Direct Competitors	30
2.3.1 Scorpius.....	30
2.3.2 Neptune 5 and 9.....	32
2.3.3 Virgin Galactic Small Launcher.....	35
2.4 Mission Definition.....	35
2.4.1 Orbit and Payload.....	35
2.4.2 Expected Market Share	38
2.5 Conclusion.....	44

3- THEORY, OPTIMIZATION AND BALLISTICS	45
3.1 Ballistic Module	45
3.1.1 Numerical integration.....	49
3.1.2 Propellants	50
3.2 Design Module	54
3.2.1 Construction Material Selection.....	54
3.2.2 Materials Slected for Analysis.	57
3.2.3 Wall Thickness and Material quality considerations.	58
3.3 DESIGN MODULE; MASS MODEL	59
3.3.1 Fairing, Satellite Adaptor and Guidance systems	60
3.3.2 Pressurization Subsystem.	61
3.3.3 PROPELLANT TANKS, UNSTIFFENED SHELLS.....	66
3.3.4 PROPELLANT TANKS, STIFFENED SHELLS	69
3.3.5 DRY BAYS AND COMPARTMENTS	70
3.3.6 COMBUSTION CHAMBER.....	71
3.3.7 CIRCUNFERENCIAL FRAMES	73
3.3.8 NOZZLE	76
3.4 Complete mass of the stages	77
3.4.1 Dry Bays.....	77
3.4.2 Propellant loading.....	78
3.4.4 Oxidizer tank	78
3.4.5 Combustion chamber and Nozzle.....	79
3.4.6 Pressurization system	79
3.4.7 Combined mass estimate for the stages.....	79
3.5 ROCKET FLIGHT LOADINGS	80
3.6 VELOCITY MODULE	85
3.7 INTEGRATED LAUNCHER SIMULATION CODE	88

3.8 SETTING OF OPTIMIZATION ALGORITHM.....	89
3.8.1 Setting the Design Space.....	89
3.8.2 Design of Experiments.....	91
3.9 OPTIMIZATION ALGORITHM.....	93
3.9.1 Adaptive Range Multi-Objective Genetic Algorithm (ARMOGA).....	94
3.9.2 Downhill SIMPLEX Algorithm (SIMPLEX).....	96
4.9.3 ARMOGA-SIMPLEX hybrid.....	97
4-RESULTS AND DISCUSSION.....	101
4.1 Design of Experiments.....	101
4.1.1 Case 1: Baseline LOX/Paraffin.....	102
4.1.2 Case 2: Hydrogen peroxide as oxidizer.....	102
4.1.3 Case 3: Nitrous Oxide as oxidizer.....	104
4.1.4 Case 4: Aluminum Trihydride additive in LOX/paraffin.....	106
4.1.5 Case 5: Turbopump feed system.....	107
4.1.6 Case 6: Hydrogen Peroxide with Paraffin+ALH3 grain.....	107
4.1.7 Case 7: Steel Tanks.....	108
4.2 Optimization Runs and Discussions.....	108
4.2.1 Case 1.....	108
4.2.2 Case 2.....	114
4.2.3 Case 3.....	119
4.2.4 Case4.....	120
4.2.5 Case5.....	123
4.2.6 Case 6.....	127
4.2.7 Case7.....	130
4.3 Comparison and Conclusion.....	134
4.4 Case 8.....	135
4.4.1 Detailed Performance analysis.....	137

5- Conclusion	140
5.1 Suggestion for future studies	140
5.1.1 Thrust Vector Control	141
5.1.2 Pressurization system	142
5.1.3- Liquid Propellant Brazilian Micro Satellite Launcher	143
Bibliography	144
Appendixes	Error! Bookmark not defined.
Appendix 2 weight for comparison of design cases	149

LIST OF FIGURES

Figure 1.1, Southern Cross Program	15
Figure 2.1: Customers share of the world's Micro and Nano satellite market.....	21
Figure 2.2: Suborbital payload market's figures	25
Figure 2.3: Number of small satellites launcher from 2000 to 2009, graphic.....	27
Figure 2.4: Orbital altitudes of small satellites launches from 2000 to 2009.....	28
Figure 2.5: Future market trend extrapolation, by Space Works Commercial.....	29
Figure 2.6: Small satellite market by 2020, by Space Works Commercial.....	30
Figure 2.7: Microcosm's Family of Low-Cost, Pressure-Fed Launch Vehicles.....	32
Figure 2.8: OTRAG Technology of clustered Launchers	33
Figure 2.9: N9 rocket and a simple CPM.....	35
Figure 2.10: Small satellite launch market share by 2020, pessimist scenario	40
Figure 2.11: Small satellite launch market share by 2020, realistic scenario.....	42
Figure 2.12: Small satellite launch market share by 2020, optimistic scenario	43
Figure 3.1: Several propellant pair and their theoretical specific impulses	53
Figure 3.2: Carbon fiber winding process	57
Figure 3.3 Detail a unstiffened shell showing the most relevant design figures	59
Figure 3.4: 3D CAD model of the launcher's fairing.....	61
Figure 3.6: The most common engine cycles in liquid rocket propulsion.	64
Figure 3.7: Merlin 1C turbopump, (copyright: SpaceX).....	65
Figure 3.8: Combine Stress State in a pressurized vessel over axial overload.	66
Figure 3.9: left, square isogrid; right, isogrid fabrication through mechanical milling	69
Figure 3.10: cross section of an unstiffened shell with exaggerates roughness	70
Figure 3.11: Simplified diagram of a hybrid rocket motor.	72
Figure 3.12: Internal tension distribution between cylindrical and spherical sections	73
Figure 3.13: Design study of the frame's mass	75
Figure 3.14: Design study, weighted sum of the normalized frame's mass and length	76
Figure 3.15: Free body diagram of a rocket in flight, resulting Forces and Moments.....	81
Figure 3.16: Loading on a typical propellant tank	81
Figure 3.17: Loading on a hybrid combustion chamber or a solid propellant motor.....	83
Figure 3.18: Loading on a typical dry bay	84
Figure 3.19: Longitudinal force along the fuselage of a typical hybrid rocket.....	84
Figure 3.20: pitch angle profile for 3 a generic stage launch vehicle.....	86

Figure 3.21: Internal data flow in the on the Simulation Code	89
Figure 3.22: Full factorial representation, 3 variables and 6 levels, 216 designs	92
Figure 3.23: Mutation Operator.....	95
Figure 3.24: Crossover Operator	95
Figure 3.25: Range adaptation employed by the ARMOGA algorithm.....	96
Figure 3.26: Different Function of a SIMPLEX Method in a 2D Design Space	97
Figure 3.27: Process flow for a typical 3-stage launcher MDO on modeFRONTIER	99
Figure 4.1: Black Arrow carrier rocket at the Science Museum (London), image by Oxyman	104
Figure 4.2: SpaceShipOne's motor on test stand.	105
Figure 4.3: Layout of Case1 rocket.	111
Figure 4.4: Different layout alternatives, credit: A. Karabeyoglu, 2011.....	112
Figure 4.5: OF shift in Case 1	113
Figure 4.6: Specific impulse shift in Case1	113
Figure 4.7: Layout of Case 2 rocket.....	115
Figure 4.8: exploratory layout study for multiple core construction.....	117
Figure 4.9: Specific impulse shift in Case2.....	118
Figure 4.10: OF shift in Case2	118
Figure 4.11: Layout of Case 4 rocket.....	121
Figure 4.12: Specific impulse shift in Case4.....	122
Figure 4.13: OF shift in Case4	123
Figure 4.14: Layout of Case 5 rocket	125
Figure 4.15: Specific impulse shift in Case5.....	126
Figure 4.16: OF shift in Case5	126
Figure 4.17: Layout of Case 6 rocket.....	128
Figure 4.18: Specific impulse shift in Case 6.....	129
Figure: 4.19 OF shift in Case 6	130
Figure 4.20: Layout of Case 7 rocket.....	132
Figure 4.21: Specific Impulse shift in Case 7	133
Figure 4.22: OF shift in Case 6	133
Figure 4.23: Third Stage general scheme	135
Figure 4.24: Layout of Case 7 rocket.....	137
Figure 5.25: Payload profile.....	138

Figure 4.26: Layout comparison of all the six cases	139
Figure 5.1: The upward spiral of Engineering Design	141

LIST OF TABLES

Table 2.1: Number of small satellites launcher from 2000 to 2009, table	27
Table 2.2: Performance characteristics of the Scorpius Sprite launcher	32
Table 2.3: Number of Launches a year for different payload capacities	36
Table 2.4: Small satellite launch market share by 2020, pessimist scenario.....	40
Table 2.5: Small satellite launch market share by 2020, realistic scenario.....	41
Table 2.6: Small satellite launch market share by 2020, optimistic scenario	43
Table 3.1: Values of a and n, for G in kg/(m ² s) and r in mm/s.	46
Table 3.2: Polynomial Coefficients for Chamber Temperature behavior perdition.....	54
Table 3.3: Polynomial Coefficients for reaction products molar mass behavior perdition.	54
Table 3.4: Polynomial Coefficients for Specific heats ratio behavior perdition	54
Table 3.5: Material employed in the analysis and their characteristics.....	58
Table 3.6: Length and diameter of the dry bay as a function of common variable.	78
Table 3.7: Conservative propellant addition.	78
Table 3.8: pitch angles used in the flight calculations	85
Table 3.9: Relevant moments in the launcher's flight.....	86
Table 3.10: Design Space for the first Stage variables.....	90
Table 3.11: Design Space for the second Stage variables	90
Table 3.12: Design Space for the third Stage variables	90
Table 3.13: Comparison between different algorithms, Launch Vehicle MDO	93
Table 3.14: Comparison between different algorithms, Rosenbrock function.....	94
Table 3.15: Comparison between different algorithms, Rastrigin function	94
Table 3.16: Setting parameter for the ARMOGA.	100
Table 3.17: Setting parameter for the SIMPLEX.	100
Table 4.1: Geometric and performance characteristics of Case1 Launcher	110
Table 4.2: Geometric and performance characteristics of Case2 Launcher	116
Table 4.3: Geometric and performance characteristics of Case3 Launcher	119
Table 4.4: Geometric and performance characteristics of Case4 Launcher	121
Table 4.5: Geometric and performance characteristics of Case5 Launcher	125
Table 4.6: Geometric and performance characteristics of Case6 Launcher	128
Table 4.7: Geometric and performance characteristics of Case7 Launcher	132
Table 4.8: Decision matrix comparing the 7 design cases	135
Table 4.9: Geometric and performance characteristics of Case7 Launcher	137

Table 5.1: Comparison of different TVC schemes..... 142

1- INTRODUCTION

Recently a tendency towards smaller satellite is appealing on the international payload market both reducing cost and sizes of satellites (FAA, 2010). The main cause of such tendency is the miniaturization of electronic components which make possible the smaller satellites to perform missions that earlier required larger platforms.

The tendency for smaller satellites has increased a secondary tendency for smaller launch vehicles capable of servicing such payload market, namely: small satellites (100kg to 500kg), microsattellites (10kg to 100kg) and nanosats (1kg to 10kg). Despite of the tendency for smaller satellites, there currently is no dedicated launch vehicle for the small payload sector, hence small satellites tend to use launch vehicle on the 1000kg to 3000kg payload capacity on shared launches.

Many launches on small launchers (up to 2000kg) (McConnaughey, 2010) are derived from retired InterContinental Ballistic Missiles (ICBMs), and some examples are: the Dniepr and the Rokot (Isarowitz, 2004). However there are newer designs developed exclusive for satellite launch applications like the Vega from the European space agency, among others. According to Ariane Space, the Vega Launcher has a very important role in their launch vehicle family strategy having a complementary role to their other launchers Soyuz (medium lift) and Ariane 5 (heavy lift).

In Brazil, the proposed launch vehicles for the near futures are: the VLS-1, VLM and the VLS-Alfa Crusis (AEB, 2012). All of those can be included in the small launch vehicles class along with Vega. The commercial exploration of VLM and VLS-Alfa was suggested on the latest strategy plan issued by the Brazilian Space Agency (AEB, 2012).

Vehicles in the Small Launcher category can be used to develop and test new critical technologies that can posteriorly be applied in larger launch vehicle. Two flagrant examples of this are SpaceX's Merlin 1C engine and the avionics used on the medium lift launch vehicle Falcon 9, both were tested on SpaceX's previously launch vehicle Falcon 1 and then employed on Falcon 9 (SpaceX, 2009).

1.1 A LAUNCHER FOR BRAZIL

Although the Brazilian Space Program (PEB) has more than 30 years history, by a series of factors it has not managed to develop and successfully launch a space rocket. Among

the main reasons for that are: small quantity and inconstancy of program's funding (AEB, 2012) and critical technologies' embargo by other nations. It is of the author's opinion that for the development of a Brazilian launch vehicle three premises have to permeate the entire design process: small development time, small cost and the utilization of technologies and techniques available in the Brazilian industrial park, in this order.

Due to PEB's history of inconstant funding the development of a Brazilian launch vehicle should take place in a relatively small time frame where the funding and the political will are favorable towards such project. Robert Zubrin (1996) argues in similar manner towards the possibility of a manned mission to Mars in the context of American Space Program. The maximum proposed timeframe for the development of a rocket in the proposed model is 6 years, considering the fund will be approved in the middle of a presidential term and being launched in the end of the second term. Any timetable longer than that could implicate in loss of funding on a critical stage of the project.

The low cost necessity is due to PEB's low available budget for the development of new launch vehicles. A launcher such as proposed in this work, cannot compete or intervene with the general availability of funding for any of the projects already in course, the most relevant being: the Southern Cross program (Figure 1.1), Geostationary Brazilian Satellite, CIBERS (Chino-Brazilian Earth Resources Satellite), Satellite Amazonia-1, the sounding rocket program and the bi-national company Alcantara Cyclone Space. Not only the development of the proposed launcher cannot interfere with other higher profile or more strategic projects but it has to contribute to them in the form of space qualification of components and in the launch of Brazilian satellites at lower costs.



Figure 1.1, Southern Cross Program

The embargo to critical technologies represents a problem of difficult solution, although it can be a driving force behind an innovative and extremely useful approach to launch vehicle design. This approach consists on only using material and processes already available in the Brazilian Industrial Park. This approach towards national technologies should permeate the entirety of the design process.

1.2 MOTIVATION

As it was said, there is a considerable trend towards the development of ever smaller satellites for application in Low Earth Orbit (LEO). The greatest evidence of this are the considerable amount of planned Cubesats and, in second place, satellites with up to 100kg (DePasquale, 2004). Currently there are no launch vehicles capable of supplying such specialized market and those devices are relegated to be launched as secondary payloads in larger vehicles.

With the ever increasing number of small payloads the necessity of a dedicated launch vehicle for such market becomes progressively greater. As presented before, the Brazilian Space Program would greatly benefit from a the development of a national launch vehicle. Moreover, considering the current situation of the space program, a micro lunch vehicle (up to 500kg payload) in the lines described on Section 1.1 is possible and realistic

1.2.1 A Simpler alternative

The imposed time and funding constraints do not allow for a strictly conventional approach. The conventional approach would be either the development of a solid launch vehicle similar to Vega or the development of a family of liquid propellant turbopump fed engines. Neither of those alternatives is suitable for a launcher such as the proposed.

A solid propellant launch vehicle could be attractive for a Brazilian micro launch vehicle for mainly 2 reasons: VLS/VLM heritage and simplicity, although such launcher would directly compete for market and funding with the cited Brazilian launch vehicles among other technical constraint. The operation of a solid propellant launcher would require the complete logistics of solid propellant production that includes high infrastructure costs. Consequently, a constant number of launches is needed to maintain the required infrastructure. Although a pure solid propellant launch vehicle is possible, it will benefit from the inclusion of a liquid propellant upper stage for improved orbit placement. An example is the Pegasus from Orbital Sciences without its HAPS hydrazine upper stage its orbital altitude accuracy is of $\pm 111km$ and with the upper stage it falls to $\pm 28km$ (Isarowitz, 2004). The inclusion of a liquid upper stage would either imply the acquisition of a foreigner system or the increased complexity of developing a solid propellant launcher and a liquid motor family.

A traditional (turbopump fed) liquid propellant approach could solve many of the problems faced by a small launcher such as proposed here, as the high specific impulse of liquid propellant systems could significantly reduce the launcher's gross mass, number of stages and ultimately its cost. On the other hand, the development of a very small turbopump fed liquid propellant engine might be as complex as developing a larger engine. The opportunity cost of developing an engine for a larger launch vehicle with almost the same effort of developing an engine for a small launcher might doom the proposed micro satellite launcher.

There is still a third alternative that combines some of the advantages of both traditional liquid and solid propellant in a simpler design. This alternative lies in hybrid propellant propulsion and pressure fed liquid propulsion. Both commonly proposed hybrid motors and pressure fed liquid engines have very simple designs, consisting only of a combustion chamber, very similar to a solid propellant motor, and tanks employing the same materials and fabrication processes, which already exist in Brazil from VLS heritage. The

propellants used both on hybrids and most pressure fed liquid engines are common industrial products, such as liquid oxygen, kerosene and paraffin, thus dispensing dedicated facilities for propellant production. The specific impulse of pressure fed liquid engines is superior to turbopump fed systems due to inefficient expansion on the gas generator nozzles (Gas Generator cycle) or losses in the turbine assembly (Staged Combustion cycle) (Sutton, 2001). Hybrid motors have a slightly specific impulse loss due to OF shift (Karabeyuoglu, 2012), although they maintain a very similar performance to general liquid propellant systems. The greatest disadvantage of both pressure fed liquid propulsion and hybrid propulsion is their relative high structural mass fractions, caused by the thick wall propellant tanks and heavy pressurization subsystems.

1.4 OBJECTIVE

This article proposes the discussion and design of a microsatellite launcher tailored for Brazilian needs and technical capabilities. Being so, a novelty design technique based on genetic optimization will be employed, this technique aims to provide a multidisciplinary analysis of the problem and the formulation of a complete solution that takes in consideration both qualitative and quantitative factors, delivering a cost effective and reasonable solution for preliminary system design.

1.5 METHODOLOGY

This article proposes not only the design of a micro satellite launcher to be constructed in Brazil but also the utilization of a multidisciplinary design optimization technique to provide the best possible options for the experienced designer to choose from. This article covers the classic product design methodology up to the point of preliminary design, this work covers: mission definition, initial design tradeoff and optimized preliminary design.

In order to define a realistic, cost effective and lucrative mission a small payload market assessment was made in the form of a market research generating a mission envelope that allies considerable high number of launches per year and flexibility maintaining the launchers size within a feasible scale. The market research took in consideration the current number of small payload launches, future previsions, political environment and competing companies to provide three future market share scenarios for the proposed launcher and an optimized mission envelope.

To provide a consistent comparison between the different propulsion technologies available for the proposed micro satellite launcher an optimization routine was developed. The proposed routine was based on the MDO developed by the University of Brasilia on “An Optimized Hybrid Rocket Motor for the SARA Platform Reentry System” (Kaled Da Cás, 2012). The methodology employed on the SARA Reentry motor was both expanded and improved to account for all the systems of a multistage launch vehicle. Among the main improvements on the MDO are: multistage capability, improved mass prediction model, Mach dependent drag prediction and the introduction of hybrid optimization algorithms. The proposed MDO provides optimal designs making possible the correct evaluation of competing technologies highlighting the true tradeoffs between them. Seven design cases were proposed each employing one or more of the commonly proposed propulsion technologies for hybrid launch vehicles. The design cases are then compared and one of them is selected. This one is optimized again including design knowledge acquired from the comparison of the first seven design cases. This procedure allows for a propulsion technology to be selected taking in account not only its performance figure, but its impact on the launcher design as a whole.

1.6 DISSERTATION STRUCTURE

The First chapter of this work provides a preliminary overview of the proposed activities outlining the motivations, objectives and proposed methodology to achieve the settled goals.

The second chapter of this work analyses the markets for a microsatellite launcher and estimates the possible market share attainable by a Brazilian launcher in the category proposed.

The third chapter presents the optimization technique employed and the various technological alternatives considered comparing then both qualitative and quantitative. The MDO algorithm is presented and detailed in this chapter.

The fourth chapter of this work proposes 7 optimization cases contemplating the most engineering and economically wise design alternatives. In the same chapter the 7 optimized designs are compared and a resulting solution is obtained. The resulting solution is then optimized again addressing design problem encountered during the optimization of the earlier 7 cases.

The fifth chapter proposes a conclusion for the work and outlines future initiatives for continued work on the design of the microsatellite launcher.

2-MARKET AND MISSION

It is highly required for a launch vehicle's success as an engineering project to correctly meet the market demands and requirements. This chapter attempts to outline the current market of small launch vehicles and predict a profitable market niche to be met by a launcher in the class this work as whole aims to design. The market analyses will require a considerable amount of guessing for the market niche of microsatellite dedicated launches does not exist.

Considering a correct prediction of the market's tendencies, it will be possible to decide the best payload capacity for the launcher being designed. This payload decision has to both maximize the profitability of the launcher, maintain the design sizing compatible to the available fabrication power of Brazilian industrial capabilities, and to be compatible with the University-oriented-design approach.

2.MARKET ANALYSIS

In recent years a considerable attention was given to the sector of Microsatellites (FAA, 2012). Microsatellites are defined as space payloads with masses ranging from 10kg to 100kg. Traditionally those payloads are fared as piggyback in a larger launcher. Although the US FAA's (Federal Aviation Administration) Office of Commercial Space transportation identifies in its 2010 report the emergence of a market for launches of payloads of less than 100 kg, according to the report that market can "cause microsatellite payloads to shift from the multi-manifest approach to individual launch on these new vehicles" (FAA, 2012).

A study realized by Fultron Corporation personnel (Chistensen, 2010) attempts to characterize the emergent market of emergent microsatellite launch vehicles, by applying Michael Porter Industry Structural Analysis. The following discussion is based in the conclusions achieved in the article.

2.1.1 Buyers

The organizations currently realizing and planning microsatellite launches intrinsically differ from the usual payload provider of larger cargoes.

In a study performed by Space Works Consulting (DePasquale, 2010) on the launch opportunities on the class of 100 to 200km, six main areas of services provided by satellites in that class were identified. Those areas are:

- Military: science and technology
- Military: intelligence, surveillance and reconnaissance
- Civil/commercial communications: polling of unattended sensors
- Civil/commercial communications: remote site communications
- Civil/commercial remote-sensing: high-resolution Earth observation
- Civil/commercial remote-sensing: Land-sat class data for environmental monitoring

As it can be seen, the military payloads play a central role in the segments of the market, although the University and research centers play an even larger role, as it is represented by the diagram bellow (Figure 2.1):

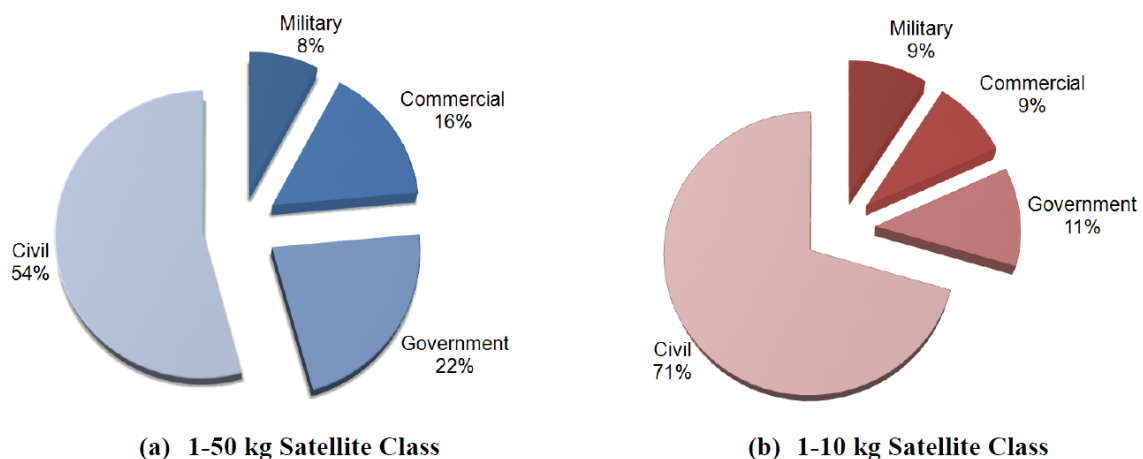


Figure 2.1: Customers share of the world's Micro and Nano satellite market

The considerable importance of the civil non-commercial (Universities) and governmental launch attempts reinforce the feasibility of a small launch vehicle developed in a University Environment financed by civil scientific foment funding.

The microsatellite operators unlike those of larger satellites normally do not possess strict timetables to be met (Chirstensen, 2010), and can easily afford delays and reschedules. In a similar way they are very versatile regarding the launch vehicles constraints and can easily adapt their payloads to different vehicles. This behavior is

caused mainly by the small budgets of those entities and the current industry standard of multi-manifest and piggyback launches.

The operators of micro and nano payloads are currently subjected to small budgets, the average Smallsats (100kg to 500kg) are normally developed with a budget between 1 and 10 million dollars (Christensen, 2010), including launch costs. This data can be extrapolated to microsatellites at a smaller scale. Unlike what happens to larger payloads, the launch cost imposes a serious liability to the satellite providers. Also the considerable number of launches indicates a large number of customers and a tendency for expansion (FAA-2010).

The most interesting orbits such as Sun Synchronous Orbit are normally difficult to be explored by the microsatellite due to the use of piggyback launches, as the auxiliary payloads cannot interfere with the main one, which is normally sent to the more desirable orbits.

By the information presented above, it is possible to prepare a superficial analysis on the consumer of small satellite launch service. The large number of costumers and relative few launch providers characterize a market with small buyer's bargaining power, a situation very similar to the market for larger payloads. Although unlike the situation in the large payloads' market the limited budgets make the costumers much more sensitive to launch costs. Even with the relative high launch cost sensitivity, the low number of adequate launch opportunities and the large number of buyers compared to suppliers result in a market characterized by low buyers bargaining power.

2.1.2 New entrants

Currently there is no launch vehicle that operates in the micro satellite class. However the the difficulties in entering this non-established market are similar to those of entering the larger satellite market: steep learning curves, high fixed costs and governmental restrictions, and high development costs of such launcher (Christensen, 2010), being the last one the most relevant. The envisioned development cost of such a small launcher is estimated around 10 million dollars (Christensen, 2010), naturally considering the cost constraints of the payloads providers in this class that cost can be possibly reduced.

Many of the companies currently considering or developing a micro satellite launcher are already players in the aerospace market (Section 2.1.1.3) or are considering spinoffs from technologies employed in the launcher, as alternatives for retrieving the investment.

Despite the predicted the high cost, it is not a barrier worth stooping the future development of small launch vehicles (Christensen, 2010). Although the learning curves might pose a problem and, especially for a launcher developed in Brazil, some governmental barriers should pose a serious problem for the project, among them the most significant being the “Sensible Technologies Safeguards Treaty” not signed by Brazil that might exclude American payloads from being launched in Brazilian Cosmodromes.

2.1.3 Suppliers

Traditionally in the space industry there have been considerably more buyers (satellite providers) than suppliers of launch vehicles. This trend is foreseen to be the general rule of the market for the next years. The number of micro launch service buyers is expected to increase over the years, first due to entry of new players in the market, Universities and small enterprises mainly, and the miniaturization of electronic components making smaller satellites capable of missions previously only possible for larger platforms.

It is still difficult for a possible micro satellite operator to set prices in its market due to the existence of other alternatives to their products, namely piggyback launches, a much more known method and currently supplying a great part of that market. Even though the suppliers in this market possess a considerable higher mark-up, they are affected by the severe budget limitation of their buyers.

Several companies are currently developing satellite launchers in the category proposed. Most of those are governmental but there are several private companies in various stages of developing. A list of those projects was compiled and those in better stage of development will be further analyzed. The most relevant are:

- Virgin Galactic Small Satellite Launch System
- Interorbital Systems’ Neptune 5 and 9
- Microcosm’s Scorpius
- IAE’s VLM

2.1.4 Competing technologies

Competing technologies are technologies that might fight for a market share in the micro satellite launch with dedicated microsatellite launchers. The most relevant of those technologies are: launch as secondary payload, the utilization of hosted payloads and for some restricted payloads suborbital launches can be considered an option.

Launch as secondary payloads is the current microsatellite industry's standard, due to the current lack of dedicated micro launch vehicles. The utilization of multi-manifest launches or piggyback has several advantages: the familiarity of the industry with this kind of system and the current availability of relatively cheap and reliable small launch vehicles (Dnieper and other repurposed ICBMs) (Isarowitz, 2004). However this strategy imposes serious liabilities to the launch of services to costumers, restricting their operations to non-optimal orbits and subjecting them to the larger payloads' launch schedules. Besides the piggybacking in larger satellite launches, there were missions where several small micro and mini satellites shared one multi-manifest launch. Although this strategy allows for more freedom in orbit placement, it imposes logistic and timeframe problems of synchronizing various payloads' schedules (sometimes as much as 18 satellites shares the same launch vehicle).

The employment of hosted payloads is a somewhat new development consisting in various experiments or equipment from different operators sharing the same satellite bus. This strategy allows for scale savings due to sharing satellite equipment: power supply, thermal protection, propulsion and communication systems can be shared by the different experiments in the same bus. Those shared satellites platforms can more easily fall within the traditional payload mass ranges and can share launch costs among the various costumers. Despite of the considerable advantages of this mission architecture, the integration of various experiments and sensor in the same spacecraft has proven itself a complicated task and only a handful to missions (mostly governmental) employing such architecture were flown.

For specific mission requiring small microgravity time, suborbital flights might be an acceptable solution. There are several countries that maintain regular suborbital civil and military launches (Figure 2.2).

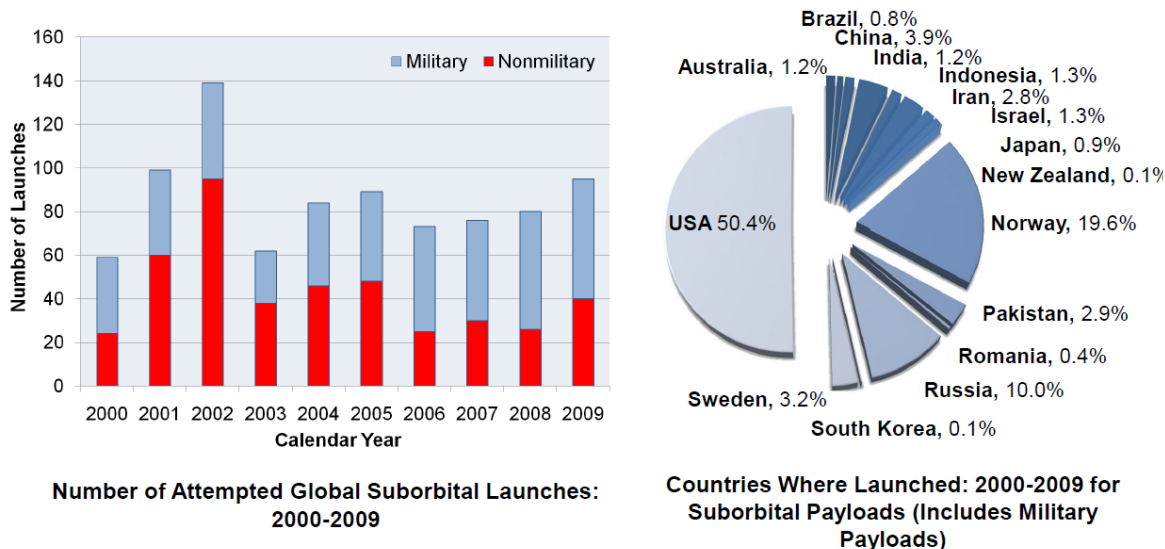


Figure 2.2: Suborbital payload market's figures

Suborbital launches are considerably cheaper than orbital, and possess a considerable higher readiness level.

For a dedicated micro satellite launch vehicle to compete with the other available technologies, it has to differentiate itself. This differentiation will come mainly from the capabilities of more responsive orbit selection and time schedule. Although the cost per launch has to be kept low due to the serious budget constraint presented by the typical micro satellite customer.

2.2 MARKET SIZE AND BEHAVIOR

The small payload market is clearly not as big as the conventional payload market, though this market going through an expansion on recent years, mainly due to electronic miniaturization and satellite component standardization. The micro satellite market possesses very specific orbit and payload mass ranges and the correct understanding of those is crucial for the design of a dedicated micro satellite launcher.

2.2.1 Mass Range

Based on the comprehensive nano, micro and small satellite database compiled by DePasquale (2010), it was attempted an estimation of a possible future market for launchers in this category. The considered database takes in to account launch attempts not successful launches and may contain data concerning satellites that failed to achieve orbit. A “launch attempt” is related to the satellite and not to the launch vehicle if a case of multi

manifest missions a “launch attempt” is accounted for each satellite sharing the carrier rocket.

Five different mass categories were considered. The first category encompasses nanosatellites, mainly cubesats, in the mass range of 1-10kg. This category possesses a considerably large number of launch attempts due mainly to the small mass and cost of nanosats. Even in a micro satellite dedicated launcher cubesats will continue to be an important secondary payload and their operators will have a much louder voice in the mission planning.

The microsatellite category (11-100kg) was broken down in two due to its relative large relative mass range. One of those categories considers satellites from 11 to 50 kilograms and the second satellites from 51 to 100 kilograms. Hence it was possible to achieve a compromise in micro satellite market and design the payload capability more acutely. Both fraction are considered the main payload range of this project.

Similarly to what was made in the microsatellite category, the Smallsat category was also broken in two for easier analysis. The first of those categories considers Smallsats in the mass range of 101 to 200 kilograms, several Brazilian satellites fall in this category among them the SCB (*Satelite Coleta de Dados*) and the *Plataforma Multi Missão* (AEB, 2012). The second category of Smallsat’s market is ranges between 201 to 500 kilograms. This second category is especially relevant because there are already operational launchers in this range of payload, among them can be cited the Orbital Sciences’ Pegasus, the Space X’s Falcon 1 and the International Launch Alliance’s Rokot (Isarowitzs, 2004).

The following table (Table 2.1) presents the number of launch attempts in each of the selected categories and the graphical representation of the same values can be seen in Figure 2.3.

Micro Nano and Small Satellite Market - Mass Ranges					
Year	0 kg-10kg	11 kg-50kg	50kg-100kg	101kg-200kg	201kg-500kg
2000	12	4	1	1	6
2001	2	2	3	0	8
2002	5	3	2	0	7
2003	6	0	7	3	5
2004	0	11	0	6	3
2005	3	1	3	3	2
2006	22	12	1	0	4

2007	13	6	1	10	14
2008	11	1	4	10	8
2009	14	12	5	8	5

Table 2.1: Number of small satellites launcher from 2000 to 2009, table

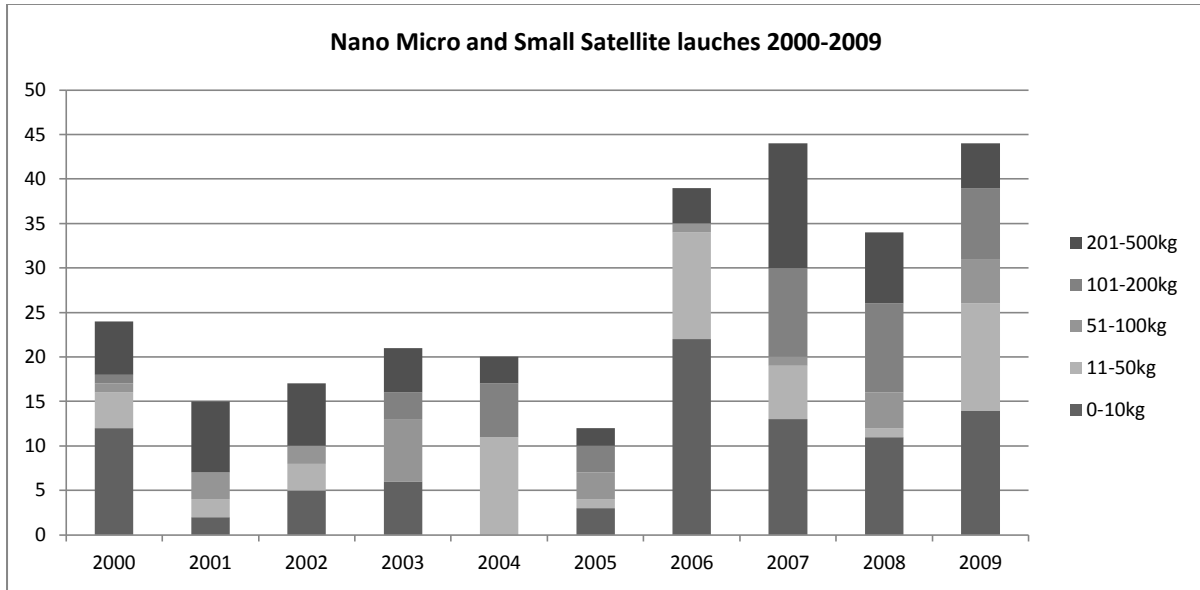


Figure 2.3: Number of small satellites launcher from 2000 to 2009, graphic

According to Christensen (2010), an average of 14 micro satellite class (10-200kg) launchers are performed a year, with a tendency for expansion, making possible for a vehicle operating in this class to perform from 4 to 6 launches a year. Although it can be seen from Table 2.1 that the number of launches in every class changes considerably each year, for example the 11-50kg launches between 2004 and 2006. This uneven market behavior will require an extremely lean managerial process. The recurrent and infrastructural cost should be kept to a minimal allowing for a great flexibility in the number of launches per year.

2.2.2 Orbital Range

Many of the satellite in the microsatellite range tended to be launched for polar orbits, more specifically in Sun Synchronous Orbits (SSO). As it can be seen in the figure below (Figure 2.4), for satellites in the 1kg-50kg class those satellites are normally located in low earth orbits with apogees ranging between 600km and 850km in inclinations around 100 degrees. This may be more due to compromises with the main payload owner than to the microsatellite operator's choice. With the advent of a dedicated microsatellite launcher this

situation can change. Although polar orbits, more specifically SSOs, are preferable for earth remote sensing and it is reasonable to assume micro satellites will remain operating in these orbits even with dedicated launchers.

The average orbital apogee for satellites with masses in the 1-50kg class launched between 2000 and 2009 was of 689km (this average excluded eight high altitude satellites with apogees between 1014 and 4500 km). The average orbital inclination for such payload class for the same period was of 87.5 degrees.

The situation in the nanosatellite class is very similar with an average apogee high of 690 km (excluding two high altitude satellites with apogees of 1015km and 1800km) and an average inclination of 86.5 degrees.

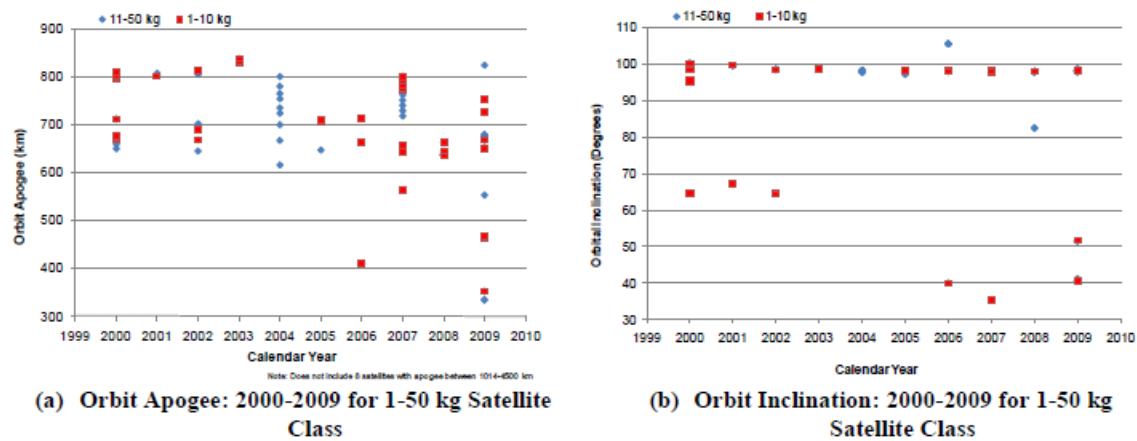


Figure 2.4: Orbital altitudes of small satellites launches from 2000 to 2009

2.2.3 The market in Brazil

The Brazilian space agency currently operates a considerably large family of suborbital sounding rocket, and those launches make up for a considerable share of the bulk of Brazilian space industry. Despite of previously attempts, due to several accidents and budget restraints the Brazilian space launcher the VLS (Satellite Launch Vehicle), a small satellite launcher, has never become fully operational. Recently and motivated mainly by a successful partnership with German Space Agency (FSCSa) (AEB, 2012) the Brazilian space research center IAE (Institute of Aeronautics and Space) has begun the development of a fully solid small satellite launcher the VLM. The development of the VLS, VLM and the improved versions of the VLS continues.

The Brazilian space agency has launched several satellites to low earth orbits and with masse ranging from micro to medium payloads classes. All those satellites were launched in foreigner vehicles but many of them were completely developed and tested in Brazil.

2.2.4 Future Forecast

It is very difficult to find an accurate quantification for number of future micro satellite payloads, though it is consensual among analysts that the market is in expansion (FAA-2010), (Christensen, 2010) (DePasquale, 2010). The only extrapolation of the future number of launches was done by Space Works (DePasquale, 2011) and focus only on the launches in the 0-50kg class. This extrapolation was based on on-going known projects. This prediction will be used as baseline for this market analysis. This data is presented below (Figure 2.5).

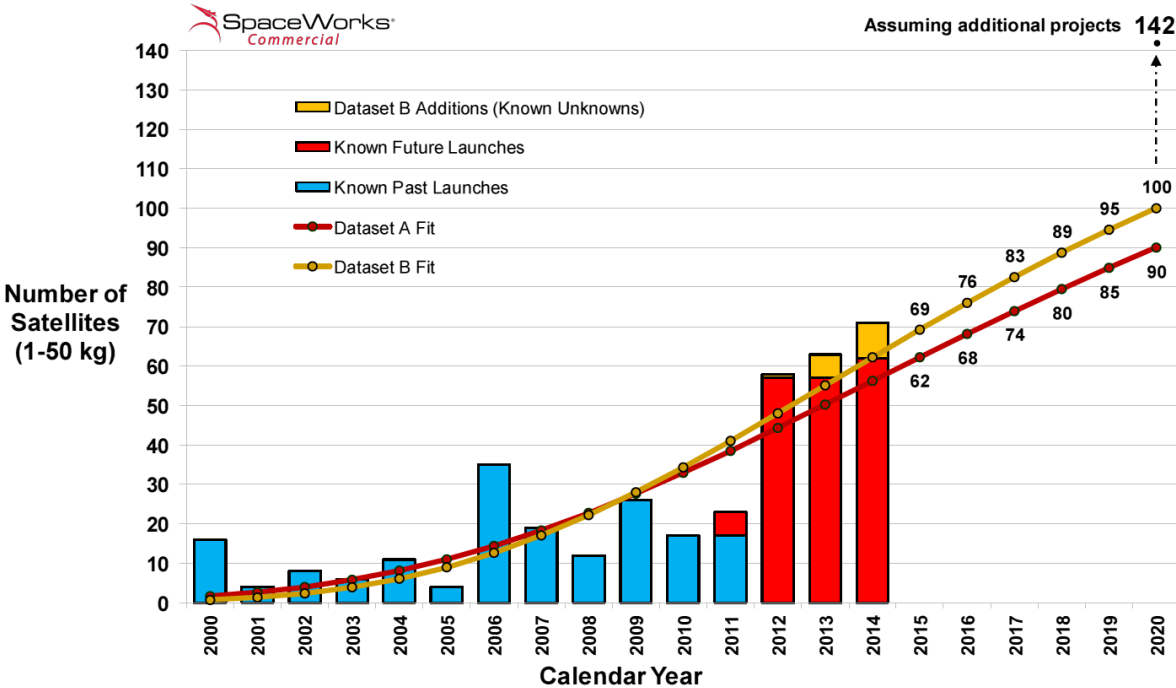
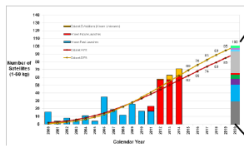


Figure 2.5: Future market trend extrapolation, by Space Works Commercial

Space works proposes a breakdown on industrial segments for 2020’s micro satellite market. This result is shown below (Figure 2.6):



Nano/Microsatellite orbital launch demand is projected to increase to over 100+ satellites needing launches in 2020



SpaceWorks Commercial Nano/Micro Satellite Launch History and Projections (2000-2020)

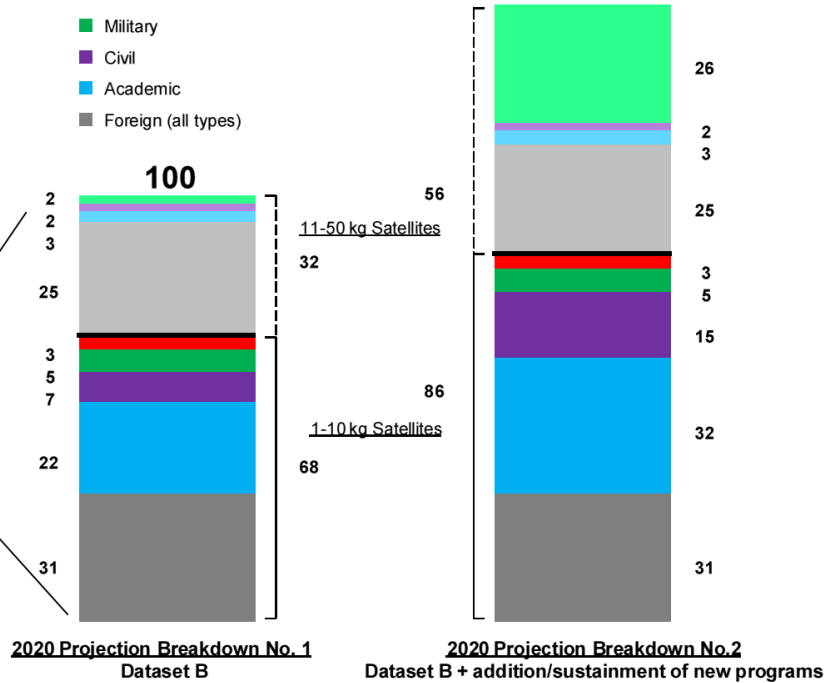


Figure 2.6: Small satellite market by 2020, by Space Works Commercial

From the predictions presented the number of payloads in the 11-50kg class by 2020 will be of 32 satellites for their more conservative scenario and of 56 for their more optimistic assumption including new programs.

2.3 DIRECT COMPETITORS

2.3.1 Scorpius

Microcosm is current working in the design of family of small sounding and orbital vehicles from the micro to medium launcher capabilities. The development is centered in the utilization of low cost approaches, namely; pressure fed injection systems and low cost ablative combustion chamber designs (Chakrobty, 2004).

As a direct consequence from the option for pressure fed propellant systems, Microcosms has engaged in the development of high pressure cryogenic all composite oxidizer tanks, and composite ablative combustion chambers. According to the company, those tanks, despite their small propellant mass fraction, are easy to manufacture and operate to the point which the pressure fed scheme becomes more attractive than traditional pump fed engines. Among the argued advantages of a thicker propellant, it is cited the easier ground operations resulting from much more shock resistant tank (Chakrobty, 2004).

Their low cost attitude permeates the entire design process of their rockets. They emphasize directives for cost reduction very similar to the ones considered necessary for developing a launch vehicle in the Brazilian Academic environment. They proposed the utilization of cryogenic propellants of low cost and available in non-aerospace industry: jet fuel and liquid oxygen. This option reduces their expenditures with complex ground operation due to security and propellant manufacturing issues. Despite of the reasonable high specific impulse achievable with LOX based propulsion Microcosm chose to employ not a 2 stage to low earth orbit system but a 3 stage system reducing the strains on propellant mass fraction. The reduced strains on the mass fraction allowed for the usage of heavier non-aerospace hardware for further cost reducing (Chakroboty, 2004).

Microcosm stresses on utilization of considerable in house fabrication to secure cost control and component availability. Several spinoffs of their IR&D and in-house fabrication are currently being commercially exploited, the most relevant of those spinoff being their light weight liquid tanks (Scorpius S.L.C., Pressuremaxx catalog).

They also utilize project architecture of incremental development, in which heavier launch vehicles are based on concepts and technologies tested on smaller previous ones and even in sub orbital rockets. They argue their low cost pressure fed designs possess very good scaling characteristics (Chakroboty, 2004). Their launch vehicle family and incremental design approach can be seen below (Figure 2.7):

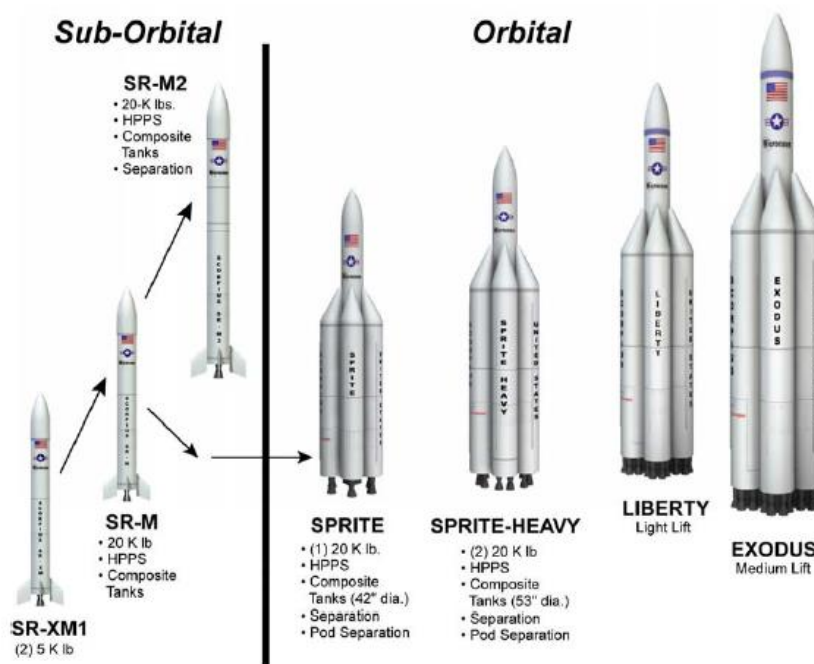


Figure 2.7: Microcosm’s Family of Low-Cost, Pressure-Fed Launch Vehicles.

The only vehicle proposed by Microcosm in the microsatellite range is the Sprite Mini-Lift, this rocket is intended for low earth orbit (LEO) launchers in the range of 200kg. The characteristics are presented in the table below Table 2.2

Scorpius Sprite Mini-Lift		
Payload	LEO 100 mi	700lb (~317kg)
	SSO	330 lb (~150kg)
Cost		1.57 Million US\$
GROSS launch mass		Not available
Configuration		3 stages (2+Boosters/Pods)
Propulsion		Liquid Pressure fed
Propellant		LOX/Aeronautical Kerosene

Table 2.2: Performance characteristics of the Scorpius Sprite launcher

2.3.2 Neptune 5 and 9

Interorbital Systems (IoS) is currently working in a family of low cost disposable launch vehicles, ranging from vary small payloads (Tubesat cluster-30kg) to considerable ambitious goals such as manned vehicles and a lunar sampler return mission.

IoS’s design philosophy is based in the concept of parallel staging and mass produced rocket stage core explored by the German company OTRAG in the 70’s. This concept is centered in the development of a standard liquid propellant rocket core and then clustering them together to form the stages. The OTRAG cores were pressure fed by a simple system of moving bulkhead using a blowdown injection profile. Their combustion chamber was ablative cooled (Figure 2.8).

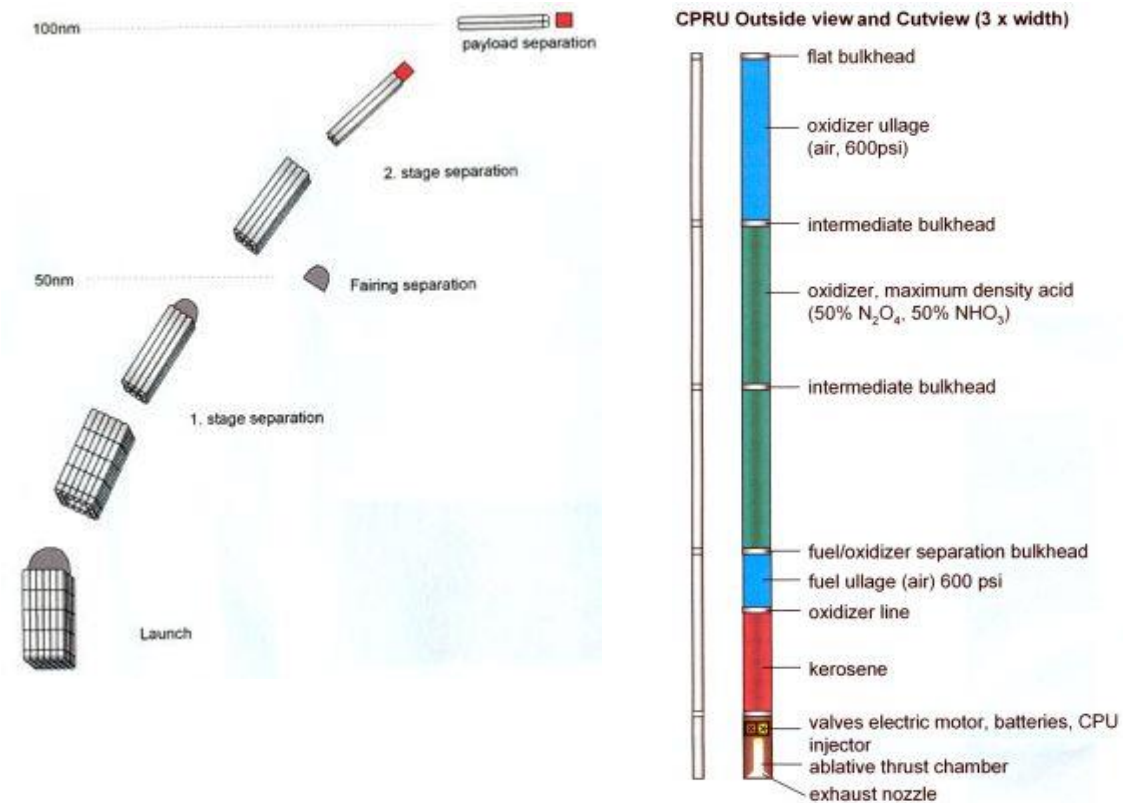


Figure 2.8: OTRAG Technology of clustered Launchers

Interorbital System’s rocket cores or Common Propulsion Module (CPM) are an updated version of the ones developed da ORTRAG. IoS’s CPMs use either blowdown schemes or pressure fed and throttling capacity for navigation and stirring. According to IoS, the modules are composed by four propellant tanks and an ablative rocket engine. The propellants used are storable hypergolic pairing of high-density white fuming nitric acid (WFNA) turpentine/furfuryl alcohol. According to the company their propellant pair was chosen for being inexpensive, storable and for providing hypergolic ignition.

Among the central problems of parallel staging are the complicated and inefficient aerodynamic of a vehicle composed of a cluster of tubular structures. Notwithstanding the company argues that the most significant part of the rockets flight and velocity increment happens outside the denser layers of the atmosphere and that the cost reduction generated by parallel staging outweighs the aerodynamic problems. Up to this date, no launch vehicle with parallel staging has ever flown.

Two of IoS’s launchers fall within the category of micro satellite launcher the Neptune 5 and Neptune 9. The Neptune 5 (N5) is capable of placing 30kg in low earth polar orbits

and was designed to support the Tubesat and Cubesat programs developed by IoS. This launch vehicle is composed of 6 engines: 4 CPM in the first stage, 1 CPM in the second and a solid motor in the third stage. The Neptune 9 is designed to carry 70kg to low earth polar orbit. The rocket is composed of 9 CPMs, 6 in the first stage 2 in the second and 1 in the third stage.

Interorbital's business approach is centered in selling pulverized low cost shares and launch services quotas via web site, similar to crowd funding. Currently is possible to buy a tube satellite development kit for a \$8239,00 with launch service included, and several groups including at least one Brazilian institution have purchased the service.





Figure 2.9: N9 rocket and a simple CPM.

2.3.3 Virgin Galactic Small Launcher

After the victory at the Ansari X-prize, the team behind the first privately funded manned spacecraft and the multimillionaire Richard Branson, owner of the Virgin Airlines and Virgin Records, founded the Virgin Galactic (VG), the first company to provide touristic flights on a dedicated suborbital spacecraft the, Space Ship 2 (SS2). The Space Ship 2 launch complex is an air launch system with a first stage composed of the White Knight 2 (WK2) a high altitude airplane and the second stage the SS2 itself. The SS2 is a winged suborbital rocket plane propelled by a single hybrid rocket motor developed by SpaceDev, a division of Sierra Nevada Company.

The Micro Satellite Launcher (MSL) project is the proposed to operate a small launch vehicle in parallel with the normal touristic operation of SS2. The MSL is composed of a 2 stage vehicle to be launched from the WK2 capable of launching 100kg to Low Earth Orbit. According to Christensen (2010), the Small Satellite Launcher project is being perceived as and secondary goal in VG's business strategy.

2.4 MISSION DEFINITION

From the number of small payload launches assessment is possible to estimate the number of launches possible for a micro satellite launcher vehicle in several mass categories, and mission architectures. The chosen mass categories were 50kg, 100kg, 200kg and 500kg.

2.4.1 Orbit and Payload

The 50kg category represents a launcher in the Neptune 5 and 9 category. Such a launcher would be the most practical and inexpensive alternative, although it might suffer from severe scale down effects. The primary mission of the 50kg launcher would be the transport of a single satellite within the range of 11 to 50kg, though secondary payloads such as Cube and Tubesats dispensers can be fitted.

The 100kg represents a launcher in the VG's Small Satellite Launcher category. Due to the considerable number of payloads in the 50kg range, two mission architectures were

considered, the first one being the launch of a single payload in the range of 51 to 100kg and the second being the launch of 2 payloads in the 11 to 50kg. Secondly Cube and Tubesats dispensers were included as alternative missions.

The 200kg class is similar to the Scorpius's. The 200kg class has considerable more payloads than the other range and represents the middle segment of the Small Satellite market. In a similar way both single and dual payload mission were considered with payloads in the 101 to 200kg and 51 to 100kg ranges respectively. Missions with 3 or more main payloads were discarded due to excessive complexity.

The 500kg range contemplates the high mass section of the Small Satellite business and was included in the analysis for comparison. This category is the only one that currently has operating dedicated launch vehicles, like the Falcon 1 and some smaller repurposed ICBMs and SLBM (Isarowitz, 2004).

For the decision of best payload range the number of possible launches per year in each category was used. Considering that underutilization of the payload capability would increase the cost per kilogram up to the point that the launcher would be unattractive, therefore missions outside the minimum payloads for each class were not counted. The assessment of number of launches for designs capable of dual payload mode was composed of the number of possible launches in the launcher's original category plus half the number of launches in the category immediately below, accounting for possibility of realizing both single and dual payload launches a year. The possible number of launches per year for each category for the period from 2000 to 2009 and from 2005 to 2009 is presented below (Table 2.3).

Class	Number of launches/year	Class	Number of launches/year
50kg 1 Satellite	5.2	50kg 1 Satellite	6.4
100kg 1 Satellite	2.7	100kg 1 Satellite	2.8
100kg 2 Satellites	5.3	100kg 2 Satellites	6
200kg 1 Satellite	4.1	200kg 1 Satellite	6.2
200kg 2 Satellites	5.45	200kg 2 Satellites	7.6
500kg 1 Satellite	6.2	500kg 1 Satellite	6.6

Number of Launches a year (2000-2009)

Number of Launches a year (2005-2009)

Table 2.3: Number of Launches per year for different payload capacities

It was expected for the 500kg class to be well positioned, considering it already represents a real market for dedicated launch vehicles. The next best alternatives were the dual manifest missions for 200 and 100kg, which is understandable considering the expanded range. The third category to present the most launches was the 50kg single manifest class. Due to the recent interest in smaller payloads payload in the 50kg range have become much more attractive in the period from 2005 to 2009 scoring the second best position, behind only the 200kg dual manifest.

The 500kg class was only included for comparison as it would result in a launch vehicle far too big to be developed in an Brazilian Academic/Private low cost environment such as proposed. Yet it is interest to notice that even though the 500kg represents a market share already possessing dedicated launchers the number of launches in the other categories is very close.

Multiple manifest launches are common although multimanifest launches to different orbital altitudes, planes or times are considerably complicated and only the most advance launch vehicles are capable of such maneuvers. The greatest deferential of a dedicated Micro Satellite launcher is the possibility of accurate orbital selection and reliability, the introduction of a multi manifest variable would possible complicate the mission design to the point that the micro launcher would not be competitive.

The 50kg payload presented a very good positioning in the comparative analyze being the category with the largest number of launches a year for a single manifest approach (excluding the 500kg class). The number of launches per year in that category is very close to the dual manifest approaches without the increased complication of multi satellite missions. The resulting size of a launch complex for a 50kg class launcher is safely within the capabilities of an Academic/Private low cost approach. In future developments the payload capacity can be increased by the addition of boosters or parallel stages. Future developments will be addressed in further sections.

The optimal orbital profile for micro satellites is easily analyzed, as the great majority of those satellites were launched to Sun Synchronous Orbits (SSO) of quasi-SSO orbits, the orbital altitudes ranging between 600 and 850 kilometers for the 11-50kg. The basic orbital altitude and profile should be a 850km SSO, making the rocket capable of operating in all the range of usual SSOs.

The primary performance profile for the proposed micro satellite launcher will be a 50kg payload to a 850km circular polar Sun Synchronous Orbit. This will allow for heavier payloads to be launched in lower SSOs or equatorial orbits. As often as possible the micro satellite launcher will also carry Cubesats and/or Tubesats dispensers to be injected in the same orbit as the main payload

2.4.2 Expected Market Share

For the estimation of a realistic market share for the proposed micro satellite launcher several factors were considered. The most significant of them concern political and industrial factors, the impact of the competing technologies and the growth of the small payload market.

The most critical political factor threatening the operation of the proposed launcher is the adhesion by the Brazilian government to the Technological Safeguards Treaty (TST). Without the TST the United States government does not allow the launch of North American payloads from Brazilian Cosmodromes. The USA is the largest producer of satellites in the world and not being able to tap into that market might doom the success of any launcher. Even with the signing of the treaty a Brazilian launcher probably will not be able to compete for the American governmental and military contracts. The imminent start of Alcantara Cyclone Space's operations will strongly increase the political pressure towards signing the TST.

The most significant industrial factor affecting the market share of the proposed launcher is the entrance of other dedicated micro launch vehicles in the market such as the ones presented earlier. The direct competitor in the 50kg class are the Neptune rockets, although vehicles like the VG's SSL and the Scorpions might compete for contracts in this smaller payload market.

The impact of competing technologies is very difficult to be evaluated for the reaction of the satellite industry to a dedicated launcher remains yet to be seen. The launching in multi-manifest missions is currently the industries' standard and some inertia is expected before the switch to dedicated launcher format. The impact of hosted payloads is even more difficult to predict. Although it requires a very high level of synchronization between the payload providers, it can provide in the future a very close level of orbital selection to

that of a dedicated launcher for a very large hosted payload platform can be the main payload of a conventional launcher.

2.4.2.1 Scenario 1 - Pessimistic

The first proposed scenario is a pessimist estimative of the achievable market share possible for a Brazilian micro launch vehicle developed in an Academic/Private environment.

The first assumption is of political nature, the Brazilian government does not sign the Technological Safeguards Treaty with the United States. Consequently, the proposed launcher does not have access to the American payload market. This assumption could be extrapolated to a saturation of the competing companies' (IoS, VG and Microcosms) launch capacities with only American payloads, although this saturation is not likely to happen and will not be further considered. Not being able to have access to North American payloads may compromise the perception of the Brazilian micro launcher by even non-American payload providers. Those difficulties in finding customers will prompt the company operating the proposed launcher to require substantial support from the Brazilian Space Agency (AEB) to survive. The possible AEB support will have to compete with the support for the VLM and VLS programs, and it is unlikely AEB will prioritize the micro launcher over its older programs.

This scenario considers that all companies currently developing micro satellite launcher will have their products in the market by 2020. The direct competitor of the proposed launcher will be the Neptune rockets, directly inserted in the 11-50kg payload range. It will be assumed that the Microcosms and the VG can compete for the 11-50kg market but with reduced effectiveness due to their non-optimal payload capacities.

This scenario is considering a smaller market growth than the proposed by Space Works. The causes for this smaller growth can be many, as direct shift from small satellites (101-500kg) to nanosats (1-10kg) without many launches in the micro satellite mass range.

Company	Estimated Number of Launches	Market Share
IoS	4.29	17.14%
Microcosm	1.29	5.14%
VG	2.14	8.57%

BR MSL	4.29	17.14%
IoS US	4.44	17.78%
Microcosm US	1.33	5.33%
VG US	2.22	8.89%

Table 2.4: Small satellite launch market share by 2020, pessimist scenario

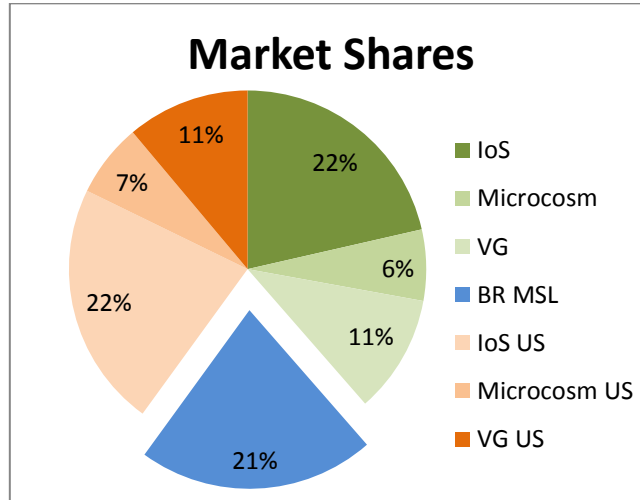


Figure 2.10: Small satellite launch market share by 2020, pessimist scenario

The market share prediction considered 40% of world’s payload providers to be from the United States (Fultron Corp., 2010). The Brazilian Micro Satellite Launcher (BR MSL) will not be allowed to compete from the American market share. Due to the non-optimal payload capabilities for the 11-50kg class the effectiveness of Microcosm and Virgin Galactic was reduced to 0.3 and 0.5 respectively. To emulate the smaller market growth the number of launches by 2020 will be considered of 25 instead of 32 as predicted by SpaceWorks. In order to emulate the impact of competing technologies, 5 of the 25 launches were considered to be performed as secondary payloads or as hosted payloads and were not included in the graph and table above.

It can be seen from the proposed market share that the BR MSL will possibly acquire a 21% of the world market for payloads in the 11-50kg range amounting for a total of 4.44 launches a year. This number of launches is sub optimal but still enough for the viability of the proposed launcher.

2.4.2.2 Scenario 2 - Realistic

The second proposed scenario is a realistic estimative of the achievable market share for a Brazilian micro launch vehicle developed in an Academic/Private environment.

The political environment for the second scenario assumes that the Brazilian government signs the Technological Safeguards Treaty with the United States and the Brazilian micro satellite launcher will be able to compete for the American market, although the American military and governmental contracts will not be available for the BR MSL due to strategic concerns. Furthermore, perception of a foreigner launcher by the American payload providers may affect their decision making them inclined to contract an American company to provide launch services.

The behavior of the market is assumed to be the one predicted by Space Corp with 32 launches in the 11-50kg class by 2020.

Company	Number of Launches	Percentage
IoS	5.8	21.4
Microcosm	1.7	6.4
VG	2.9	10.7
BR MSL	5.8	21.4
IoS US	2.9	10.8
Microcosm US	0.9	3.2
VG US	1.5	5.4
BR MSL US	2.3	8.6
Military and Governmental	3.2	12.0

Table 2.5: Small satellite launch market share by 2020, realistic scenario

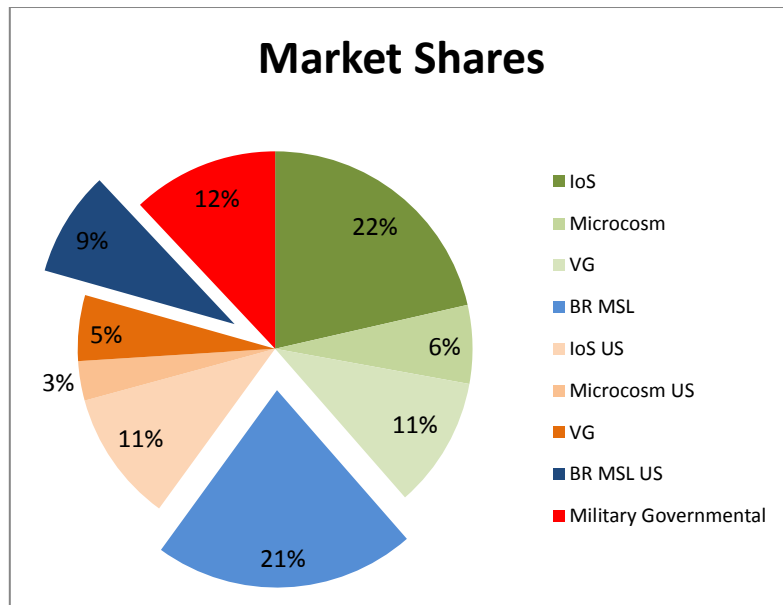


Figure 2.11: Small satellite launch market share by 2020, realistic scenario

Scenario 2 considers 30% (12% of the world’s total) of the American Payloads to be either from Governmental or military sources (DePasquale, 2010) (Figure 2.1). This market was considered voided to the BR-MSL. The preference for national products by the American payload providers was emulated by setting the effectiveness of the BR MSL to 0.8 in the American Market. Similarly to Scenario 1 the effectiveness of Microcosm and VG was set to 0.3 and 0.5 respectively. In order to emulate the influence of competing technologies, the 5 of the predicted 32 launches were excluded from the analysis, representing hosted and secondary payload launches.

It can be seen from the proposed market share that the BR MSL will possibly acquire a 30% of the world’s market for payloads in the 11-50kg range amounting for a total of 8.1 launches a year. This number of launches is considerable, possibly above the production and launch capabilities envisioned for the BR MSL.

2.4.2.3 Scenario 3

The third proposed scenario is an optimistic estimative of the achievable market share for a Brazilian micro launch vehicle developed in an Academic/Private environment.

Politically Scenario 3 is similar to Scenario 2. The Brazilian Government signs the TST with the US enabling access to the North American payload market. The resistance to foreigner launch providers and the restriction to military and governmental contracts were maintained.

In this scenario one of the companies currently proposing a micro satellite launcher does not manage to deliver a product to the market by 2020. The company most likely not to deliver an operational launch complex is the Virgin Galactic. VG’s main business is space tourism and they are currently engaged in developing the SS2, the Small Satellite Launcher is being perceived as a secondary objective. Although VG is by far the largest and well-funded of the competing companies, and either Microcosm or Interorbital Systems can bankrupt due to financial problems.

The size of the market was based on the most optimistic predictions by Space Corp assuming a number of 56 payloads per year in the 11-50kg class.

Company	Number of Launches	Percentage
IoS	12.00	26.09
Microcosm	3.60	7.83
BR MSL	12.00	26.09
IoS US	6.13	13.33
Microcosm US	1.84	4.00
BR MSL US	4.91	10.67
Military Governmental	5.52	12.00

Table 2.6: Small satellite launch market share by 2020, optimistic scenario

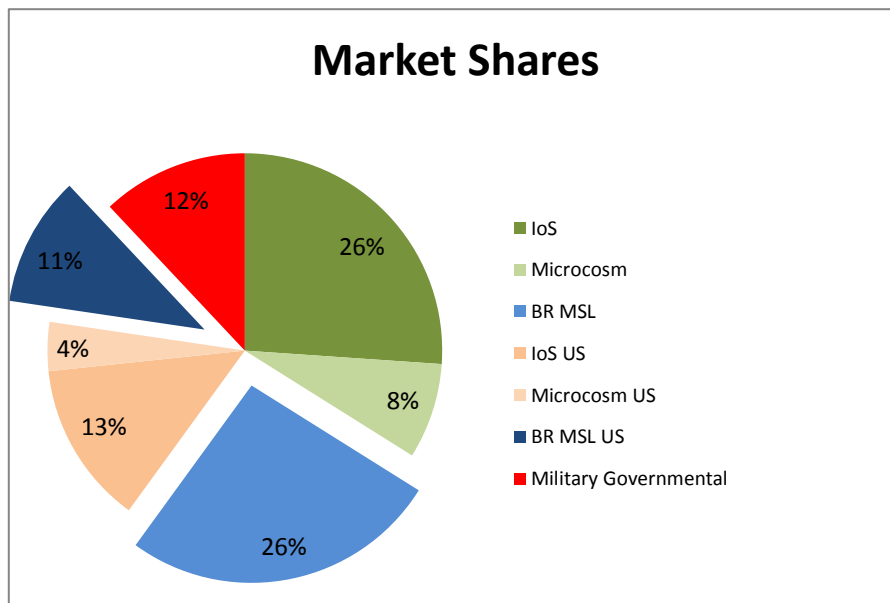


Figure 2.12: Small satellite launch market share by 2020, optimistic scenario

The scenario 3 considers 30% (12% of the world's total) of the American Payloads to be either from Governmental or military sources (DePasquale 2010) (Figure 2.1). This market was considered voided to the BR-MSL. The preference for national products by the American payload providers was emulated by setting the effectiveness of the BR MSL to 0.8 in the American Market. The effectiveness of Microcosm was reduced to 0.5, and VG was removed from the analysis. In order to emulate the influence of competing technologies, the 10 of the predicted 56 launches were excluded from the analysis, representing hosted and secondary payload launches.

It can be seen from the proposed market share that the BR MSL will possibly acquire a 37% of the world market for payloads in the 11-50kg range amounting for a total of 16.91 launches a year. This number of launches is very high, certainly above the production and launch capabilities envisioned for the BR MSL. If this scenario materializes, many other companies will enter the dedicated micro satellite launch market incentive by the excessive demand.

2.5 CONCLUSION

Based on this preliminary market analysis a micro satellite launcher is viable. The launcher's primary objective orbit will be Sun Synchronous Orbit, being capable of delivering 50kg to a polar orbit with altitude of 850km. Naturally the proposed Brazilian Micro Satellite Launcher should be capable of delivering payloads heavier than 50kg at lower altitudes and competing at the 51-100kg market as a secondary business strategy. The launch of nanosatellites such as Cubesats should also represent an important secondary business branch, with Cubesat dispensers being included in every possible flight and even a full nanosatellite multi-manifest launch per year is possible.

3- THEORY, OPTIMIZATION AND BALLISTICS

This chapter is dedicated to presenting the theory behind the various subprograms employed on the preliminary design studies, along with the theoretical background behind them. This methodology first simulates the internal motor performance solving the internal ballistics problem, then the structural mass of the rocket is calculated and finally a velocity loss estimator is used to predict orbit attainment. This design calculator is then employed inside a commercial hybrid optimization solver.

As aforementioned, the design calculator is divided in three blocks, the first one dedicated to internal ballistics and called Ballistic Module, the second one the Design Module is used for structural calculations and the Velocity Module for flight performance estimation.

The Ballistic Module employs a modified version of the ballistic calculation routine already used in several publications by University of Brasilia's group (Kaled Da Cás, 2012). The greatest modification is the exclusion of the chamber's internal pressure as a design variable and its replacement by the nozzle's radius, the oxidizer tank's external diameter was also added as a design variable and also the exclusion of the internal diameter as a design variable. These changes simplified the calculations but complicated the setting of the design variable's boundary limits. The code will be explained in detail on the next section. The design variables limits and ranges are presented on Section 3.8.1.

The Design Module employs a mixture of dimensioning calculation and semi-empiric formulas. The bulk of equations employed in the calculation were extracted from the Ukrainian design experience (Lynnyk, 2008).

The Velocity Module accounts for both aerodynamic and gravitational losses during flight. This code takes in consideration Mach variable drag coefficient, height variable density, pressure and temperature among other dynamic parameters.

3.1 BALLISTIC MODULE

The Model behind the Ballistic model is inspired by the one proposed by Casalino and Pastrone (2005). The basic objectives while evaluating a hybrid propellant motor are the estimation of the thrust level, mixture ration, oxidizer tank's pressure and loading, nozzle geometry, and grain geometry. Since hybrid motors do not allow for constant burn grain geometries, the combustion port's area changes during the rocket's operation, hence it

follows that a geometry that reduces those effects is considered a secondary objective in designing the motor.

The following procedure describes the algorithm used in the Ballistic Module. The initial input data for the ballistic calculation also dub as many of the Design Variables for the optimization calculations, the Design variable are shown below:

- External Grain Diameter: D_{ext}
- Fuel Grain's Length: L_g
- Propellant Mass Flow rate: \dot{m}_{oxi}
- Nozzle Throat Radius: R_t
- Oxidizer tank diameter (rocket's diameter, used only by the Design Module): D_r
- Internal grain diameter (Used only on post optimization, Case 8): D_{int}

First the solid fuel regression rate, as a function of the oxidizer mass flux, is calculated through the relation

$$\dot{r} = aG_{oxi}^n. \quad (3.1)$$

The values for a and n are obtained from experimental research. In the table below values obtained both by UnB's group and by other research teams are presented. Table 3.1 shows values for several propellants pair of interest in hybrid propulsion.

Propellants	a	n	Reference
N2O/paraffin	0.722	0.67	Bertoldi (2007)
N2O/paraffin	0.488	0.62	Karabeyoglu et al. (2004)
H2O2/paraffin	0.034	0.96	Brown and Lydon (2005)
H2O2/paraffin40%ALH3	0.034	0.96	Extrapolation, no experimental data available
O2/paraffin	0.488	0.62	Karabeyoglu et al. (2011)
O2/ paraffin40%ALH3	0.488	0.62	Extrapolation, no experimental data available

Table 3.1: Values of a and n , for G in $\text{kg}/(\text{m}^2\text{s})$ and \dot{r} in mm/s .

The oxidizer volumetric flow G given by:

$$G = \frac{\dot{m}_{oxi}}{\pi D_{int}^2} = \frac{\dot{m}_{oxi}}{A_p} \quad (3.2)$$

The value of G controls the processes of combustion port regression on the rocket. High values of G can lead to combustion processes not governed by convection but by gas dynamic, and rendering the experimental data on regression rate useless. Therefore the

maximum value of G is set to be $500 \frac{kg}{m^2s}$ (George, 2001). This value corresponds to the maximum value of G found in literature that held up the convection controlled burning. Maximum values of G always happen in the first moment of burning, thus the minimum internal combustion port diameter can be found from:

$$D_{int} = \sqrt{\frac{4\dot{m}_{oxi}}{\pi G}} = \sqrt{\frac{4\dot{m}_{oxi}}{\pi 500}} = 0.0505\sqrt{\dot{m}_{oxi}} \quad (3.3)$$

On post processing and refining of the optimization the internal diameter D_{int} will be used as a Design Variable and equation 4.3 will not be used on the Design Module.

Paraffin as a fuel is interesting due to its low toxicity and wide availability. Among the oxidizers employed on hybrid rocket propulsion Nitrous Oxide (N_2O , NOX), Hydrogen Peroxide (H_2O_2 , $[H_2O_2]>90\%$, HTP) and Liquid Oxygen ($O_{2(l)}$, LOX) are the most common and well known. The usage of paraffin with addition of Aluminum Tri-hydride shows promising results (Karabeyoglu, 2011) and was considered in the optimization, although there is no experimental regression rate data availed. Further discussion on propellants can be found in Section 4.1.2. Due to the high regression rates presented by paraffin in comparison to other fuels one combustion port configuration is possible, therefore the fuel mass flow rate is given by:

$$\dot{m}_{fuel} = \rho_{fuel} L_g \pi D_{int} \dot{r} \quad (3.4)$$

Where ρ_{fuel} is the fuel's specific mass (Section 4.1.2), L_g and D_{int} are the grain's length and diameter, respectively.

The mixture ratio or oxidizer/fuel ratio (OF) is given by the instantaneous ratio between the vaporized fuel and the injected oxidizer

$$OF = \frac{\dot{m}_{oxi}}{\dot{m}_{fuel}} \quad (3.5)$$

The mixture ratio is the most relevant parameter governing the propellant burn processes and, unlike what happens on solid motors, the pressure has little influence on the grain regression rate. In order to save computational power it was chosen not to run the chemical equilibrium software inside the Ballistic Module, instead a series of polynomial were

regressed from chemical equilibrium data. The data and the polynomials are presented on the propellant subsection of this chapter (Section 3.1.1.1).

The average chamber temperature T_c , the average molar mass of the combustion products MW and the ratio of specific heats γ are given by the regressed polynomials:

$$T_c = P_1(OF) \quad (3.6)$$

$$MW = P_2(OF) \quad (3.7)$$

$$\gamma = P_3(OF) \quad (3.8)$$

The propellant's characteristic velocity, c^* is given by the following relations:

$$c^* = \frac{\sqrt{\gamma R_g T_c / \gamma}}{\sqrt{\left[\frac{2}{\gamma+1}\right]^{\frac{\gamma+1}{\gamma-1}}}}, \quad (3.9), \quad R_g = 8314 / MW, \quad (3.10)$$

The pressure in the post-combustion chamber p_1 is given by (Sutton, 2001):

$$p_1 = (\dot{m}_{oxi} + \dot{m}_{fuel}) c^* A_t, \quad (3.11) \quad , \quad A_t = \pi R_t^2, \quad (3.12)$$

Where R_g is the specific gas constant and A_t is the nozzle's critical section area.

For purposes of proper dimensioning of the oxidizer injection system, the pressure in the pre-combustion chamber is needed (Veras, 2003):

$$p_c = \frac{p_1}{1 + 0.2 \left(\frac{A_t}{A_p}\right)^2}, \quad (3.13)$$

The nozzle exit area A_{exit} is calculated from the aero-thermal expansion of the combustion gasses. The exit pressure is fixed at 0.5, 0.1 and 0.01 atmospheres for the 1st, 2nd and 3rd stages respectively. In post processing of the optimized motor (i.e. with trajectory data) a more suitable exit pressure will be employed.

$$A_{exit} = A_t \cdot \left(\left(\frac{\gamma+1}{2} \right)^{\frac{1}{\gamma-1}} \cdot \left(\frac{p_{exit}}{p_1} \right)^{\frac{1}{\gamma}} \sqrt{\frac{\gamma+1}{(\gamma-1) \cdot \left(1 - \frac{p_{exit}}{p_1}\right)^{\frac{\gamma-1}{\gamma}}}} \right)^{-1}, \quad (3.14)$$

The expansion ratio is an important instrument for comparison with other existing motors; this parameter is calculated using the relation below:

$$\varepsilon = \frac{A_{exit}}{A_t} \quad (3.15)$$

The thrust coefficient C_F represents how efficiently the nozzle is working and takes into account the influence of the pressure drag (or thrust) caused by atmospheric pressure:

$$C_F = \sqrt{\left(2 \frac{\gamma^2}{\gamma-1} \cdot \left(\frac{2}{\gamma+1} \right)^{\frac{\gamma+1}{\gamma-1}} \left(1 - \left(\frac{p_{exit}}{(\dot{m}_{oxi} + \dot{m}_{fuel}) \frac{c^*}{A_t}} \right)^{\frac{\gamma-1}{\gamma}} \right) \right)} + \frac{p_{exit} - p_{atm}}{(\dot{m}_{oxi} + \dot{m}_{fuel}) \frac{c^*}{A_t}} \varepsilon, \quad (3.16)$$

The thrust F can then be calculated from the thrust coefficient, the chamber pressure and the throat's Area:

$$F = p_1 A_t C_f, \quad (3.17)$$

The specific impulse is the most significant performance indicator of a rocket motor. This parameter is calculated using the following relation:

$$I_s = \frac{F}{(\dot{m}_{fuel} + \dot{m}_{oxi}) g_0} = \frac{F}{(\dot{m}_{prop}) g_0} \quad (3.18)$$

Where g_0 is the average earth gravity acceleration and \dot{m}_{prop} is the propellant mass flow rate.

3.1.1 Numerical integration

The equations cited above are representative of only one instant in the burning of the fuel grain, for a complete and transient performance prediction it is needed to integrate the above represented algorithm in time through the whole consumption of the propellant grain.

Although the integration of the propellant burning is aimed to provide a time variant performance prediction the integration step was chosen not to be a time step but a fuel diameter step. It was done this way, so it would not matter the size of the grain or the average regression rate possible in any given geometry, the resolution of the internal

ballistic would be done in the same scale, considering the regression rate is not a strong function of the grain's mass.

The time differential δt is represented as a function of the diameter differential δd and the regression rate:

$$\delta t = \frac{\delta d}{\dot{r}} \cong \Delta t = \frac{\Delta d}{\dot{r}} \quad (3.19)$$

After the first run of the algorithm described above the value of the Nozzle's exit is saved and the subsequent run of the algorithm are performed without Equation 4.14. The process proceeds with subsequent runs of the algorithm with ever increasing internal diameter until the propellant grain is completely consumed.

The Mass of oxidizer utilized to burn the propellant grain is found by simple numeric integration of the oxidizer mass flow rate. A similar process can be employed in many other variables such as velocity variation and the total burn time.

$$m_{oxi} = \int_{D_{int}}^{D_{ext}} \dot{m}_{oxi} \frac{\delta d}{\dot{r}^2}, \quad (3.20)$$

3.1.2 Propellants

Several propellant pairs were considered as viable alternatives for the proposed Space Launch System. The oxidizer choices reflect the most common and affordable alternatives for hybrid rocket propulsion, namely: Liquid Oxygen, Nitrous Oxide and Hydrogen Peroxide. Paraffin was the only fuel considered, as it presents average regression rate characteristic only matched by cryogenic fuels such as solid methane (Karabeyoglu, 2004). In recent studies, the impact of paraffin doping with Aluminum Hydride (AlH_3) was proposed to generate significant specific impulse and impulse density improvements (Karabeyoglu 2011). This additive will also be considered in the analysis.

Nitrous oxide is a common medical and industrial gas, its most common application, diluted in oxygen, is as mild anesthetic. Although it is by far the most expensive oxidizer, it is still considered affordable. Nitrous oxide retail price averages around 20 dollars per kilo in Brasilia, though this value is bound to be reduced for larger acquisitions. Nitrous Oxide/paraffin possesses intermediate level of specific impulse, but it also allows for wise implementation of Blowdown injection systems due to NOX's condition of saturated

vapor at room temperature and high pressures (~5MPa). Due to the Vapor-Liquid equilibrium, the reductions in tank pressure during tank evacuation are met by vaporization of oxidizer, and the internal tank pressure can be maintained, to some extent, constant without any external pressurization subsystems. NOX/paraffin possesses a regression rate exponent very close to 0.5 and according to some author equal to 0.5 (Karabeyoglu, 2011; Bertodi, 2007). Regression rates exponents of 0.5 result in cancelation of the grain geometry change effect on the available vaporized propellant mass flow. This characteristic results on specific impulse and thrust values along the burn despite of grain internal geometry changes.

Hydrogen Peroxide is a common and low cost bleaching agent commonly used on cellulose industry. In retail prices, this oxidizer can be normally found in the 2 to 4 dollars per kilogram price tag depending on the concentration. Hydrogen Peroxide was employed as oxidizer in earlier liquid propulsion systems such as the English vehicle Black Arrow (Hill, 2006), but was abandoned in favor of other storable oxidizers such as Nitrogen Tetroxide. However recently High Test Peroxide (HTP) (H_2O_2 at concentrations above 90%) has received renewed interest due to its low toxicity, cost and reasonable performance. Those characteristics combined with the oxidizer's room temperature storage capabilities are making HTP a viable alternative for low cost rocket propulsion. Additionally, HTP/paraffin possesses one of the greatest regression rates in hybrid propulsion. Despite of hydrogen peroxide's reasonable performance, it possesses a very high regression rate exponent and due to that, this oxidizer causes severe specific impulse changes due to grain geometry shift.

Liquid Oxygen is produced by liquefaction and further fractionated distillation of atmospheric air. Liquid Oxygen is commonly used in large medical facilities due to its cheaper storage when compared to the gaseous form of the oxidizer. The average price of the oxygen cubic meter averages around 2 dollars at retail prices. Liquid Oxygen is probably the most common oxidized in space rocket propulsion (Isarowitz, 2004). LOX is usually combined with space rated kerosene (RP-1) or hydrogen. In hybrid rocket propulsion LOX has being combined with virtually every solid fuel ever tested, the most common combinations are LOX/HTPB and LOX/Paraffin. LOX/paraffin pair presents both high regression rate and high specific impulse (Karabeyoglu, 2004), though liquid

oxygen is a cryogenic liquid and needs constant cooling or venting therefore requiring more complex prelaunch operations.

Paraffin presents a very high regression rate, only rivaled by cryogenic propellants like solid methane (Karabeyoglu, 2004). This increased regression rate is theorized to be due mainly to the formation of a layer of liquid paraffin between the solid fuel grain and the flame film. The formation of ripples and waves in this layer is responsible for increased in burn surface. Also it is theorized that the liquefied paraffin layer emits droplets of liquid fuel that burn inside the main oxidizer rich stream above the flame layer. Due to its high regression rate paraffin hybrids allow for the usage of a single combustion port greatly simplifying fuel grain production and reducing unburned propellant sleeves from a typical of 5% to almost zero (Karabeyoglu, 2011).

It was recently proposed the addition of Aluminum Hydride to the paraffin to increase performance characteristics (Karabeyoglu, 2011). This additive increases the solid propellant grain density contributing to the a impulse density increase, as it increases the energetic characteristics of the fuel by adding aluminum's high energy fuel particles, and lowers the average molar mass of the combustion products by the increasing hydrogen content and finally shifts the optimum OF ratio to lower values (Figure 3.1), further improving the impulse density. An interesting fact from this additive is that it is not possible to be employed on liquid rockets due to decantation of the solid AlH_3 particles in the fuel tank. The impact of this additive on the propellant mass fraction of the rocket is yet unclear for it allocates much of the reaction mass in the combustion chamber (due to small optimum OF), which is less structurally efficient than the oxidizer tank. Although a relative smaller oxidizer tank allow for a much lighter pressurization subsystem, the heaviest individual component of the propulsion system.

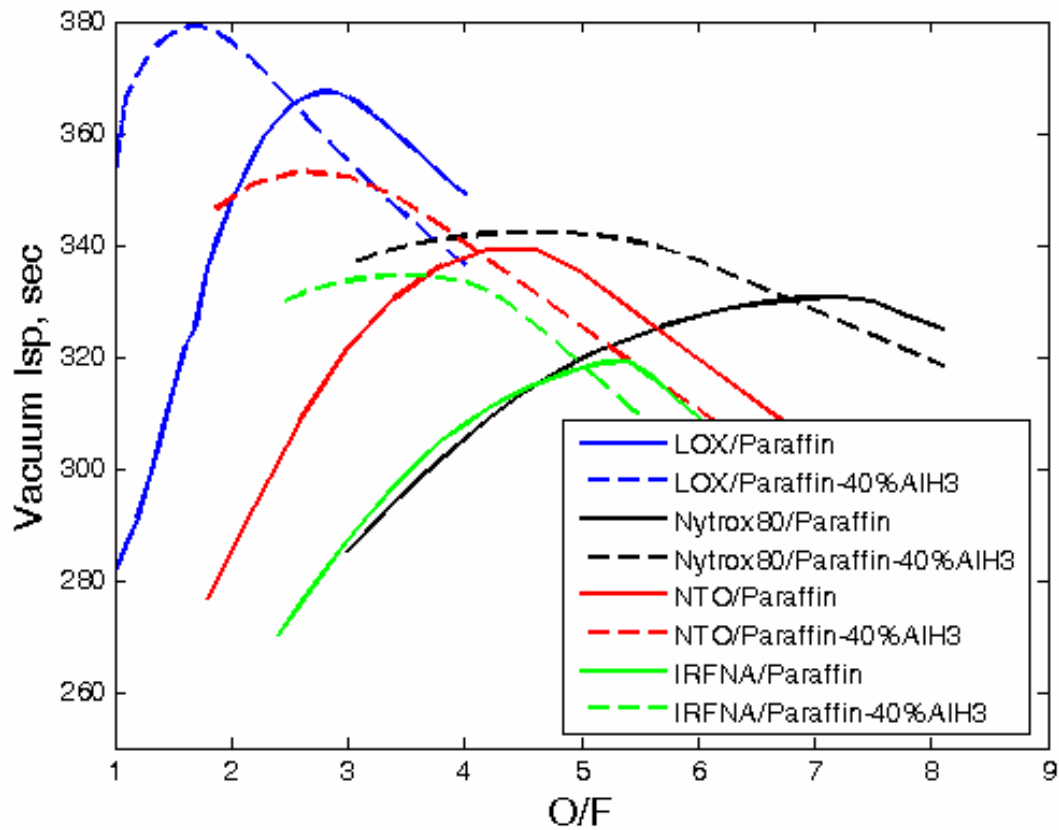


Figure 3.1: Several propellant pair and their theoretical specific impulses, (Karabeyoglu, 2011)

3.1.1.1 Propellant Regression Polynomials

As it was said in the Internal Ballistic subsection (Section 3.1), for reduced computational time, the combustion of the various propellant pairs was represented not with chemical equilibrium software but with a series of interpolated polynomials. The interpolation data was extracted from the commercial software Rocket Propulsion Analysis (Lite Edition) version 1.2.5.2 available online for free.

Three interpolated polynomials were: the combustion chamber's temperature (T_c), the average reaction product's mass (MW) and specific heats' ratio (γ). The interpolated polynomial values are presented in the table below:

Chamber Temperature ($y = a_5 * x^5 + a_4 * x^4 + a_3 * x^3 + a_2 * x^2 + a_1 * x^1 + a_0 * x^0$)						
Propellant pair	a_5	a_4	a_3	a_2	a_1	a_0
LOX/Paraffin	-61.9680	870.9486	-4540.4	10379.0	-8731.6	3531.3
NOX/Paraffin	-0.1095	4.2592	-57.8743	286.4257	59.0641	255.8041
HTP/Paraffin	-0.0239	0.8526	-7.0182	-61.5510	1027.3	-555.0811
LOX/Parafin40% AlH ₃	-28.1238	354.5791	-1.578*10 ⁻³	2694.7	-688.2527	2335.7
HTP/Paraffin40% AlH ₃	-0.0556	1.3787	-6.1727	-93.1106	884.5338	1061.2

Table 3.2: Polynomial Coefficients for Chamber Temperature behavior perturbation

MollarMass ($y = a_5 * x^5 + a_4 * x^4 + a_3 * x^3 + a_2 * x^2 + a_1 * x^1 + a_0 * x^0$)						
Propellant pair	a_5	a_4	a_3	a_2	a_1	a_0
LOX/Paraffin	-0.0437	0.7136	-4.3033	10.9892	-6.3360	13.4787
NOX/Paraffin	-4.136*10 ⁻⁴	0.0158	-0.2219	1.2714	-0.9269	15.2262
HTP/Paraffin	-9.066*10 ⁻⁵	0.0037	-0.0462	0.0602	2.5133	9.8157
LOX/Pa40% AlH ₃	-0.0345	0.3820	-1.3844	0.5830	9.1599	8.8994
HTP/Paraffin40% AlH ₃	-2.236*10 ⁻⁵	0.0062	-0.0432	-0.2130	3.7288	10.8502

Table 3.3: Polynomial Coefficients for reaction products mean molar mass behavior perturbation

Gamma ($y = a_6 * x^6 + a_5 * x^5 + a_4 * x^4 + a_3 * x^3 + a_2 * x^2 + a_1 * x^1 + a_0 * x^0$)							
Propellant pair	a_6	a_5	a_4	a_3	a_2	a_1	a_0
LOX/Paraffin	0.0023	-0.0277	0.1123	-0.1292	-0.1794	0.3714	1.1498
NOX/Paraffin	2.2684*10 ⁻⁵	-8.8857*10 ⁻⁴	0.0138	-0.1082	0.4449	-0.9337	2.0913
HTP/Paraffin	-5.651*10 ⁻⁷	3.6347*10 ⁻⁵	-9.2285*10 ⁻⁴	0.0116	-0.0712	0.1787	1.0947
LOX/Parafin40% AlH ₃	-0.0018	0.0249	-0.1238	0.2542	-0.1402	-0.1254	1.2772
HTP/Paraffin40% AlH ₃	-3.9820*10 ⁻⁶	1.4569*10 ⁻⁴	-0.0021	0.0141	-0.0430	0.0229	1.2414

Table 3.4: Polynomial Coefficients for Specific heats ratio behavior perturbation

3.2 DESIGN MODULE

In order to provide minimally decent performance estimations, a very precise mass estimation and design algorithms are needed. The equationing behind the presented algorithm was based on traditional Ukrainian design methodologies and design knowledge specific of hybrid rocket motors. The Ukrainian methodology is based both in analytical solutions for the main load bearing elements of a rocket launcher and also on semi empirical relations for usual element's mass. The bulk of the design procedures described next were extracted from *Основи Конструювання Ракет-носіїв* (Principles for the Design of Launch Vehicles) (Lynnyk, 2008).

3.2.1 Construction Material Selection

A central point in the structural designing process of a launch vehicle is the selection of structural materials, for it defines the technological paradigm to be used. At a superficial analysis, carbon based composites pose as the best materials for lightweight applications, although several other factors should be considered for a complete and responsible evaluation.

At the first glance, the problem of material selection for rocket structural design is already solved to its excellence, resulting in only three common solutions (Lynnyk, 2008): pressure stabilized vessels using steel, aluminum Isogrid structures for liquid propellant rockets and composite cocoons for solid motors. However there is currently is definitive solution for pressure feed schemes. Aluminum, steel, titanium and composites are equally employed, due mainly to the restricted application of this kind of system. For optimization both innovative solutions and more classical approaches will be evaluated.

Three common materials were considered as suitable candidates to be used on the designing of the proposed Brazilian Micro Launcher, although several others were evaluated and discarded as not suitable. The discussion of all the materials analyzed will be presented below, and then several qualitative and quantitative comparison tables will be presented.

Aluminum-Magnesium alloys are the most commonly used material for propellant tank construction in liquid propellant rockets, due mainly to their weldability, chemical compatibility with corrosive propellants such as liquid nitric acid and hydrazine, small price and general industrial familiarity. Al-Mg does not possess a remarkable specific strength nor to yield nor to rupture and does not allow for aggressive thermal treatments such as aging. The most common chemical treatment used in AL-Mg alloys are cold or hot rolling. The general low yield tensions allow for easy and cheap milling even of the cold rolled alloys making complex shapes possible and to some extent economically wise. Recently Aluminum-Lithium alloys are being used with impressive results in launch vehicle tanks. SpaceX states the Li-Al alloys used in the Falcon9 launcher have better specific strength than average carbon composites.

Duraluminums and Aeronautical Aluminums occupy almost the same design niche. They both possess considerable yield and break limits low density and allow for artificial aging. Although they are very difficult to be welded and even so they lose their thermal treatments very easily. These types of materials are best suitable for application on riveted dry compartments, machined parts such as injectors, valves and structures critical on stiffness such as stringers and frames. The cost of Duraluminums is smaller than the Aeronautical, but both can be considered not expensive materials when compared to other aerospace materials.

High Strength Steels refers to a wide range material composed of steel alloys, including stainless steels, molybdenum and niobium alloys, among others with various applications. These possess very high yield and break limits, very high density and usually their specific strength is considerably above the aluminum alloys. Usually, the specific stiffness of the steels is inferior to those of aluminum alloys, making steel less desirable for stringers and frames. The combination of very high yield strength and high density of steel alloys with the small tank pressures of liquid propellant tanks usually results in very thin tank walls. The thin walls cause severe fabrication problems and make it difficult to employ stiffeners such as isogrids. Those design inconveniences resulted on the developments of pressure stabilized tanks, in which the internal pressure is maintained above atmospheric from fabrication up to launch. This decision results in severe logistical challenges, though the reduced mass fraction pays off and this configuration is employed on the Centaur upper stage, one of the most successful American stages. Steel saw considerable application on solid rocket motors, the Brazilian VLS is an example (Isarowitz, 2004), but now composite casings are much more common among newer motors (Isarowitz, 2004). The cost of steel alloys is considerably smaller than any other types of material used in aerospace application. The utilization of steel tanks might show itself interesting in hybrid pressure feed systems due to their unusually higher tank pressures and tight cost constraints.

Recent developments on material sciences have both lowered the cost and increased the strength of several composite material, the most relevant being Carbon Fiber, Glass Fiber and Kevlar. The greatest disadvantages of composite materials are in cost and fabrication complexity. Composites materials are composed of a very resistant filament material fiber and a binder, usually polymeric resin. For their very nature composite materials severally limit the use of usual fabrication processes and also require a considerable time for the resin to cure, these result in very complex and time consuming fabrication processes. On the other hand, the low density and high resistance of carbon composites can allow for lighter and simpler launch vehicles, in the sense that a higher propellant mass fraction possible with composites allow for fewer stages. To this date composite tanks were commonly used in high pressure gas tanks and in pressure feed systems (Isarowitz, 2004), the only known pump fed system to employ such material was the DC-1 SSTO prototype. Until recently composite tanks were not considered practical for cryogenic liquids, such as liquid oxygen, although that is changing for Microcosm Ltd. (Scorpius S.L.C.,

Pressuremaxx catalog) developed and is commercializing aerospace cryogenic composite tanks. On a deeper analysis the fabrication challenges of carbon composites might become an advantage to a small launch vehicle fabrication plant, since the demand is small, unlike automotive industry, and the specific carbon winding machinery might be cheaper than a conventional fabrication plant (Figure 3.2).

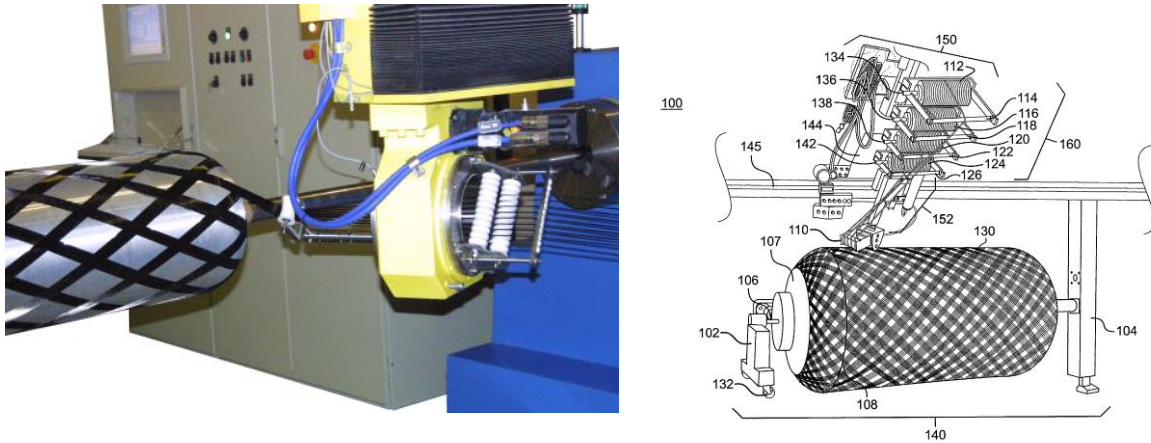


Figure 3.2: Carbon fiber winding process

3.2.2 Materials Selected for Analysis.

In order to evaluate the technological level and to provide an accurate comparison between the various materials, the author chose to perform the initial estimation and design optimization, using all the selected materials. A representative of each material design class will be selected and used in this first estimation, later in the design refinement the specific material might be changed for a similar and more adequate and better estimated configuration.

The selected materials are: AMG6M weldable AL-Mg Alloy of soviet origin used in complex shape devices, AMG6H 20% work hardened AMG6M used in tank walls and bottoms; AISI E4340 Steel, oil quenched 845°C, 425°C temper; Carbon Fiber Simulacrum that accounts for the carbon fiber liner and other necessary components of carbon fiber tanks and A543 Gr. 2 cryogenic stainless steel. Those materials try to represent high quality materials but without using unrealistically advanced and materials difficult to obtain. The characteristics of each of the materials can be seen below (Table 3.5):

Material	Specific mass	Yield Limit	Proportionality limit	Break Limit	Modulus of Elasticity	Reference
AMG6M	2640 kg/m ³	120 MPa	160 MPa	320MPa	68 GPa	Lynnyk, 2008
AMG6H (Cold Rolled)	2640 kg/m ³	200 MPa	280 MPa	380MPa	68 GPa	Lynnyk, 2008
AISI E4340 Steel	7800 kg/m ³	1475 MPa	1530 MPa	1595 MPa	205GPa	Matweb, 2013
Carbon Composite	1422.5 kg/m ³	NA	NA	679 MPa	NA	Pressuremaxx Catalog, 2013
A543 Gr. 2 (Cryosteel)	7800kg/m ³	690 MPa,	690 MPa,	931 MPa	200GPa	Key to Metals, 2013

Table 3.5: Material employed in the analysis and their characteristics

3.2.3 Wall Thickness and Material quality considerations

Due to sheet material's imperfections and form deviations, the design thickness should be smaller than the sheet's actual mean thickness. This procedure can be seen in the picture below (Figure 3.3):

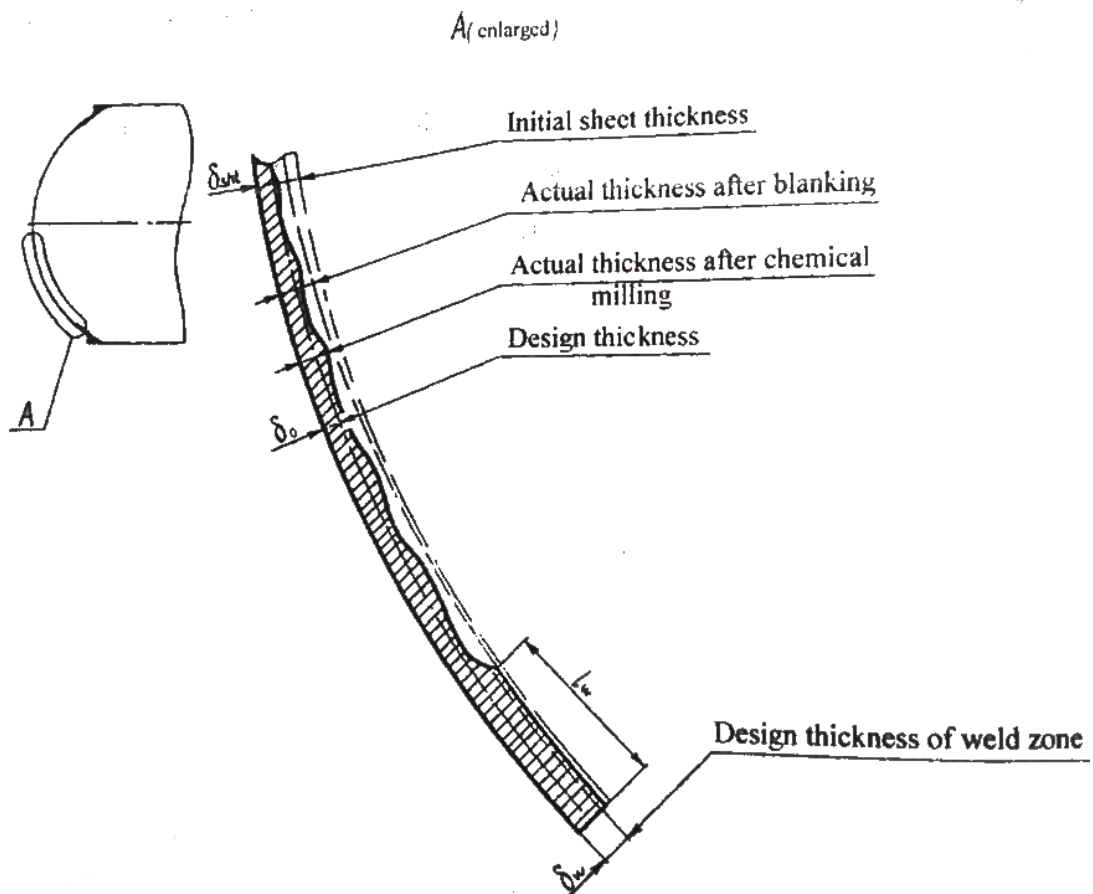


**Figure 3.3 Detail a unstiffened shell showing the most relevant design figures
(Lynnyk, 2008)**

The picture (Figure 3.3) illustrates the thickness after chemical milling, but the representation stands for the most common fabrication processes. To safely design thin metal sheet structures the effects of imperfection from the machining processes must be taken into account for they might amount for a considerable increase in the final mass of the designed part. Two divergent thickness values should be defined the design thickness and mass calculation thickness; δ_0 and δ_{mass} respectively.

The design thickness is the value resulting from the tension and factor of safety calculations and mass thickness is the sheet's average thickness used for mass calculations. Those values are related by the equation bellow:

$$\delta_{mass} = \delta_0 + \Delta_{for} + \Delta_{ch} \quad (3.21)$$

Where Δ_{for} is half the average corrugation after forging and Δ_{ch} is half the roughness after chemical milling (or other fabrication process).

Also it is useful to define the process to obtain the thickness of the raw material sheet to be used in the fabrication of the component δ_{sht} :

$$\delta_{sht} = \delta_{mass} + \Delta_{for} + \Delta_{sht} \quad (3.22)$$

Where Δ_{sht} is half of the average thickness deviation of the raw material sheet.

3.3 DESIGN MODULE; MASS MODEL

The Mass Model employed on this analysis is composed of the most important loading bearing components, heavier subsystems and includes allowances for unknown component's masses. The components included on the mass model of each of the stages are shown below, the method employed for the estimation of each one of them detailed in the next sections.

Third Stage:

- Fairing with satellite adaptor
- Guidance and control, computer and power supply
- Pressurization Subsystem
- Oxidizer tank
- Intertank Dry bay
- Combustion Chamber
- Nozzle

Second Stage:

- Interstage Dry Bay
- Pressurization Subsystem
- Oxidizer tank
- Intertank Dry bay
- Combustion Chamber
- Nozzle

First Stage:

- Interstage Dry Bay
- Pressurization Subsystem
- Oxidizer tank
- Intertank Dry bay
- Combustion Chamber
- Nozzle
- Aft Bay

3.3.1 Fairing, Satellite Adaptor and Guidance systems

There is no current standard Satellite adaptor for a launch vehicle in the class proposed on this study, although there are several adaptors currently used in piggyback schemes for satellites in the mass range of the Proposed Brazilian Micro Launcher, for example the launch service broker Space Flight Services Ltda. employs an 8 inch diameter payload adaptor for a 70kg satellite.

An estimation of the fairing's shell mass is a very straight forward procedure, although inside the fairing there are several other components and subsystems that amount for much of the assembly's total mass. For a correct estimation of the total mass a CAD model of the fairing was made including the most important components (Figure 3.4).

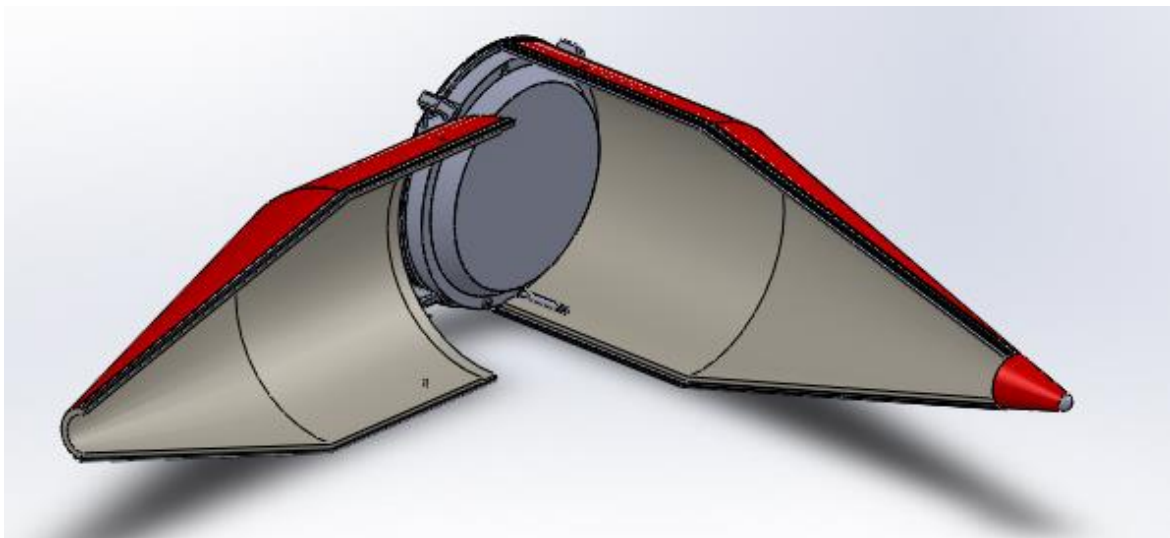


Figure 3.4: 3D CAD model of the launcher's fairing

The mass of a generic 0.57m diameter Fairing's complete assembly was then obtained using a CAD tool (12.5kg). The mass of a generic similar fairing was argued to be proportional to the third power of the rocket's diameter.

$$m_{Fairing} = 12.5 \frac{D_{r3}^3}{0.57^3}$$
$$m_{Fairing} = 67.49 * D_{r3}^3 \quad (3.23)$$

Where D_{r3} is the third stage's diameter.

The mass of the guidance and control system is the largest point of uncertainty on the mass model. The mass of the electronic and measurement equipment is not scalable and it is normally not a problem on large launchers, though it can be a major problem in such a small vehicle like the Brazilian Micro Launcher. No data concerning this kind of system's mass was found and no accurate guess was possible. A mass of 15 kg was then attributed to the Avionic systems.

3.3.2 Pressurization Subsystem

On a hybrid propellant rocket the pressurization subsystems is responsible injecting liquid oxidizer into the combustion chamber. Three different types of systems were considered and included in the calculation; pressure fed, simplified blowdown and turbopump.

3.3.2.1 Pressure Fed

The methodology for the pressure fed follows from the methodology presented by Sutton on *Rocket Propulsion Elements* (2001). The total mass and volume of the pressurization gas can be calculated by the following relation:

$$M_g = p_p \frac{V_{toxi} 1.05}{R_g * T_{inj1}} \left(\frac{y_g}{1 - \frac{p_g}{p_o}} \right) \quad (3.24)$$

$$V_g = R M_{gas} \frac{T_O}{p_o} \quad (3.25)$$

Where M_g is the pressurization gas's mass, p_g is the pressure remaining in the pressurization gas tank a after evacuation of the oxidizer, p_p is the pressure to be maintained in the oxidizer tank, p_o is the initial pressure inside the pressurizing tank, V_{toxi} is the volume of the oxidizer tank a 5% extra volume was added for safety (Sutton 2001),

V_g is the pressurization gas's volume at storage condition, T_{inj} is the temperature in which the pressurization gas is injected in the combustion oxidizer tank, T_o is the gas's storage temperature, γ_g and R_g are the specific heat ratio and the specific gas constant, respectively, for the pressurization gas.

It was proposed that the pressurization gas could be injected in the combustion chamber after the depletion of the liquid oxidizer (Karabeyoglu, 2011), for that reason the chosen pressurizing gas was oxygen. As a conservative measure the reaction mass correspondent to the pressurization gas was not included on the Δv calculations

It is common on large liquid rocket propulsion systems for the pressurization gas's tanks to be located inside a cryogenic propellant tank. This procedure reduced the gas's volume and therefore the gas's tank mass ($T_o \cong 90K$). If cryogenic storage is employed the pressurization gas must be expanded prior to injection, it can be attained by exchanging heat between the gas and the hot combustion chamber walls. This procedure will lower the required pressurization gas's mass (Equation 4.24) not only on cryogenic storage. Also the pressurization system can be composed of a reactive system such as thermocatalytic decomposition of Hydrogen Peroxide instead of inert gas injection. This system reduces mass, the specific mass of liquid peroxide is much higher than that of gas and through increased injection temperature, the thermo decomposition of HTP generate $T_{inj} \cong 700K$ depending on the concentration. Although this scheme introduces unwanted complexity.

The first optimization approach will employ a simple system using oxygen stored at room temperature, cryogenic storage, heating of the gas or thermocatalytic pressurization will be analyzed on project detailing phases.

3.3.2.2 Blowdown

A blowdown system could theoretically be applied to every oxidizer, although it would result in a loss combustion chamber pressure along the burn. Nitrous Oxide is at room temperature a saturated vapor and can be stored at high pressures, with a vapor and liquid phases, this equilibrium allows for self-pressurization. In a self-pressurizing environment, such as in a N₂O tank, whenever the pressure in the vapor phase drops due to evaluation of liquid oxidizer a portion of oxidizer evaporates raising the pressure to the vapor pressure for the current temperature of the tank. A complete blowdown repressurization

model that correctly represents the shifting equilibrium inside the Nitrous oxide would be ideal, although none of the options available in literature could be implemented inside the optimization environment (Whitmore, 2010). Alternatively a simplified methodology was implemented to represent the Blowdowns peculiarities. Three changes were introduced to represent a Blowdown system:

1: Raise the ullage volume to 40% of the tank's volume. According to Sutton (2001), conventional blowdown systems (no self-pressurization) have an ullage volume of up to 40% of the total tank volume.

2: Reduce the average specific impulse by 10%. According to Sutton (2010) blowdown systems suffer of about 10% loss of specific impulse due to pressure loss,

3: Zero the mass of pressurization tank and pressurization gas.

3.3.2.3 Turbopump fed

Turbopump fed systems absolutely dominate liquid rocket propulsion and equip a least one stage of every single majority liquid propulsion launcher in operation today (Isarowitz, 2004). In spite of its relative mechanical complexity, turbopump fed engines have been used since the Vergeltungswaffe 2 (V-2 missile) entered in operation in 1944, although Oiknine (2006) has argued that hybrid rockets will only attain commercial success if the current launch costs remain high for hybrid pose as low cost alternative. It can be inferred from that turbopump systems may not be suited for usage in hybrid propellant rockets, since the added complexity would outweigh the great cost and simplicity advantages of hybrid rockets. Besides the complexity issues, there are some operational issues in using turbopump on hybrid rocket, the majority of the liquid propellant rockets employ the gas generator or staged combustion cycles, in which hot gas is generated by the combustion of the propellants is used to drive the turbine (Figure 3.6). On hybrid rockets the implementation of a Gas Generator or a Staged Combustion would demand a dedicated liquid propellant supply unnecessarily increasing the complexity of the motor.

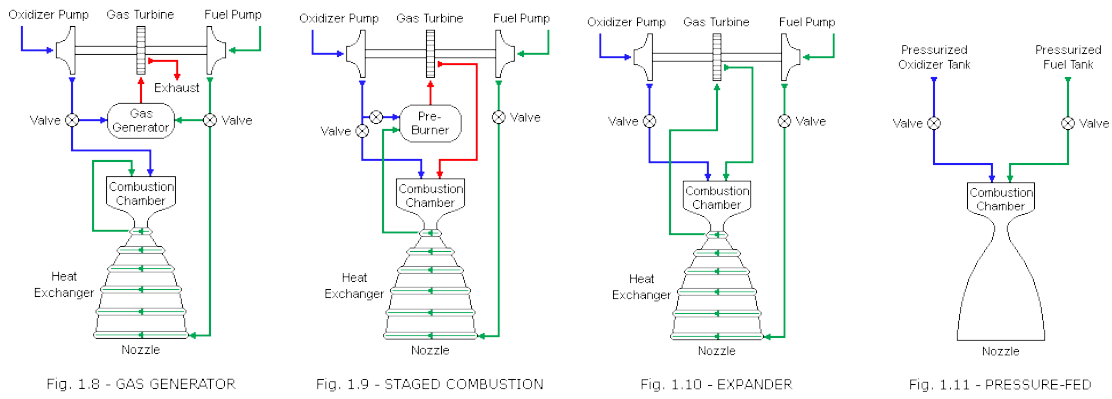


Figure 3.6: The most common engine cycles in liquid rocket propulsion.

The expander cycle might be an interesting alternative for it does not need any type of pre burner or gas generator, only a cooling jacket where the fuel is heated then expanded to drive the turbine. A problem with using the expander cycle in hybrid rockets is that there is only liquid oxidizer available to be used in cooling and protecting the cooling jacket, and the turbine from chemical oxidation by the heated oxidizer vapor might be challenging.

As a variation from the Gas Generator cycle a monopropellant can be used instead of burning a propellant pair to generate hot gas. High Test Peroxide has been widely used as monopropellant on several aerospace thrusters and can easily be fitted to operate on a gas generator. Another alternative to be considered is the usage of a solid propellant gas generator. Solid propellant gas generators have been used as auxiliary gas generators during start-up of some Soviet liquid engines and can theoretically be adapted for full burn time operation.

In the more common gas generator cycles, some of the propellant, 5% (Sutton, 2001), is expanded at the gas generator's low pressure nozzle reducing the average specific impulse. This behavior can be represented in the context of this Design Module as follows:

$$F' = 0.95(\dot{m}_f + \dot{m}_o)I_s g_0 + 0.05(\dot{m}_f + \dot{m}_o)g_0 I_{s\,gg}, \quad (3.26)$$

$$I'_s = \frac{F'}{(\dot{m}_f + \dot{m}_o)g_0}, \quad (3.27)$$

Where F' and I'_s are the modified thrust and specific impulses and $I_{s\,gg}$ is the gas generator's specific impulse, 136s for a peroxide monopropellant.

It is also very important to consider the turbopump in the mass model. The turbopump, and other plumbing systems, are of difficult estimation, a procedure similar to the one employed for the fairing estimation was also used here. It is argued that the mass of a turbopump is proportional to the propellant mass flow rate, for similar propellants and chamber pressures. Only one turbopump assembly mass was found for comparison, the Merlin 1C's turbopump weighting 150 pounds (~75kg) (SpaceX, 2003) (Figure 3.7).



Figure 3.7: Merlin 1C turbopump, (copyright: SpaceX)

A Mass extrapolation was made to predict the mass of a hypothetical oxidizer turbopump for this hybrid rocket. It is assumed that the weight of a turbopump is linearly proportional to the propellant mass flow rate dispensed by the pumps and the mass flow rate is also proportional of the thrust (Equation 3.18). Additionally, in hybrid rockets only the oxidizer flows through the pumps. These assumptions are summarized by the equation below:

$$M_{tp} = \left(F \frac{M_{tp\ Merlin}}{F_{Merlin}} \right) * \frac{OF}{OF+1} * 1.1 * 1.5; \quad (3.28)$$

Where M_{tp} indicates mass of the turbopump, F indicates thrust and OF the mixture ratio for the hybrid rocket in question. The subscription “Merlin” indicates data relative to the Merlin engine. The merlin turbopump is one of the lightest in the market, so a 10% mass

increase was added for safety, another 50% mass increase was added to account for the pre-burners and plumbing masses.

3.3.3 PROPELLANT TANKS, UNSTIFFENED SHELLS

A considerable fraction of the structural mass and nearly all the volume of a typical liquid propellant rocket are composed by its propellant tanks. Similarly in a solid propellant motor, the major structural component is a solid propellant casing, which is structurally similar to a propellant tank.

There are two main forces acting on propellant tank during its operation; overload (Linear and transversal) and internal pressure. These forces can be seen in the diagram below (Figure 3.8):

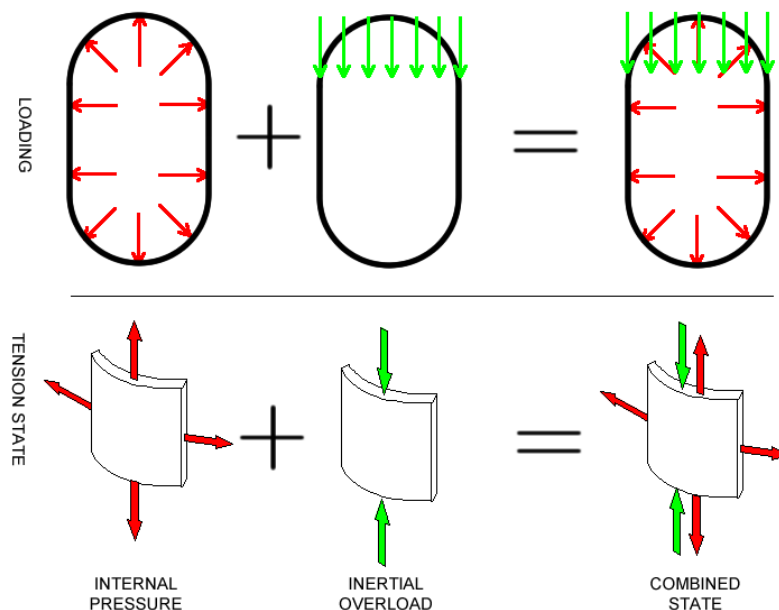


Figure 3.8: Combine Stress State in a pressurized vessel with axial overload.

As it can be seen from the above illustration (Figure 3.8) that the axial overload acts against and reduces the effect of the internal pressure.

The process to design a propellant tank, or pressures vessel, consists in analyzing two different design cases and evaluating which the defining processes is controlling the specific propellant tank being designed:

1. The pressure vessel's loading is dominated by internal pressure and the longitudinal acceleration has a secondary roll, only lowering the stress.
2. The longitudinal (or transversal) acceleration is the main loading and the tank walls are subjected to buckling.

The required wall thickness to withstand internal pressure can be calculated by the evaluation of both the longitudinal σ_{long} and circumferential σ_{θ} tensions caused in thin wall pressure vessels. The equation can be seen below:

$$\sigma_{\theta} = \frac{p_{max} r}{\delta_{wall}}, \sigma_{long} = \frac{p_{max} r}{2 \delta_{wall}} \quad (3.29)$$

Where p_{max} is the pressure vessel's maximum internal pressure during operation, r is the vessel's radius and δ_{wall} the wall thickness. The circumferential tension has the same value of the longitudinal on spherical shells (spherical vessels and cylindrical tank bottoms) and consequently the thickness is half of that on cylindrical sections with the same radius and pressure loading.

The mass of a cylindrical pressure vessel with hemispherical ends (bottoms) is given by the equation below:

$$m_t = 2\pi r^2(r + W)p_{max} \frac{\rho_t}{\sigma_b} = 4\pi r(r + W)\delta_{wall}\rho_t, \quad (3.30)$$

$$\delta_{wall} = \frac{p_{max} r}{2 \sigma_{long}}, \quad (3.31)$$

Where W is the length of the cylindrical section of the vessel (the overall length being $W + 2r$), ρ_t is the density of the material used in the vessel construction and σ_b is the ultimate strength (break limit). It is considered appropriated to use ultimate strength instead of the yield strength for geometric deformation is an accepted tradeoff for a lighter pressure vessel (Lynnyk, 2008); this rule only applies to metallic pressure vessels. Similarly the mass of a spherical pressure vessel can be obtained from the same equation (Equation 3.30) making $W = 0$. As it can be seen from Equation 3.30 the construction material selection for pressure vessels should be guided by specific ultimate yield strength (ρ/σ_b), thus making carbon composites and high strength steels the ideal materials for this application.

Although it can be observed that the vast majority of liquid rocket propellant tanks employ aluminum alloys (similar to AGM6H) tanks instead of steel or carbon composite (Isaowitz, 2004). Aluminum tanks are used due to the comparatively low tank pressure of pump fed propellant tanks (usually 0.5MPa while pressure fed system use 5MPa), the lower pressure and high specific strength of steel and carbon composite would result in much thinner tank walls that cause considerable fabrication and logistical problems that outweigh the structural mass fraction improvement. The only exception are the Centaur stages that employ pressure stabilized tanks, where the internal pressure counter balance the transportation stresses and the longitudinal and transversal overloads during flight, allowing for very thin steel walls. Although this design requires the pressure vessel to remain pressurized from fabrication to launch which generate a considerable logistic inconvenient.

The second design case corresponds to the wall thickness required to withstand the longitudinal overloads caused by the rocket's acceleration, the transversal overload cause by the aerodynamic stresses and during transport to the launch facility. The longitudinal overload is the most severe of those loadings and it is the most difficult to be avoided by smart design. In terms of system mass the highest the acceleration the smallest the gravitational losses (this will be explained in further sections) and ultimately infinity acceleration would result in the smallest possible gravitational loss (Hoffman Transfer). Although high accelerations cause significant structural problems, mainly in the delicate electronics contained in the payload. The payload's resistance to longitudinal acceleration cannot be controlled since it is provided by a third part company. Therefore it is usual for launch vehicle to assume a maximum longitudinal acceleration of 6 in their design and the payload providers usually guarantee at least this level of acceleration tolerance (Isarowitz, 2004).

The most common effect caused on tank wall by overload is localized buckling of the tank walls; failure over normal compression is a much secondary effect due to the slenderness of the wall. The wall thickness of an unstiffened tank (thin wall pressure vessel) to withstand buckling caused longitudinal acceleration is given by:

$$\delta'_0 = \sqrt{\frac{T_e - \pi r^2 P_{min}}{2\pi k E}}, \quad (3.32)$$

Where P_{min} is the minimum internal pressure during operation, E is the material's modulus of elasticity, k is a factor of stability and is related to the tank's connections to other parts of the rocket ($k = 0.2 \dots 0.4$). T_e is the combined equivalent axial compression force (Section 3.5).

In the case that $\delta'_0 \leq \delta_0$, the tanks loading is controlled by pressure and the thin wall pressure vessel is the lightest, cheaper and simplest alternative. On the more common case among liquid propellant rockets, the opposite is true and the loading is dominated by longitudinal acceleration. In this case the thin walled pressure vessel is not the wisest alternative and a more complex design should be considered.

3.3.4 PROPELLANT TANKS, STIFFENED SHELLS

The common tank design to withstand majorly longitudinal forces is stiffened or reinforces thin wall pressure vessels. The most common stiffener designs are the isogrid; isogrids consist in milled protrusions in the form of square or triangular honeycombs (Figure 3.9).

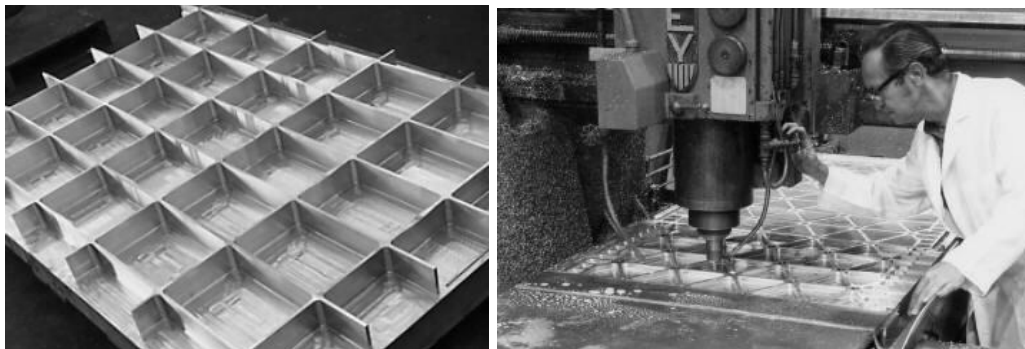


Figure 3.9: left, square isogrid; right, isogrid fabrication through mechanical milling

In a square isogrid pressure vessel, the longitudinal stiffeners withstand the longitudinal compression while the circumferential one works limiting the longitudinal slenderness, the internal pressure is withheld by the tank wall segment between the stiffeners.

The proper design of an isogrid shell can be found in Lynnyk (2008, pp. 39-42). Although the same source provides an approximation for preliminary estimation of the of an isogrid wall's mass:

$$\delta_e = A \sqrt{\frac{T_e}{2\pi k E (\varphi + B)}}, \quad (3.33)$$

A and B are numerical factors derived from the fabrication process, their appropriate values are shown below:

- Chemically milled shells: A=1.78, B=0.2
- Mechanically milled shells: A=1.48, B=-0.25

φ is the ratio of stiffener effectiveness and can be approximated, in preliminary calculations by $\varphi = (0.6 \dots 0.8)$. δ_e is the equivalent thickness of an isogrid shell and can be used for mass calculations with Equation (3.30) in the place of δ_{wall} .

As aforementioned, many of the described tanks are welded structures that often employ some sort of heat treatment to improve material's quality. The process of welding usually destroys the heat treatment resulting on a lower material resistance, the alternative to deal with such inconvenience is increasing the thickness of the shell near the welded areas, and this can be seen in the picture below:

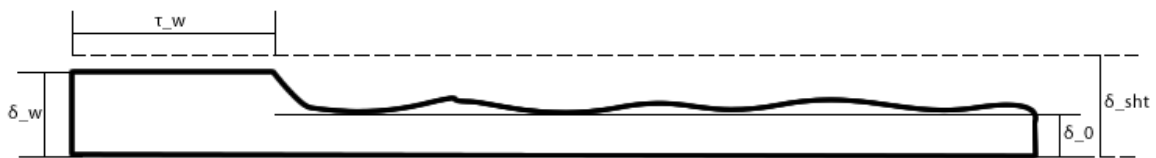


Figure 3.10: cross section of an unstiffened shell with exaggerated roughness

The larger thickness δ_w to withstand the loss of thermal treatment can be found by the equation below:

$$\delta_w = \delta_0 \frac{\sigma_{0t}}{\sigma_0} 1.1, (4.34)$$

The sigma σ_{0t} and σ_0 are the design tensions for the heat treated material and the the untreated material, respectively. A 10% increase on the σ_w is introduced to account for the tension concentrator on the seam. The length of the thickness increase is approximated by the empirical relation: $\tau_w = (3 \dots 7) \sigma_w$

3.3.5 DRY BAYS AND COMPARTMENTS

The term dry bay generally describes compartments that are not propellant storage tanks. Dry bays work much the same as propellant tank in the regards of structural calculations, with the exception that they usually are not pressurized. Dry bay can be either unstiffened shells or isogrid and are subjected to much the same loadings.

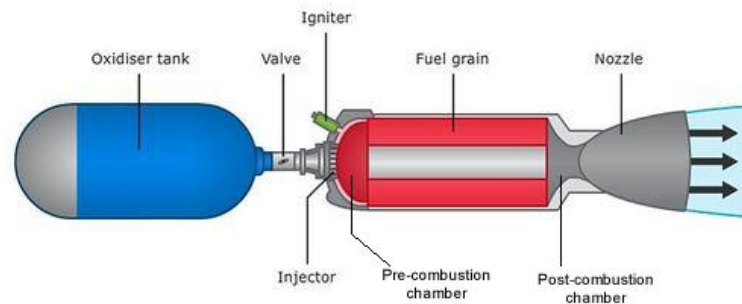
Dry bays have several different usages inside a launch vehicle, the most relevant being:

- Command & Control bay: where the Avionics are located. Usually located in the third stage.
- Inter-tank bay: located between two propellant tanks or a propellant tank and the combustion chamber (on hybrids), it contains propellant distribution manifolds injectors (on hybrids) and other propellant related apparatus.
- Propulsion bay: where the liquid propellant engines are located, it dubs are Aft bay in the first stages.
- Inter-stage bay: usually connected to a propulsion bay, which disconnects during staging, contains the staging subsystem - hydraulic or mechanical pushers, explosive bolts, and others.
- Aft Bay: special propulsion bay in the first stage, it is used to hold the launcher in place during pre-launch operations and in some systems (Falcons 1 and 9) to hold the launcher during engine startup.
- Fairing: the launcher's fairing is a dry bay located in one of the upper stages that houses and protects the payload from aerodynamic loading and is responsible for much of the launcher's aerodynamic behavior.

Besides the main loading bearing shells, similar to tanks, dry bays usually have other devices such as manholes, inspection windows equipment shelves and the motor mountings. Those devices require considerable designing efforts and cannot be approximated easily; a 10% increase on the rocket's total mass was added in the ballistic code to cope with those minor details.

3.3.6 COMBUSTION CHAMBER

The combustion chamber of a hybrid rocket is very different from a liquid propellant combustion chamber and is more similar to a solid propellant motor fitted with an injector plate at the upper end. Normally hybrid rockets need a pre-combustion chamber and a post-combustion chamber for effective reaction efficiency (Karabeyoglu, 2011). Figure 3.11, below, represents the basic configuration of a hybrid rocket's combustion chamber and tank:



© Copyright. 2011. University of Waikato. All Rights Reserved.

Figure 3.11: Simplified diagram of a hybrid rocket motor.

A pre-combustion chamber is where the injected propellant film breaks up and the oxidizer atomization occurs. It can possibly be very small on peroxide rockets, where a catalytic bed is employed, although a volume will always be needed before the fuel grain, usually the pre-combustion chamber does not need to have thermal protection for the constant evaporation of oxidizer cools the chamber walls.

The post combustion chamber is where a considerable part of the ablated fuel reacts with the oxidizer. The post combustion chamber needs to be either cooled or thermally protected to withstand the hot gas coming from the propellant grain.

Both the pre and post combustion chamber cannot be properly designed without either extensive testing or CFD codes, although a good estimation for them is to be shaped as hemispheres with the same diameter of the combustion chamber itself. This procedure was employed in the optimization coding.

In order to account for the thermal protection employed in the combustion chamber, a layer of 5mm of HTPB thermoplastic was added in the inside of the chamber. This thermal protection is super-estimated for both the pre combustion chamber and the cylindrical section where the propellant grain is located do not need protection; this measure was adopted as a safety margin of the chamber's design. The equation below shows the mass estimation for the combustion chamber:

$$m_c = 2\pi \left(\frac{D_{cc}}{2}\right) \left(\frac{D_{cc}}{2} + L_{cc}\right) p_c \frac{\rho_{cc}}{\sigma_{cc}} + 2\pi \left(\frac{D_{cc}-\delta_{tp}}{2}\right)^2 \left(\frac{D_{r1}-\delta_{tp}}{2} + L_{g1}\right) \delta_{tp} \rho_{tp}, \quad (4.35)$$

Where D_{cc} and L_{cc} are the diameter and length of the cylindrical section of the chamber, respectively, p_c is combustion chamber pressure, ρ_{cc} and σ_{cc} are the specific mass and ultimate strength of the combustion chamber's material. δ_{tp} and ρ_{tp} are the thickness (5mm) and specific mass (1400kg/m^3) of the thermal insulation

3.3.7 CIRCUNFERENCIAL FRAMES

In order to reduce the length of a pressure vessel the diameter of the spherical section can be increased; and if it is done so, the use of reinforcement circumferential frames becomes necessary.

In a vessel with hemispherical ends, the longitudinal stresses of the cylindrical section possesses the same direction and magnitude of the ones from the spherical bottom. In a bottom with larger diameter a resulting force is generated. This effect can be seen in the figure below:

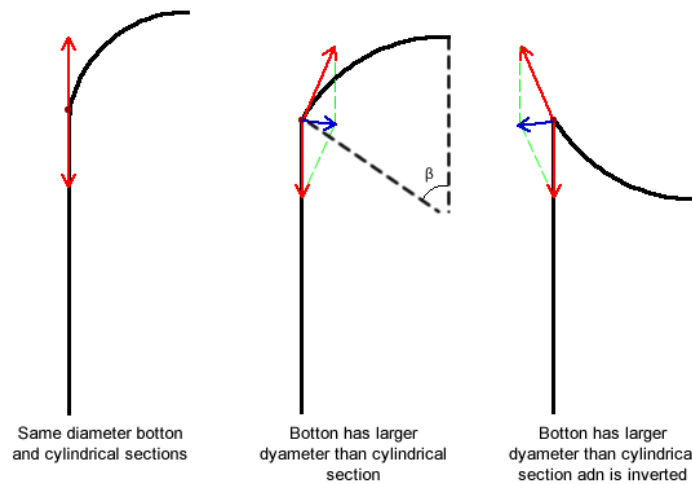


Figure 3.12: Internal tension distribution between cylindrical and spherical sections

In the figure above (Figure 3.12), it can be seen that the normal bottom with larger diameter imposes a compression tension over the tank's reinforcement ring which may cause it to buckle. The figure also shows the alternative of using an inverted bottom, which creates a reinforcement ring under traction which might be lighter and simpler than the conventional one under compression. The inverted bottom reduces the tanks internal volume and normally is avoided safe for cases when the inverted bottom also dubs as the

bottom of an upper tank. A simplified estimation of the frame's required cross-section are can be seen below:

$$A_{fr} = \frac{p_{max} r^2}{2[\sigma] \tan(\beta)}, \quad (4.36)$$

Where $[\sigma]$ is either equal to the yield limit $[\sigma] = \sigma_y$ in case of compression of the frame or equal to the break limit $[\sigma] = \sigma_b$ in the traction case, r is the tank's radius. The angle β can be seen in the figure above (Figure 3.12). The frame can then be modeled as a thin ring and its mass is given by the following equation:

$$m_{fr} = 2\pi r A_{fr} \rho_t, \quad (4.37)$$

The mass of a tank with bottoms of different diameters is a modified version of the equation presented earlier for the cylindrical tanks with hemispherical ends (Equation 4.30):

$$m_t = 2\pi r W \delta_{wall} + 2\pi R (R - \sqrt{R^2 - r^2}) \delta_{bottom} \rho_t + m_{fr}, \quad R = \frac{r}{\tan(\beta)}, \quad (4.38)$$

$$\delta_{bottom} = \frac{p_{max} R}{\sigma_\theta}, \quad (4.39)$$

Where δ_{bottom} is the thickness, and R is the radius of the spherical end caps.

In order to evaluate the impact of the β angle in the tank's the mass a comparative study was made to find the most appropriate angle for a compromise between length reduction and mass reduction. The results are present in graphic for below (Figure 3.13):

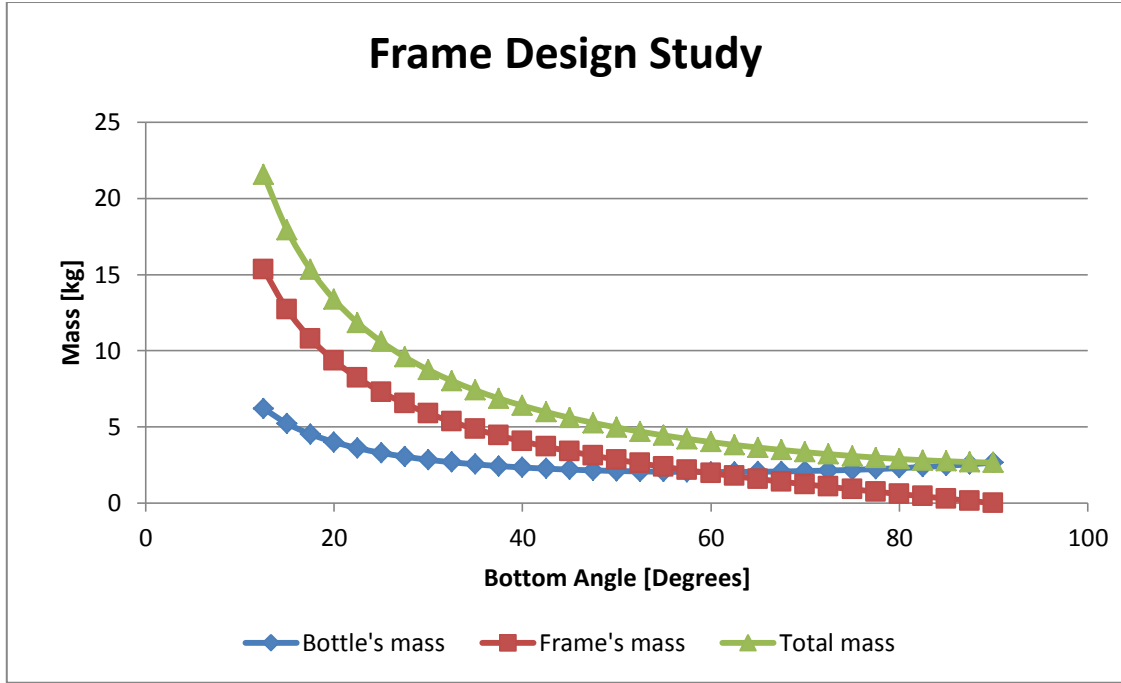


Figure 3.13: Design study of the frame's mass

The Frame design study showed the lowest possible mass was found when $\beta = 90$, the equivalent to a tank with simple hemispherical caps of the same diameter as the tank itself.

The first study did not contemplate the benefic impact of the overall length reduction on the rocket. This impact is difficult to be measured for it depends on the rocket as a whole; the impact of tank length reduction is insignificant in a short rocket or in a long rocket where the aspect ratio is high, although it could be very important on a long rocket with an average aspect ratio. On the other hand any dry mass reduction always has a drastic impact in the rocket's performance.

The chosen way to select a preliminary value for β employed the classic optimization technique of weighted sum of the objectives: length, $L_b(\beta)$, and mass, $m_t(\beta)$. The sum objective N consisted in the combination of the non-dimensional length and mass:

$$N = \frac{m_t(\beta)}{m_t(45^\circ)} + \frac{L_b(\beta)}{L_b(45^\circ)}, \quad (3.40)$$

$$L_b(\beta) = \left(\frac{r}{\tan(\beta)} - \sqrt{\frac{r^2}{\tan^2(\beta)} - r^2} \right), \quad (3.41)$$

The results of the weighted sum showed the existence of a minimum at $\beta = 45, N = 1$, the results are presented below:

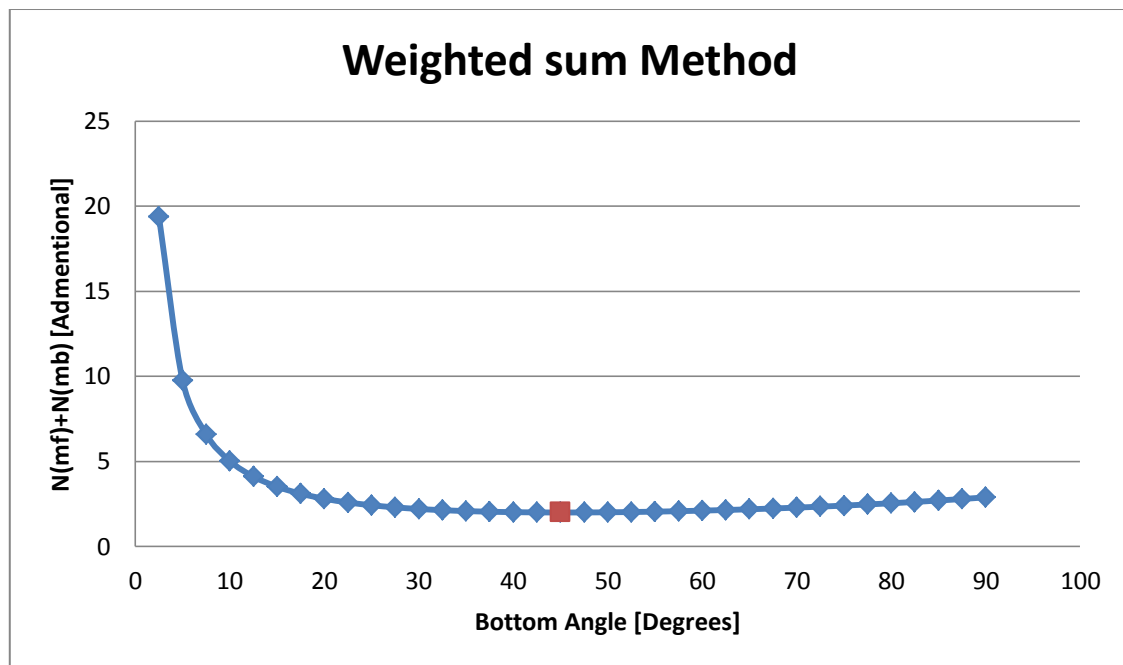


Figure 3.14: Design study, weighted sum of the normalized frame’s mass and length

Considering both studies, the compromise solution was chosen, the pressure fed optimization cases will employ tanks with $\beta = 90$ and lowest possible mass and the pump fed optimization cases will employ the compromise solution of $\beta = 45$. This decision was made because relative mass increase by a smaller β on the pressure fed systems would be much greater because of their higher internal pressures.

3.3.8 NOZZLE

The rocket’s nozzle is one of its most important components for it is there where the expansion processes occur and thrust is generated. Only supersonic convergent–divergent nozzles are used in rockets. Supersonic nozzles have first a convergent section where the combustion products are expanded and accelerated up until the speed of sound, after the combustion products have reached sonic speeds they enter in a divergent section where the transversal section increases and the gasses are accelerated up until they reach the end of the nozzle. There are two main types of nozzles: conic and bell shaped

Conic nozzles consist of a conic divergent with usually a 15 degree half angle (Sutton, 2001). A conic nozzle is usually simpler, although heavier and generates greater losses from spreading of the propellant stream.

Bell shaped nozzles start with a high half angle ($\sim 50^\circ$) and then this angle is reduced to about 5° . This procedure results in a shorter nozzle and smaller losses due to spreading of

the propellant stream, although they generate losses due to expansion waves, absent on conic nozzles. The inconveniences of bell nozzles are mainly regarding fabrication of its complex shape. Currently almost all commercial rocket systems employ bell shaped nozzles and conical nozzles are restricted only to very small military systems.

For the optimization program, it was chosen to employ a conic nozzle for ease of coding and to better account for the losses. The nozzle mass model consists on a conic trunk with base and top diameters equal to the exit and throat diameters calculated on the Ballistic Module (Equation 4.14). The nozzle's convergent section was already accounted for in the post combustion chamber. A 5mm thick ablative thermal insulation, similar to the one in the combustion chamber, was also added.

$$l_{tb} = \frac{(R_{exit}-R_t)}{\tan(15^\circ)}, \quad (3.42)$$

$$m_{tb} = \left(\pi R_{exit}^2 + \pi R_{exit} \sqrt{L_{tb}^2 + R_{exit}^2} \right) (\delta_{cc} \rho_{cc} + \delta_{tp} \rho_{tp}), \quad (3.43)$$

Where m_{tb} is the nozzle's mass and l_{tb} is the nozzles length.

3.4 COMPLETE MASS OF THE STAGES

The equations presented above describe each of the relevant components of a hybrid rocket's stage, in this section the components of each stage's mass are combined.

3.4.1 Dry Bays

The dry bays on the hybrid rocket being simulated are: one aft bay, for connection with the launch pad in the first stage; three inter-tank bay, where the oxidizer manifolds are located; and two inter-stage bays, where the stage disconnection mechanisms are located for the second and third stages. In the context of the optimization algorithm, each of the dry bays may have conic shape. The length and diameter of each of the dry bays is given in Table 3.6 below:

Dry bay	Length	Lower diameter	Upper diameter
Aft bay (1st stage): 1.1	L_{tb1}	D_{cc1}	D_{cc1}
Inter-tank bay (1st stage): 1.2	$\frac{D_{cc1}}{2} + \frac{D_{r1}}{2} + 0.1m$	D_{cc1}	D_{r1}
Inter-stage (1st stage): 1.3	$\frac{D_{cc2}}{2} + \frac{D_{r1}}{2} + L_{tb2} + 0.1m$	D_{r1}	D_{cc2}
Inter-tank bay (2nd stage): 2.1	$\frac{D_{cc2}}{2} + \frac{D_{r2}}{2} + 0.1m$	D_{cc2}	D_{r2}

Inter-stage (2nd stage) 2.2	$\frac{D_{cc3}}{2} + \frac{D_{r2}}{2} + L_{tb3} + 0.1m$	D_{r2}	D_{cc3}
Inter-tank bay (3rd stage) 3.1	$\frac{D_{cc3}}{2} + \frac{D_{r3}}{2} + 0.1m$	D_{cc3}	D_{r3}
Payload Fairing	1.5m	D_{r3}	D_{r3}

Table 3.6: Length and diameter of the dry bay as a function of a common variable.

The subscripts 1, 2 and 3 refer to the first second and third stages respectively. A 0.1m tolerance was included in each of the dry bays. The fairing will always have 1.5m length despite of the rest of the rocket.

4.4.2 Propellant loading

The propellant loading on the rocket needs to be somewhat above the values calculated on the Ballistic module. The estimates made here reflect the highest recommended values and only extensive testing on hybrids can provide better estimates.

Tolerance	Value	Explanation
Ignition	$m_{prop} * 0.05$	5% of the propellant might be lost in the ignition transient
Unusable propellant	$m_{prop} * 0.03$	3% of the propellant cannot be used due to inefficiencies in the drainage of the oxidizer tanks and/or are left in the propellant manifolds
Spare propellant	$m_{prop} * 0.05$	5% extra propellant for correction maneuver and other unforeseen events

Table 3.7: Conservative propellant addition.

3.4.4 Oxidizer tank

The oxidizer tanks in the equation presented for the calculation of the tank's mass requires the length of the tank to be provided. The diameter of the oxidizer tanks is given by the Design Variable D_{r1} . An extra 20% ullage volume was included (except on blowdown cases where 40% is used) to account for changes in specific mass of the oxidizer.

$$V_{toxi} = \frac{m_{oxi}}{\rho_{oxi}} 1.2, (3.44)$$

$$L_t = \frac{4(V_{toxi} - 2*V_{Botton})}{\pi * D_{r1}^2}, (3.45)$$

Where ρ_{oxi} is the oxidizer's specific mass, V_{Boton} is the volume of the oxidizer tank's bottom. The material for the oxidizer tanks is carbon composite, to the exception of pump fed systems that consider aluminum and Cryogenic Steel as low cost alternatives. The factor of safety for the carbon composite equal 1, for the data regarding the material was

extracted from a commercial carbon tank and the factor of safety is already contained in the ultimate strength value. For Aluminum and Steel the factor of safety equals 1.2. The same factor of safety is also used in the combustion chamber, frames and dry bays.

3.4.5 Combustion chamber and Nozzle

The combustion chamber's diameter equals the design variable D_{ext} for each of the stages. The Length of the cylindrical section of the combustion chamber equals the length of the propellant grain, which is the Design Variable L_g . The nozzle's throat diameter is the Design Variable r_t and the exit diameter is an output from the Ballistic Module, r_{tb} .

3.4.6 Pressurization system

In each of the pressure fed cases, the system's gas is oxygen which gives the smallest overall system mass and the possibility of gas phase combustion. Moreover, the mass of the pressurization sub system is calculated considering the tank to be a sphere, in post processing this will be changed into more convenient shapes. One of the considered arrangements is a series of cylindrical pressure vessels arranged around the combustion chamber. Another arrangement would be locating the pressurization gas tanks inside the oxidizer tank (in the cases using LOX only), so the cryogenic temperatures would reduce the gas volume and the mass of the tanks. Although if this configuration would be chosen, provisions for heating the gas before injection in the oxidizer tank are required. The mass of a spherical pressure vessel to contain the pressuring gas is presented below:

$$m_{tg} = \frac{3}{2} p_0 V_g \frac{\rho}{\sigma}, \quad (3.45)$$

Where m_{tg} is the pressurization gas's tank mass.

For the pump fed systems, the reaction mass for driving the turbopump and the vessel to contain it are included in the mass of the pump and in the specific impulse reduction (section 3.3.2.3).

3.4.7 Combined mass estimate for the stages.

The mass of each of the components presented in the earlier sections are combined to provide the stage's dry mass. The propellant tolerances and the pressurization gas are considered dry mass, since they do not participate on propulsion. An extra 12% of

structural mass tolerance was added to account for design errors and connections between the components. The mass equation of each of the stages is presented below:

$$m_{dry1} = (m_{c1} + m_{t1} + m_{db11} + m_{db12} + m_{db13} + m_{gas1} + m_{tg1})1.2 + 1.3 m_{prop}, \quad (4.46)$$

$$m_{dry2} = (m_{c2} + m_{t2} + m_{db21} + m_{db22} + m_{gas2} + m_{tg2})1.2 + 1.3 m_{prop}, \quad (4.47)$$

$$m_{dry3} = (m_{c3} + m_{t3} + m_{db13} + m_{Fairing} + m_{gas3} + m_{tg3} + 15)1.2 + 1.3 m_{prop}, \quad (4.48)$$

Where m_{dry1} , m_{dry2} and m_{dry3} are the dry masses of each of the stages. m_{dbxx} corresponds to the dry bay's mass, the two number code is presented in Table 3.6 above. The 15 kilogram addition on 3rd stage's mass represent the unsalable computer guidance system.

For optimization proposes the launcher's gross mass (m_t) and its aspect ratio (LoD) are calculated. These calculations are not done inside any of the modules but in Simulation Code environment:

$$LoD = \frac{L_{g1}+L_{g2}+L_{g3}+L_{tb1}+L_{tb2}+L_{tb3}+D_{r3}+L_{t1}+L_{t2}+L_{t3}+D_{ext1}+D_{r1}+D_{ext2}+D_{ext2}+D_{ext3}+1.5}{D_{r1}}, \quad (4.49)$$

$$m_t = m_{dry1} + m_{dry2} + m_{dry3} + m_{prop1} + m_{prop2} + m_{prop3}, \quad (4.50)$$

3.5 ROCKET FLIGHT LOADINGS

In order to properly dimension the structural components of the rocket it is necessary to correctly estimate the loading to which the vehicle is subjected during flight and transport. The most important loading the launch vehicle is subjected during flight are caused by: dynamic pressure and thrust. Those forces can be seen in the figure 3.15 below:

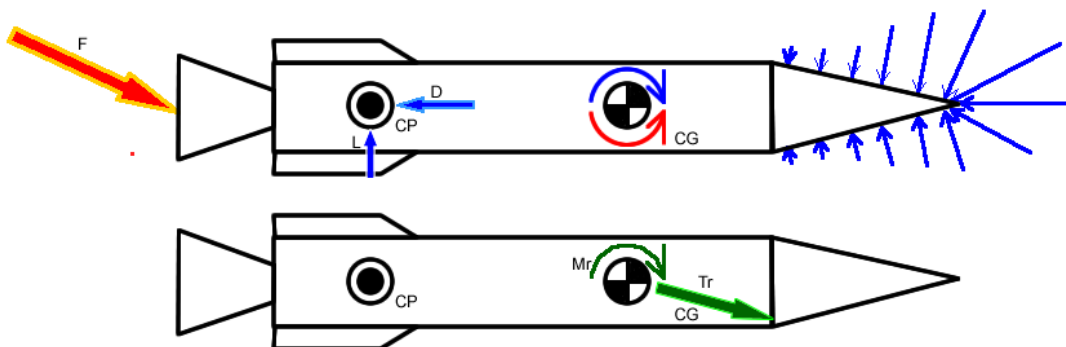


Figure 3.15: Free body diagram of a rocket in flight, resulting Forces and Moments

As it can be seen from the figure above, the rocket in flight is not in equilibrium and a resulting force is present. The resulting force causes the vehicle to accelerate causing inertial effects (force) to act, by the D'Alembert principle the structure of the vehicle is subjected to a field force proportional to the linear and angular accelerations:

$$\Sigma \bar{T} = \bar{T}_r = m\bar{a}, (3.51)$$

$$\Sigma \bar{M} = \bar{M}_r = I\bar{\alpha}, (3.52)$$

Where \bar{T}_r and \bar{M}_r are the resulting force and moment, $\bar{\alpha}$ and \bar{a} are the resulting angular and linear accelerations and I is the angular moment of inertia in the direction of the resulting moment.

As it was said before, tanks are a major constituent of a rocket's structural mass. Tanks are majorly subject to: inertial compression from the upper parts of the vehicle, localized forces (thrust), pressure and the weight of the propellant inside, see below (Figure 3.16):

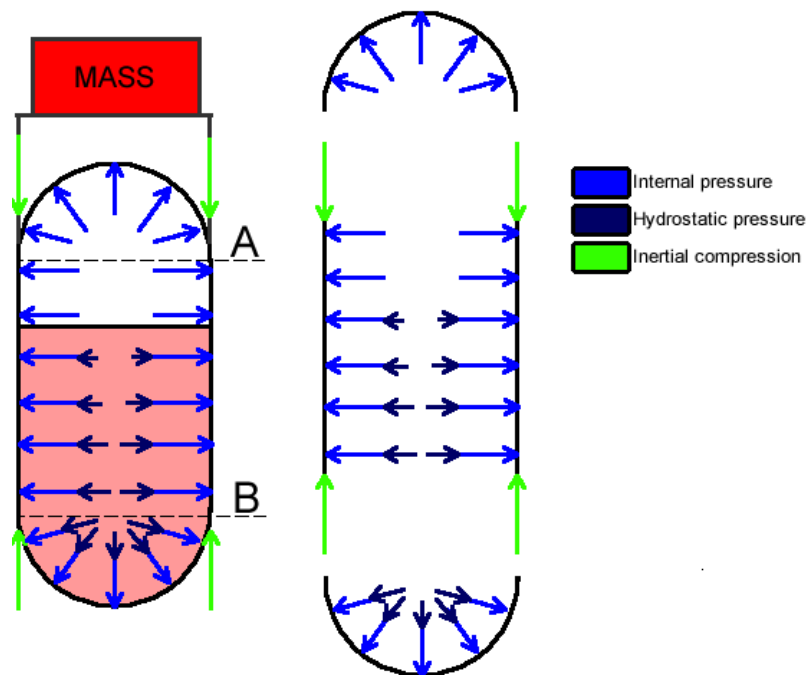


Figure 3.16: Loading on a typical propellant tank

It can be seen from the image above the upper bottom of a typical propellant tank is subjected only to the tanks internal pressure. The lower bottom is subjected to internal

pressure and to hydrostatic pressure caused by the liquid propellant; hydrostatic pressure could be a major concern especially in large rockets. In typical designs the cylindrical section of the tank also dubs as a monocoque fuselage and is subjected to internal pressure, hydrostatic pressure and inertial compression.

The internal pressure p_t and the hydrostatic p_h pressures are easily calculated resulting on the pressure vessels design pressure p_{max} :

$$p_{max} = p_t + p_h = (p_c + 0.5 \text{ MPa}) + \rho_o \bar{a} h , (3.53)$$

Where ρ_o is the oxidizer's specific mass, and h in height of the fluid column above the considered transversal section. The tank pressure is 0.5MPa greater than the chamber pressure to account for pressure loss on the injector (Karabeyoglu, 2011).

For the inertial calculations, the resulting moments M_r and resulting force T_r are combined into an equivalent compressive force:

$$T_e = T_r + \frac{2M_r}{r} , T_r = \bar{a} \sum m_{abv} , M_r = \bar{a} \sum I_{abv} , (3.54)$$

Where T_r and M_r are the resulting force and moment on the given section of the rocket, m_{abv} and I_{abv} are the masses and moments of inertia of the components above the considered transversal section.

The loading in a hybrid propellant combustion chamber is similar to the one in a solid propellant motor. The thrust is caused by an asymmetrical pressure distribution in the combustion chamber. This can be seen in the Figure 3.17 below:

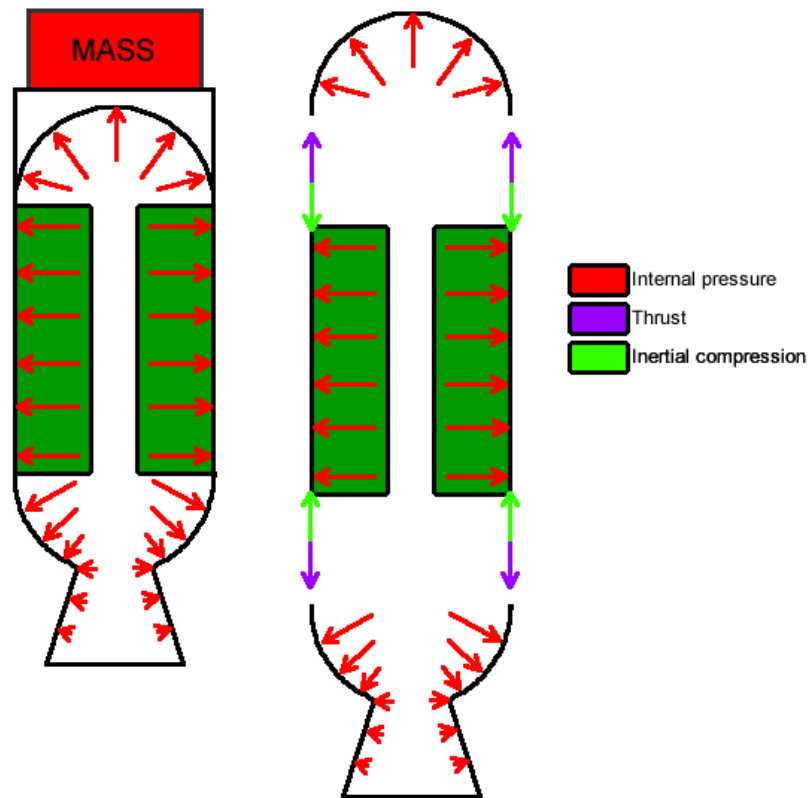


Figure 3.17: Loading on a hybrid combustion chamber or a solid propellant motor

As aforementioned, the loading and design of a dry compartment is very similar to the one of a tank. In a usual design, the inertial forces are transferred from the wall of a lower tank directly to the dry bay above without compressing the tank bottom, as it is represented by the image (Figure 3.18) below:

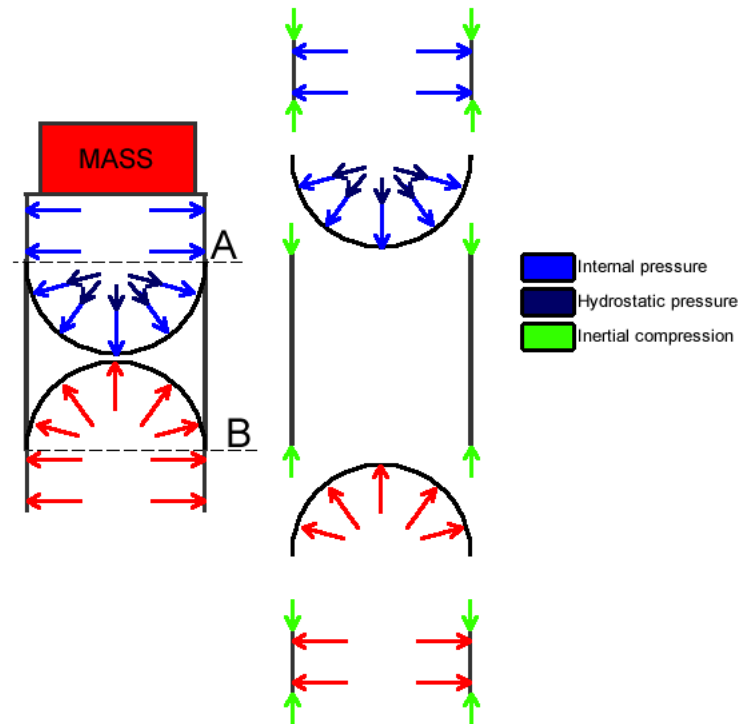


Figure 3.18: Loading on a typical dry bay

The internal transversal force in a typical hybrid rocket can have both negative and positive values; positive meaning traction (in propellant tanks) and negative meaning compression (in dry compartments). A typical internal force distribution in a pressure fed hybrid can be seen below (Figure 3.19); the pressure effects have been understated and the inertial effects exaggerated.

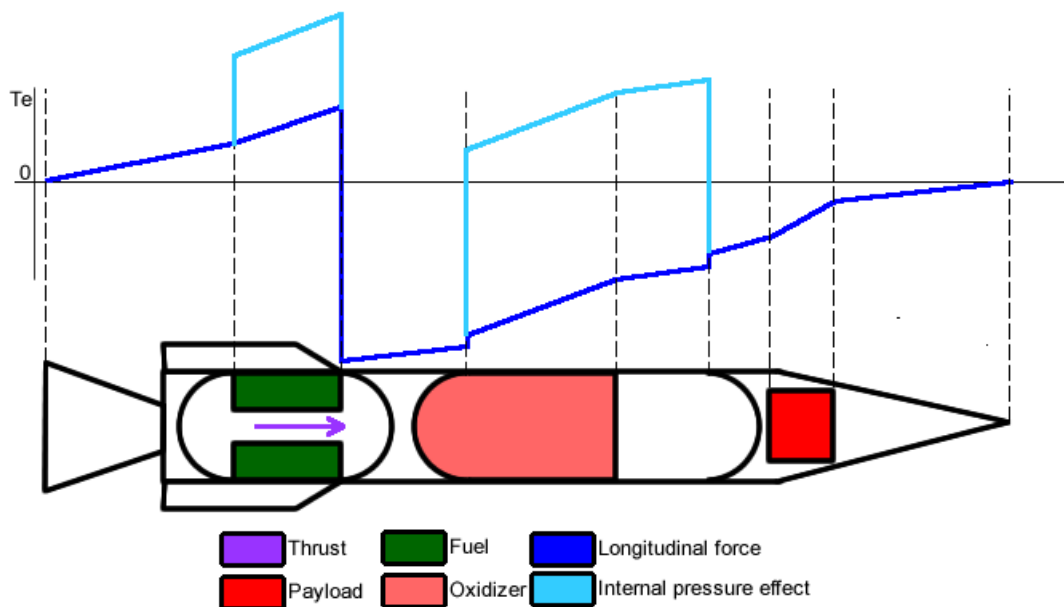


Figure 3.19: Longitudinal force along the fuselage of a typical hybrid rocket

3.6 VELOCITY MODULE

The velocity module aims to provide a coherent prediction of the aerodynamic and gravitational losses during flight, not simulated the flight trajectory *per si*. The equations employed on this module derive from the ones used in the commercial program DBallistic develop by the University of Dnepropetrovsk's team (DBallistic Manual, 2003).

The algorithm utilizes a fixed trajectory with shifting pitch angles, following a previously determined profile for a typical 3 stage launch vehicle (DBallistic Manual, 2003).

$$\vartheta_{np}(t) = \begin{cases} \vartheta_0, 0 \leq t < t_1 \\ \vartheta_0 - 2(\vartheta_0 - \vartheta_{k1})\frac{t-t_1}{t_2-t_1} + (\vartheta_0 - \vartheta_{k1})\frac{(t-t_1)^2}{(t_2-t_1)^2}, t_1 \leq t < t_3 \\ \vartheta_{k1}, t_2 \leq t < t_3 \\ \vartheta_{k1} - (\vartheta_{k1} - \vartheta_{k2})\frac{t-t_3}{t_4-t_3}, t_3 \leq t < t_4 \\ \vartheta_{k2}, t_4 \leq t < t_5 \\ \vartheta_{k3} - (\vartheta_{k2} - \vartheta_{k3})\frac{t-t_5}{t_6-t_5}, t_5 \leq t < t_6 \\ \vartheta_{k3}, t_6 \leq t < t_7 \end{cases}, (4.55)$$

Where $\vartheta_{np}(t)$ is the pitch angle for any given t moment of the trajectory, ϑ_0 is the initial launch pitch angle; ϑ_{k1} , ϑ_{k2} and ϑ_{k3} are the final pitch angle after the burning of the first second and third stages, respectively. The angles employed can be seen in below (Table 3.9). $t_1 \dots t_7$ and are relevant moments in the flight of a three stage vehicle.

The second degree approximation of pitch angle behavior on the first stage tries to represent smoother maneuvers required in the denser layers of the atmosphere. The second and third stages fly in less dense environments, thus making it possible more abrupt maneuvers. The equation system above is plotted for a generic case in the figure below (Figure 3.20):

Angle
Launch angle, $\vartheta_0 = 90^\circ$
First stage burnout, $\vartheta_{k1} = 23.39^\circ$
Second Stage burnout, $\vartheta_{k2} = 17.44$
Thrid stage burnout, $\vartheta_{k3} = 0$

Table 3.8: Pitch angles used in the flight calculations

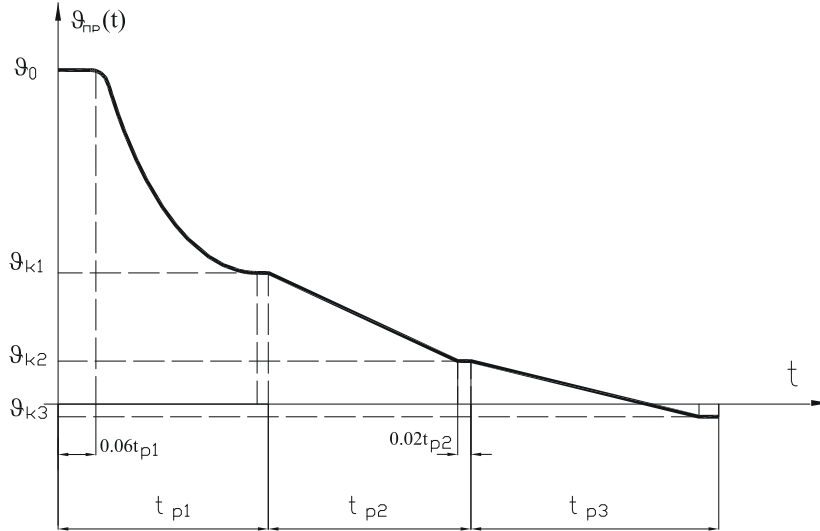


Figure 3.20: Pitch angle profile for 3 a generic stage launch vehicle (DBallistic Manual, 2003)

The moments $t_1, t_2, t_3, t_4, t_5, t_6$ and t_7 are explained and related to t_{p1}, t_{p2} and t_{p3} , the burning time of the 3 stages of the rocket. See table below (Table 3.9):

Moment	Relation	Meaning
t_1	$t_1 = 0.06t_{p1}$	Period of vertical flight to overcome the dense layer of the atmosphere
t_2	$t_2 = t_1 + 0.92t_{p1}$	Main flight of the first stage
t_3	$t_3 = t_2 + 0.02t_{p1}$	Staging and pitch angle correction maneuvers
t_4	$t_4 = t_3 + 0.98t_{p2}$	Main flight of the second stage
t_5	$t_5 = t_4 + 0.02t_{p2}$	Staging and pitch angle correction maneuvers
t_6	$t_6 = t_5 + 0.98t_{p3}$	Main flight of the second stage
t_7	$t_7 = t_6 + 0.02t_{p3}$	Satellite alignment maneuver

Table 3.9: Relevant moments in the launcher's flight

The flight environment predictions were also extracted from DBallist manual (2003). The most important parameters to be predicted are: temperature $T_{atm}(H)$, specific mass of the air $\rho_{atm}(H)$, local atmospheric pressure $p_{atm}(H)$ and local sound speed $a_{atm}(H)$. The height dependent equations for those parameters are shown below:

$$T_{atm} = 300 - 0.0065H, \quad (3.56)$$

$$\rho_{atm}(H) = \begin{cases} \rho_0 \left(1 - \frac{H}{44350}\right)^{4.25}, & 0 \leq H < 11000m \\ 0.298 \exp\left(\frac{11000-H}{6400}\right), & 11000 \leq H < 100000m \\ 0, & H > 100000m \end{cases}, \quad (3.57)$$

$$p_{atm}(H) = \begin{cases} p_0 \left(1 - \frac{H}{44350}\right)^{5.25}, & 0 \leq H < 11000m \\ 0.224 \exp\left(\frac{11000-H}{6400}\right), & 11000 \leq H < 100000m \\ 0, & H > 100000m \end{cases} \quad (3.58)$$

$$a_{atm}(H) = \begin{cases} 340.3 - 0.00411H, & 0 \leq H < 11000m \\ 295, & 11000 \leq H < 20000m \\ 295 + 0.0011(H - 20000), & 20000 \leq H < 51400m \\ 330 - 0.018(H - 51400), & 51400 \leq H < 100000m \end{cases} \quad (3.59)$$

Where H is the current altitude of the launcher, and ρ_0 and p_0 are the specific mass and pressure of the air at sea level, respectively.

The velocity and the height can be found by the integration of the launcher's acceleration. The algorithm is presented below:

$$m_l(t) = m_0 - \dot{m}_{prop}t, \quad \dot{m}_{prop} = \frac{F}{I_s g_0}, \quad (3.60)$$

$$D = \frac{1}{2} \rho_{atm}(H) |v|^2 C_D A_{aero}, \quad (3.61)$$

$$G = g_0 \left(\frac{6371000}{H+6371000}\right)^2 m_l(t), \quad (3.62)$$

$$\bar{a}(t) = \frac{F(\cos(\vartheta_{np}(t))) - D(\cos(\vartheta_{np}(t)))}{m_l(t)} \hat{i} + \frac{(F(\sin(\vartheta_{np}(t))) - D(\sin(\vartheta_{np}(t)))) - G}{m_l(t)} \hat{j}, \quad (3.63)$$

$$\bar{v}(t) = \int \bar{a}(t) dt, \quad \bar{s}(t) = \iint \bar{a}(t) dt, \quad (3.64)$$

$$H(t) = \bar{s} \hat{i}, \quad (3.65)$$

Where D and G are the drag and weight forces, C_D is the drag coefficient of the rocket (shown below), $v_l(t)$ is the instantaneous velocity of the launcher, $m_l(t)$ is the launcher current mass and A_{aero} ($A_{aero} = \pi D_r^2$) is the aerodynamic reference area.

$$C_D = \begin{cases} 0.2 + 0.2M, & M \leq 0.85 \\ M - 0.51, & 0.85 < M \leq 1.2 \\ 0.3 + \frac{1}{2M}, & M > 1.2 \end{cases}$$

While the above described code can in theory estimate the flight trajectory accurately, it was not done so. Although the changes needed to execute that estimation can be easily implemented by a reasonable programmer.

The aerodynamic velocity loss A_{loss} is given by the integration of the drag force:

$$A_{Loss} = \int_0^{t_7} \frac{D}{m_l(t)} dt; \quad (3.66)$$

The gravitational velocity loss G_{loss} is given by the integration of the weight force:

$$G_{loss} = \int_0^{t_7} \frac{G}{m_l(t)} dt, \quad (3.67)$$

The final velocity of the rocket can then be calculated by a modified version of the Tsiolkovsky rocket equation:

$$\Delta v = \sum_{x=1}^3 \ln \left(\frac{m_{0x}}{m_{0x} - M_{propx}} \right) I_{sx} g_0 - A_{loss} - G_{loss}, \quad (3.68)$$

3.7 INTEGRATED LAUNCHER SIMULATION CODE

This section describes the information flow inside the simulation code and how the three modules interact during the simulation of each individual. The Ballistic and Design modules are run three times, one for each stage and the Velocity module is run only once. The simulation code outputs not only the required objectives and constraints variables but also other interesting variables, useful for analysis. The image below shows the interaction workings of the simulation code (Figure 3.21):

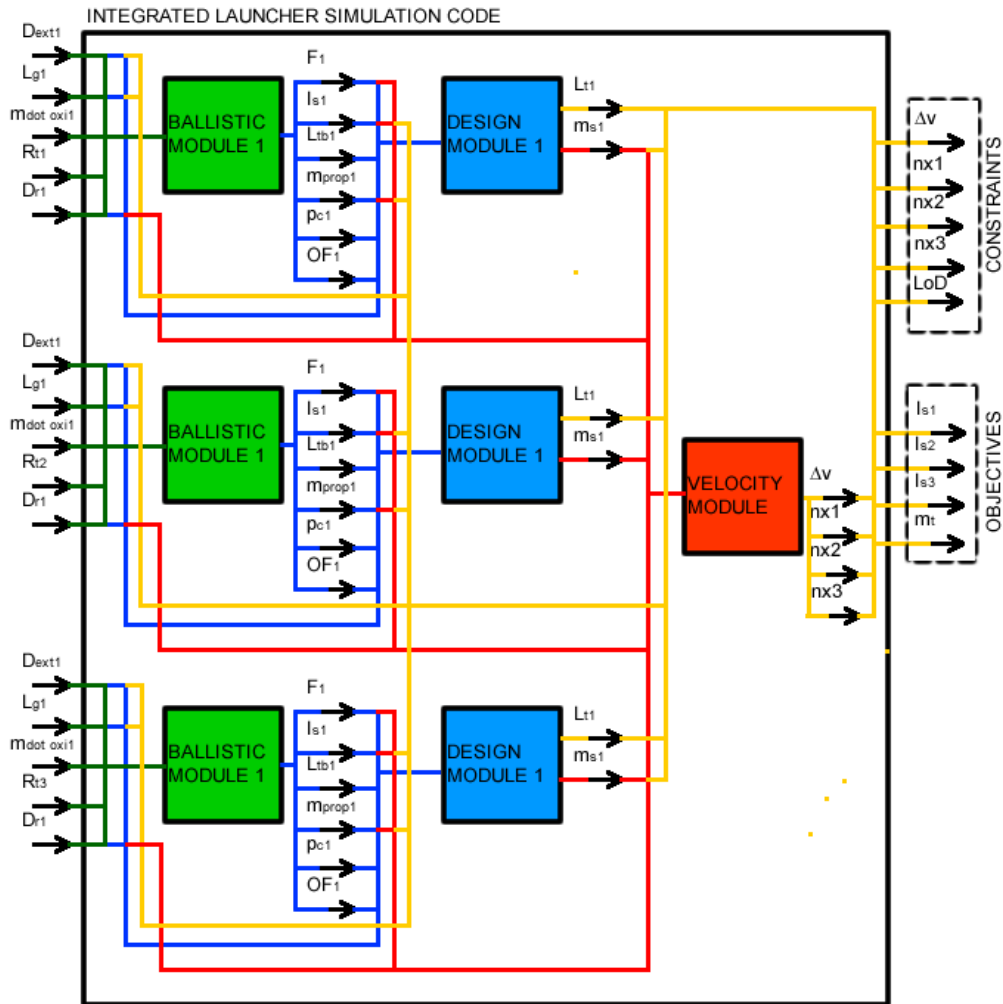


Figure 3.21: Internal data flow in the on the Simulation Code

3.8 SETTING OF OPTIMIZATION ALGORITHM.

In order to probe and explore the problem's design space a progressive methodology was employed, under this methodology several preliminary optimizations were run and their results served as the basis for the formulation of the subsequent optimization runs. Although with the exception of the preliminary setting of the design space, the resulting individuals from previous runs were never used in subsequent runs, only design insights acquired from the previous were used.

3.8.1 Setting the Design Space.

The considerable large number of initial variables (12) and the relatively narrow set of feasible combinations resulting in working individuals required an accurate setting of the design space in order to allow for a proper optimization algorithm.

The process employed to the initial setting of the design variables range (design space) consisted of the initial sizing of the launcher, from that it was possible to establish the ranges of each of the design variable.

For the initial sizing a mass fraction optimization code was employed. This code consisted in a δv loss estimation and a structural mass fraction estimator based on historic data for solid rocket motors. This data, though not precise, gave an initial idea of the needed sizes of the launcher. Subsequently each of the stages was optimized using a simplified version of the Ballistic Model, similar to the one employed in the SARA deboost motor's case study (Kaled Da Cás, 2012). This preliminary optimization yielded data concerning structural mass fraction of hybrid propellant rockets, which was then substituted in the simplified mass fraction optimization code, generating more accurate results. Those new results were then taken as basis (central value) for the setting of the Design Space:

	Upper limit	Central	Lower Limit	Step	Base
Tank Diameter D_{r1}	1	0.85	0.7	0.033	10
External Diameter D_{ext1}	1.175	0.8	0.425	0.01	76
Grain Length L_{g1}	4.4	3.2	2	0.016	151
Oxidizer Mass Flow Rate \dot{m}_{oxi1}	54.5	30.25	6	0.538	91
Nozzle Radius R_{t1}	0.19	0.105	0.19	0.0024	71

Table 3.10: Design Space for the first Stage variables (Case1)

	Upper limit	Central	Lower Limit	Step	Base
Tank Diameter D_{r2}	0.6	0.75	0.9	0.033	10
External Diameter D_{ext2}	0.925	0.55	0.175	0.01	76
Grain Length L_{g2}	3.1	1.9	0.7	0.016	151
Oxidizer Mass Flow Rate \dot{m}_{oxi2}	25	15.5	6	0.21	91
Nozzle Radius R_{t2}	0.1	0.06	0.02	0.0011	71

Table 3.11: Design Space for the second Stage variables (Case1)

	Upper limit	Central	Lower Limit	Step	Base
Tank Diameter D_{r3}	0.2	0.4	0.6	0.044	10
External Diameter D_{ext3}	0.775	0.4	0.250	0.01	76
Grain Length L_{g3}	2.7	1.5	0.3	0.016	151
Oxidizer Mass Flow Rate \dot{m}_{oxi3}	19.5	10.0	0.5	0.2	76
Nozzle Radius R_{t3}	0.09	0.05	0.01	0.0011	71

Table 3.12: Design Space for the third Stage variables (Case1)

Some of the design cases explored required new variable ranges to be employed, especially those employing oxidizers different than liquid oxygen. The technique to

provide those new ranges will be explained on Case 2 (Section 4.2.2). The variable range shown above was used on the design cases where liquid oxygen was employed, Case 1, Case 4 Case 5 and Case7.

3.8.2 Design of Experiments

The requirement of diverse and representative initial populations for the genetic algorithm was met through a combination of two different sampling methods: reduced factorial and pseudo random individual generation. For the later implementation of gradient search method a Monte Carlo distribution was implemented around the chosen best individual generated by the genetic search.

3.8.2.1 Full Factorial and Reduced Factorial

Full Factorial is a classical Design of Experiment (DOE) strategy for studying interactions between variables. The Full Factorial (FF) algorithm generates every possible combination of a defined number of points in the variable's domain. A common Full Factorial has for example the input variables set at 2-levels each (lower bound and upper bound). A design with all possible lower and upper combinations of all the input variables is called a "full factorial design in two levels".

The number of experiments N generated by a Full Factorial is given by the product:

$$N = \prod_{i=1}^k n_i, (4.69)$$

Where n_i is the number of levels and k the number of variables.

The disadvantage of this method is the large number of experiments generated in the case of a large number of variables. A full factorial is practical when less than five or six input variables are being analyzed, with more than that, testing all combinations becomes time consuming.

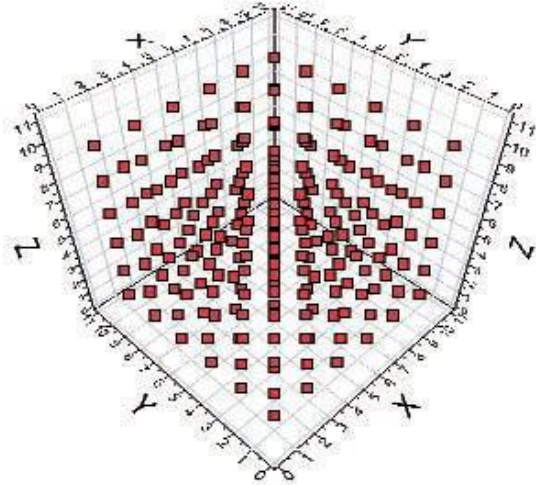


Figure 3.22: Full factorial representation, 3 variables and 6 levels, 216 designs

The Reduced Factorial (RF) is a two level full factorial aimed to reduce the amount of Designs; this approach assumes the system to be controlled by low order interactions and excludes designs resulting from high order interactions of the variables. Furthermore, even though the RF method is a two level factorial, the individuals are not the upper and lower limits of the design space, they are positioned in relative position to the extremes, usually 15% to 25% distance of the extremes. This method was used when generating all the initial population, a 15% distance from the extremes was used.

3.8.2.2 Random

Additionally to the Reduced Factorial experiments, there were added 10 randomly generated designs, in order to introduce further variety on the initial population for the genetic searcher. The algorithm for this experiment generation was based on traditional random number generation treatment and generates random experiments on the whole of the Design Space.

3.8.2.3 Statistical Distributions-Monte Carlo

After the initial genetic search the, and in the context of the hybrid algorithm, a second run is performed using a gradient based algorithm. For that second run, a new Design of Experiment population is created using a Mont Carlo defined algorithm. This algorithm randomly positions a chosen number of Designs around a chosen mean value. The chosen mean value being the best individual found by the previously genetic search.

3.9 OPTIMIZATION ALGORITHM

Due to the relative high number of variables employed in this multidisciplinary problem, the relative narrow set of feasible individuals and to achieve a better overall result a combination of two different methods is employed: the first evolutionary and the second gradient based, search resulting in what is known as hybrid algorithm. Hybrid algorithms have shown promising result in similar problems (Hartfield, 2006).

Historically genetic algorithms have shown great performance both in multi-objective problems and in large spectrum searches, although this type of algorithm has not assured convergence (Deb, 2009). Genetic algorithms were used both inside and outside the UnB's research group in solving similar multidisciplinary problems showing good performance (Deb, 2009; Kaled Da Cás, 2012; Hartfield, 2006; Casalino, 2012). In spite of UnB's group previous experience in solving multidisciplinary design problems in hybrid rocket propulsion, designing a multistage launcher was never attempted.

Gradient based algorithms are very efficient in finding minima, although they often incur in local minima. Gradient Based algorithms, such as the one chosen, have assured and relative fast convergence to the nearest minimum.

A hybrid algorithms aim to solve the greatest challenges of both genetic and gradient based algorithms, convergence issues and local minimum issues respectively. Initially the genetic algorithm performs a large spectrum exploration of the design space presumably arriving on a group of solutions near the global minimum. From the set of best solution from the genetic algorithm, a Design of Experiments set is formed and used in the gradient based algorithm. This procedure showed better results than each of the previous cited algorithms employed separately; this can be seen on the table below applied to the launch Vehicle MDO and to other classic optimization functions:

Optimization Problem		Mass	Number of Designs
Genetic, Armoga	First feasible	7836.7	208
	Optimum	4825.6	3154
Gradient, SIMPLEX	First feasible	19475.0	19
	Optimum	5885.5	301
Hybrid	Optimum	4526.4	3983

Table 3.13: Comparison between different algorithms, Launch Vehicle MDO

Optimization Problem		Function Value	Number of Designs
Genetic, Armoga	First feasible	103950	1
	Optimum	86.9	3047
Gradient, SIMPLEX	First feasible	103950	1
	Optimum	33.6	224
Hybrid	Optimum	27.3	3287

Table 3.14: Comparison between different algorithms, Rosenbrock function

Optimization Problem		Function Value	Number of Designs
Genetic, Armoga	First feasible	346	1
	Optimum	13.81	3101
Gradient, SIMPLEX	First feasible	346	1
	Optimum	55.4	214
Hybrid	Optimum	13.81 (no Improvement)	3101

Table 3.15: Comparison between different algorithms, Rastrigin function

3.9.1 Adaptive Range Multi-Objective Genetic Algorithm (ARMOGA)

The Adaptive Range Multi-Objective Genetic Algorithm (ARMOGA) was the Genetic Algorithm (GA) of choice for the initial optimization search. This algorithm is an improvement on the more common Multi-Objective Genetic Algorithm (MOGA), and as all GAs, employs a strategy of simulated evolution inspired by the natural selection and the evolution of species (Deb, 2009). As in every evolutionary algorithm the result of the algorithm is not a single optimal solution but rather an optimal population (Deb, 2009). The basic function of any GA are: mutation, crossover and dominance (Deb, 2009).

In a Genetic Algorithm the various experiments (Designs) are represented as chromosomes, a string vector that contain the values of each of the design variables and those values are used to obtain the values of the various objectives functions.

The Mutation function is aimed to introduce diversity in the population, and it is inspired by natural mutation processes that affect the evolution of living organisms. The Mutation function randomly alters one of the genes in the individual's chromosome. Higher percentage of mutation can introduce diversity but if too high it causes a negative effect on the convergence of the algorithm (Deb, 2009). Parallel to Mutation, Elitism can be employed for better performance of the algorithm. Elitism consists on preserving some

good individuals from previous generations unaltered in later generations to allow them to spread their genes further. Mutation is explained visually below (Figure 3.23)

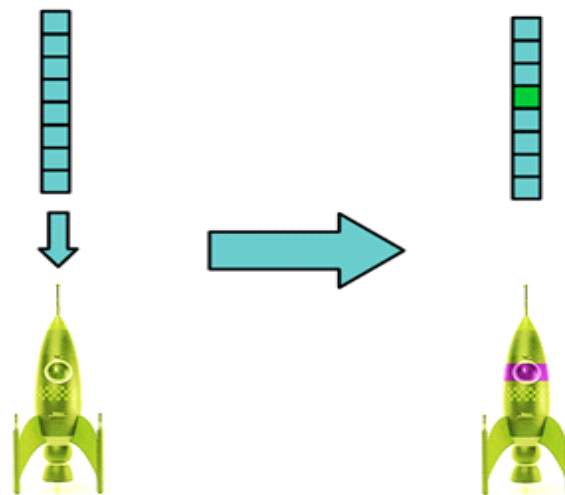


Figure 3.23: Mutation Operator

The Crossover function represents the individual generation through normal reproduction. In this process, two parent individuals have the genes on their chromosomes swapped and the combination to generate new children individuals. The Crossover is intended to spread good genes among the population and to find useful combinations of those genes (Figure 3.24):

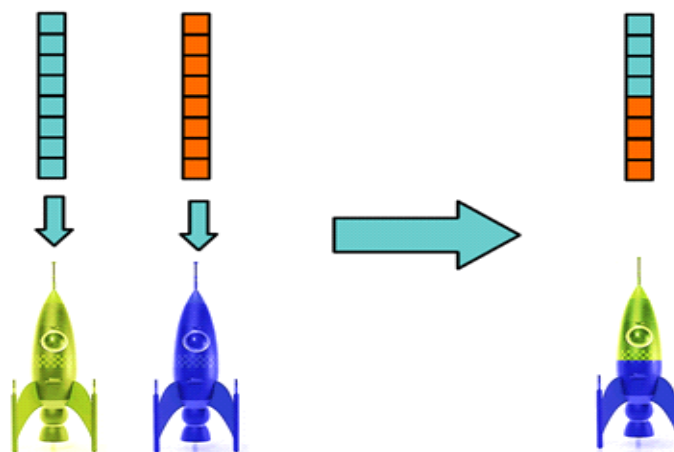


Figure 3.24: Crossover Operator

Most multi-objective optimization algorithms use the concept of domination, on these algorithms, two solutions are compared if whether one dominates over the other or not. According to Deb (2009) the concept of dominance is defined as:

A Solution $x^{(1)}$ of optimization problem with M objectives is said to dominate the other solution $x^{(2)}$, if both conditions 1 and 2 are true:

1. The solution $x^{(1)}$ is no worse than $x^{(2)}$ in all objectives, or $f_j(x^{(1)}) \leq f_j(x^{(2)})$, for all $j=1,2,\dots,M$.
2. The solution $x^{(1)}$ is strictly better than $x^{(2)}$ in at least one objective or $f_j(x^{(1)}) < f_j(x^{(2)})$, for at least one $j \in \{1,2, \dots, M\}$

The set of solutions that are not dominated by any other solutions is named Non-Dominated Set, and for most evolutionary algorithms those are considered the best solutions for a given generation. The next generation is then set applying the mutation and crossover functions to the non-dominated set.

The chosen GA for this optimization was the Adaptive Range Multi-Objective GA (ARMOGA) (Sasaki, 2005). This is a type of GA designed for rapid convergence or Pareto Front formation. ARMOGA employs variable and adaptive range methodologies that in predetermined periods reevaluate the variable boundaries excluding zones that yielded poor results (Figure 3.25). The ARMOGA uses the classic GA parameters, such as mutation, crossover and number of generations, and also the ones for the range adaptation process. The values of these parameters were selected based on several tests and can be seen on Table 3.16.

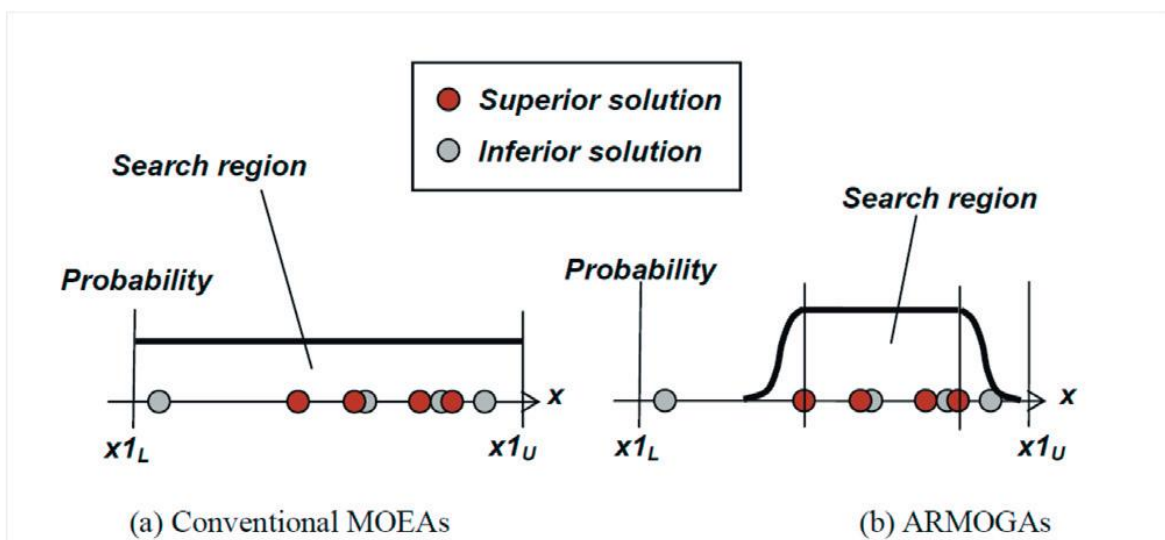


Figure 3.25: Range adaptation employed by the ARMOGA algorithm (Sasaki, 2005).

3.9.2 Downhill SIMPLEX Algorithm (SIMPLEX)

The SIMPLEX Method or Nelder–Mead method is a heuristic gradient descent method, and unlike evolutionary optimization methods generate a single optimal individual as

result. The SIMPLEX is a single objective optimization tool, although it can be employed inside a multi-objective algorithm using a cooperative or concurrent strategy, Nash Equilibrium or Game Theory, respectively. The SIMPLEX's Multi-objective possibilities will not be used in this dissertation. The Nelder-Mead method is based on simplexes a category of polytopes with $N+1$ vertexes in N dimensions; a segment of line, a triangle and a tetrahedron are examples of simplexes. This method operated generating a simplex in the N -dimensional Design Space and subsequently moving the vertexes in search of ever smaller (i.e. better) values for the objective function. Moving the simplex's vertexes on the Design Space is performed by three functions: Expansion, Contraction and Reflection.

The Downhill SIMPLEX method is started from an initial set of $N+1$ designs, where N is the Number of Design Variables to be optimized. Each of the designs in the set is evaluated for the objective function and the one of the designs is moved. The design is moved along a line connecting itself and the centroid of the shape formed by the other N designs. The Design can be moved farther from the other designs, Expansion; closer, Contraction or reflected about the centroid, Reflection. Expansion is used when the one of the design is slightly better than the others; the next design is placed away from the centroid in the direction of the better design. Similarly, Contraction is used when one of the designs is slightly worse than the rest. Finally, Reflection is used when one of the designs is much worse than the others. Those operations can be seen below for a 2 variable problem (Figure 3.26):

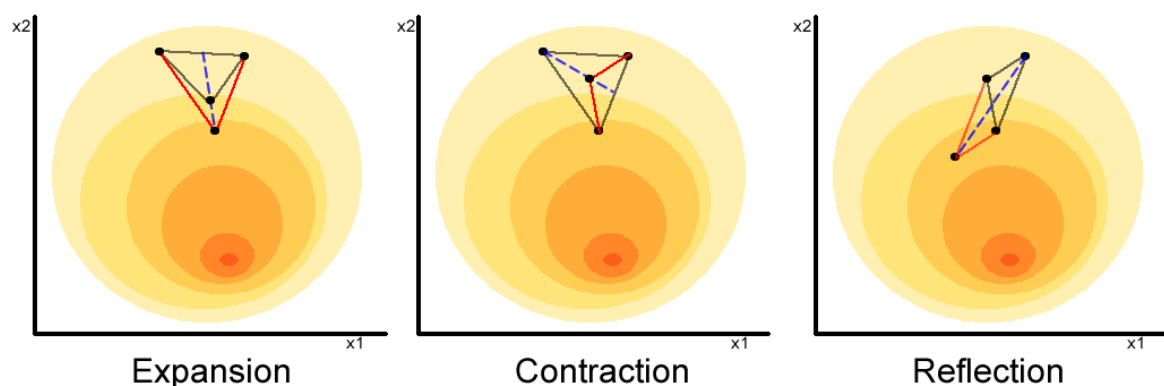


Figure 3.26: Different Function of a SIMPLEX Method in a 2D Design Space

4.9.3 ARMOGA-SIMPLEX hybrid

The hybrid optimization algorithm has yielded the best solution in all tests done (except for the Rastrigin function where it tied with the ARMOGA), and it showed itself capable

of combining good characteristics from both the evolutionary and the gradient algorithms. The implementation of this hybrid algorithm was the combination of two stages: on the first stage an evolutionary algorithm is used and on the second a gradient based.

The first stage is a multi-objective search in which the specific impulse of each of the stages is maximized and the total mass of the rocket is minimized. The specific impulse and the mass have little correlation, although several tests showed that the overall quality of the final population increased if the specific impulse was also optimized. On several test performed, the absence of a specific impulse optimization resulted on the algorithm finding a local minimum with low chamber pressures and higher mass than the found using the specific impulse in the optimization.

For the initial evolutionary search fifteen Design Variables (Section 3.1), four objectives and five constraints were used:

- Design Variables
 - External Grain Diameter: D_{ext}
 - Fuel Grain's Length: L_g
 - Propellant Mass Flow rate: \dot{m}_{oxi}
 - Nozzle Throat Radius: R_t
 - Oxidizer tank diameter: D_r
 - Internal grain diameter (Used only on post optimization, Case 8): D_{int}
- Objectives:
 - Minimize gross mass
 - Maximize 1st stage's specific impulse
 - Maximize 2nd stage's specific impulse
 - Maximize 3rd stage's specific impulse
- Constraints:
 - $\Delta V > 7454.0$ m/s (850Km SSO orbit)
 - Longitudinal overload (Nx1) < 6gs
 - Longitudinal overload (Nx2) < 6gs
 - Longitudinal overload (Nx3) < 6gs
 - Aspect Ratio (LoD) < 25

The commercial optimization platform modeFRONTIER (Version: modeFRONTIER 4.0 b20080131) was used as optimization management environment. The processes flow chart generated by the modeFRONTIER optimization environment for a typical MDO of a 3-stage hybrid rocket can be seen bellow (figure 3.27):

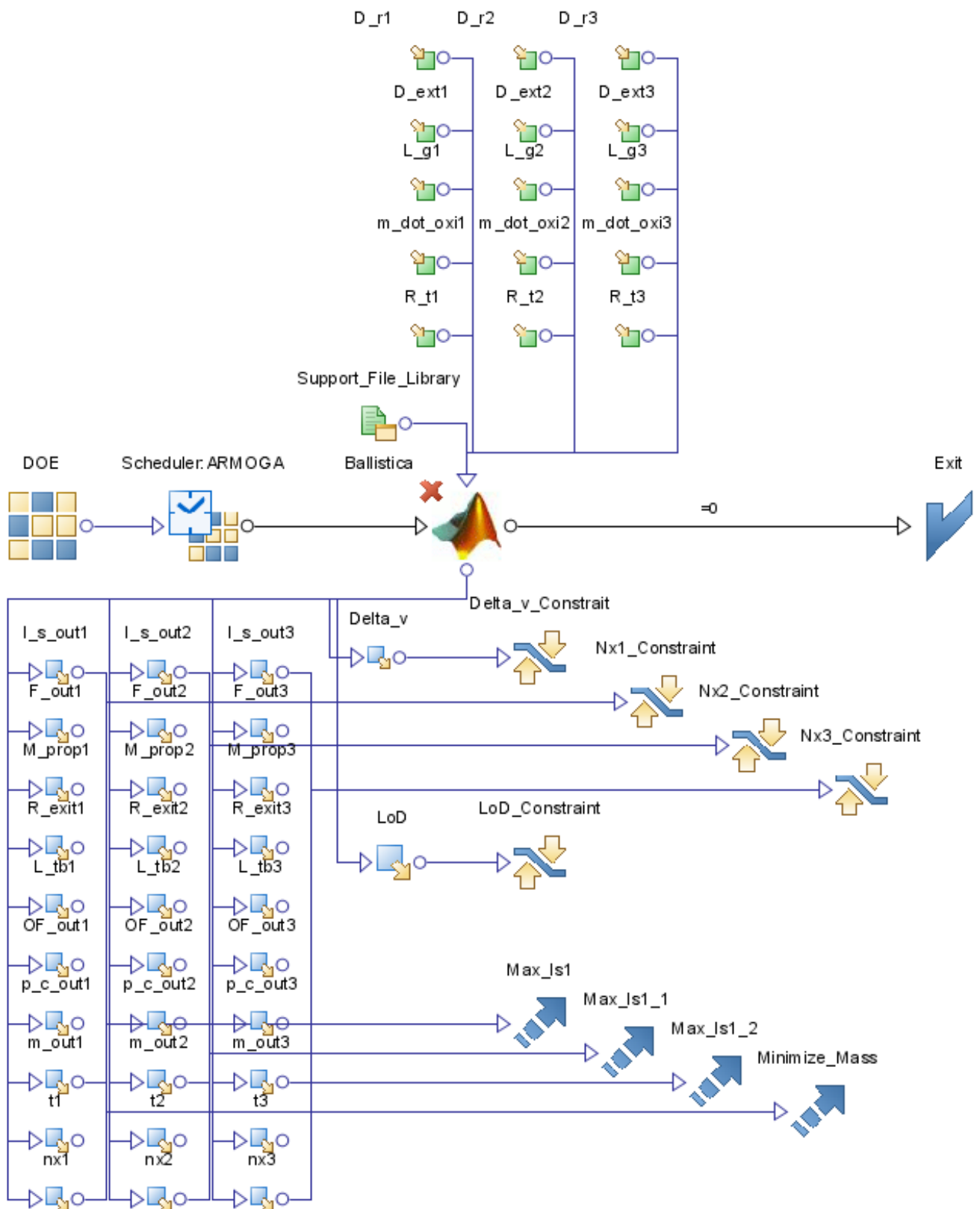


Figure 3.27: Process flow for a typical 3-stage launcher MDO on modeFRONTIER

For all of the MDOs performed the following parameters were used in setting the initial evolutionary search:

Algorithm	ARMOGA
Number of Generations	120
Individuals per generation	32
Start generation or Range adaptation	20
Probability of Crossover	1
Probability of Mutation	0.1
Average number of Individuals per run	~4400

Table 3.16: Setting parameter for the ARMOGA.

The second stages consist in selecting the best individual from the ARMOGA run and use it as basis for a SIMPLEX run. Considering the ARMOGA as a multi-objective evolutionary algorithm there is no single best individual, but a population of Pareto optimal designs. In a regular multi-objective optimization the designer is supposed to choose from the Pareto optimal set the most adequate individual. Although in the specific case of this MDO, the specific impulse objectives are of secondary importance when compared to the mass minimization. Therefore the selected optimal individual is the one with the smallest mass.

Once the optimal individual is selected, its design variable values are used as mean values for the generation of a Design of Experiments set using the Monte Carlo algorithm. This procedure intents to generate an initial population close to the supposed global minimum region found by the ARMOGA. The Monte Carlo algorithm is set to Generate 13 designs (N+1 designs)

Using the Monte Carlo initial population the Downhill SIMPLEX algorithm is then set to minimize the mass parameter. For all of the MDOs performed the following parameters were used in setting the gradient search:

Max number of Integrations	500
Final Termination Accuracy	10^{-5}

Table 3.17: Setting parameter for the SIMPLEX.

The resulting Design from the Downhill SIMPLEX is considered the best solution for the given hybrid algorithm MDO.

4-RESULTS AND DISCUSSION

The previous chapter outlined the theory and explained the construction of the Multidisciplinary Design Optimization (MDO) code developed for this work. This chapter presents the results found by testing several technological alternatives. Several design alternatives were chosen to represent readily available technological options and also to evaluate the improvements of employing state-of-the-art techniques over more standard and affordable ones.

In order to represent the various coherent design alternatives, a total of eight design cases were conceived and evaluated. The cases consist are presented below:

- Case 1: Base line reference, pressure fed LOX-Paraffin and standard materials.
- Case 2: Hydrogen Peroxide is used as oxidizer, instead of LOX.
- Case 3: Nitrous Oxide is used as oxidizer, blowdown injection is used.
- Case 4: Aluminum Hydride (AlH₃) is used as additive in the paraffin grain with LOX.
- Case 5: Turbopump feed system is used instead of pressure fed.
- Case 6: Hydrogen Peroxide is used with paraffin grain doped with AlH₃.
- Case 7: Low cost alternative with steel tanks instead of carbon composite.
- Case 8: Post Optimization based on the output from the first 7 cases.

The cases represent the most commonly proposed engineering alternatives for a hybrid propellant space launcher (Sutton, 2001), and also explore some innovative propellants, motor designs and construction materials. The cases will be explained in the next Section (4.1), then results will then be presented and compared in section 4.2. Finally in Section 4.3 a general high level tradeoff comparison of the first seven cases resulting in the selection of one of them for further design detailing.

4.1 DESIGN OF EXPERIMENTS

The various cases proposed above are explained and their relevance is explained with regard to both scientific and technological aspects.

4.1.1 Case 1: Baseline LOX/Paraffin

Case 1 represents the most commonly proposed alternative for high power hybrid rocket propulsion (Sutton, 2001): pressure fed system using Liquid Oxygen as oxidizer. The only deviation from the most standard propulsion was the usage of a paraffin grain instead of the more commonly proposed HTPB (Hydroxyl Terminated PolyButadiene). Even so paraffin has more than 17 years of extensive experimental testing by the Stanford group and more than 12 of testing experience in the University of Brasilia (Karabeyogly, 1995; Viegas, 2000). Paraffin was chosen for its high regression rate characteristics and for its low cost and easy handling.

On the other hand, the materials employed in this case are not standard metals but composite tanks, for the structural mass fraction of pressure fed hybrid rockets is expected to be very high and possibly, if common materials were used, render those rockets unfeasible. Even though the carbon-epoxy composite tanks are not standard in aerospace industry they are commercialized with cryogenic rating by Microcosm Space Mission Engineering (Scorpius S.L.C., Pressuremaxx cathalog). The integration of screws in a carbon composite material might be complicated due to its anisotropic structure. The combustion chamber is to be made of high strength steel to allow for easier integration and fitting of the various components of the motor assembly (valves, nozzle, injectors, etc...).

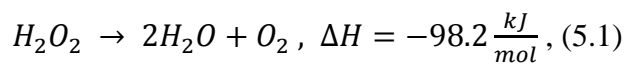
This case is expected to figure among the best results in this optimization due to paraffin/oxygen's high specific impulse. Comparatively speaking liquid oxygen is the most inexpensive oxidizer studied in this work, although operating a cryogenic fluid might result in logistic problems and more expensive infrastructure.

4.1.2 Case 2: Hydrogen peroxide as oxidizer

This case explores the usage of hydrogen peroxide (HTP) as an oxidizer in a pure paraffin propellant grain using a carbon composite oxidizer tank, a steel combustion chamber and a pressure fed injection system. Hydrogen peroxide was already successfully used in space launch application; the most famous vehicle to employ this oxidizer being the retired British launcher Black Arrow (Hill, 2006). Hydrogen peroxide possesses a high boiling point rendering this oxidizer storable in ambient conditions, it is also relatively inexpensive and possesses a moderate specific impulse with paraffin (263s at sea level and 323s in vacuum). Ambient temperature storage greatly reduces and simplifies pre-launch logistics and reduces the infrastructure in the launch pad. A storable propellant pair even

allows for tank filling during fabrication and shipping of the pre-filled stages to the launch complex. The optimum OF ratio for this propellant combination is ~7.5; it allocates much more of the reaction mass in form of oxidizer, which contributes to reducing the structural mass fraction due to the low specific ultimate tension of steel compared to the carbon composite, and the higher density of the peroxide compared to paraffin.

Additionally HTP is a monopropellant that can be exothermically decomposed in water on a hot silver catalyst bed accordingly to the equation below:



The thermo-catalytic decomposition of HTP can generate specific impulses of ~170s on vacuum at chamber temperatures of 1140K, which easily allows for uncooled radiated chambers. Thermocatalytic trusters can be used to steers the launcher in a much simpler and cost effective way than the normaly employed (in solid propellant rockets) in Flexible Nozzles. The hot gas produced by decomposition of HTP can be used to pressurize the oxidizer tank tank significantly reducing the stage's dry mass (if a high pressure HTP dedicated tanks is used). Hot peroxide is hypergolic with organic fuels; and this property can make the motor's ignition restart (Costa, 2010), very simple and straight forward (Gouvêa, 2008).

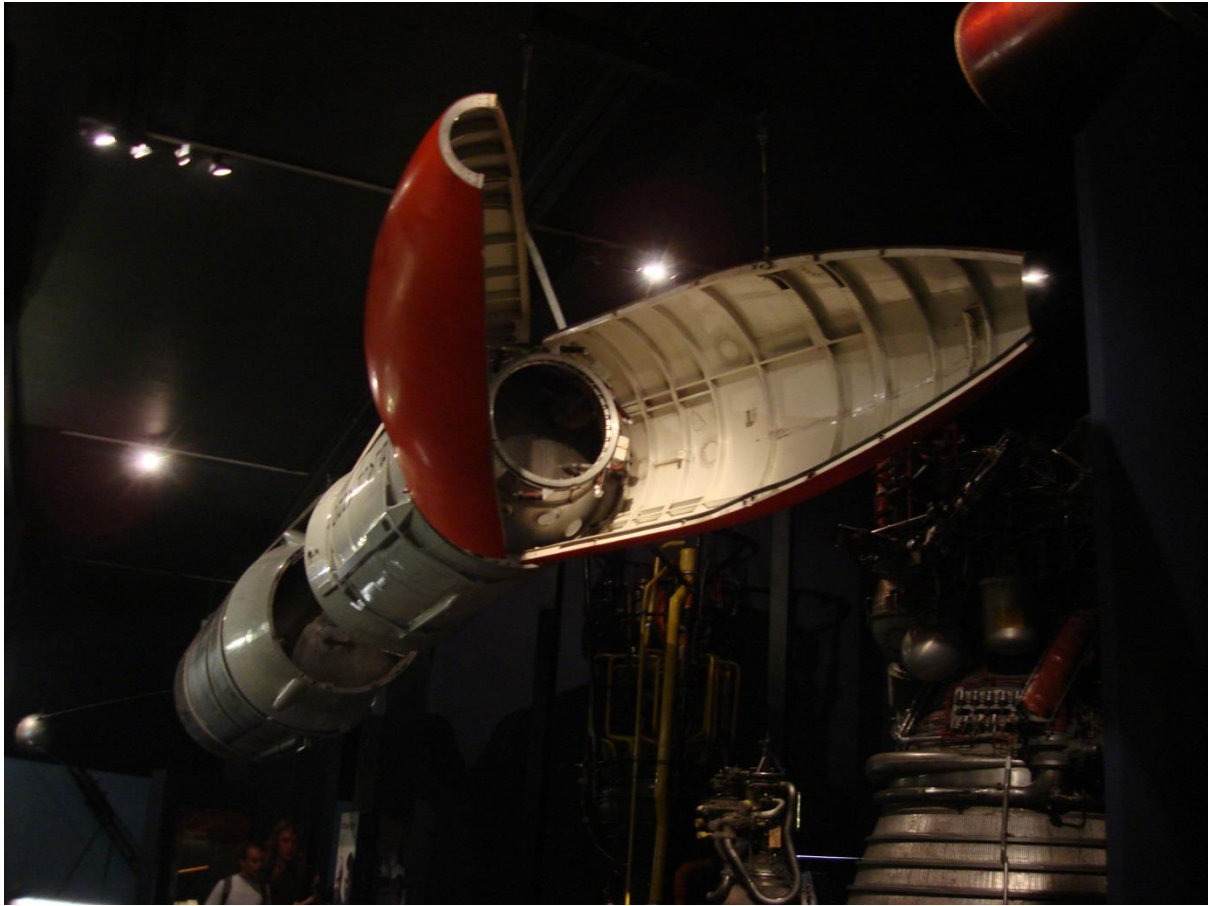


Figure 4.1: Black Arrow carrier rocket at the Science Museum (London), image by Oxyman

Hydrogen peroxide chemical formulation is H_2O_2 possessing a very high hydrogen content per mollar resulting in a relatively low average molar mass of the reaction products, contributing for a higher specific impulse. Unfortunately, the oxidation of paraffin with HTP 95% is not very energetic, 2851.40 K at optimal specific impulse OF. Also the regression ratio of paraffin/HTP is much higher than paraffin/LOX with a much bigger regression rate exponent (0.96 against 0.62 of LOX) which render the motor much more vulnerable to OF change due to combustion port diameter change; this peculiarity reduces the average specific impulse and might render HTP/Paraffin hybrids very difficult to design.

4.1.3 Case 3: Nitrous Oxide as oxidizer

Nitrous Oxide (NOX) has being used as rocket oxidizer since the dawn of space propulsion; it was first proposed by pioneer Robert Goddard as an oxidizer in liquid rockets. Hybrid rockets using NOX/paraffin were extensively researched by Stanford

propulsion group which also proposed a blend combination with liquid oxygen called NYTROX (Dyer, 2007). The greatest industrial exponent in the design of NOX hybrid motors is SpaceDev that bought NASA's research on hybrids, designed the motor for SpaceShipOne and currently is working on SpaceShipTwo's propulsion system, both systems employ NOX as oxidizer and HTPB as fuel (Figure 4.2).



Figure 4.2: SpaceShipOne's motor on test stand.

NOX/Paraffin possesses a very low specific impulse (247s at sea level. and 307s in vacuum) due to its moderate chamber temperatures $\sim 3200\text{K}$ and to relative heavy reaction products introduced by Nitrogen compounds. Even though the performance characteristics of NOX being inferior to even those of solid motors, this oxidizer allows for some interesting engineering solutions like self-pressurization and Thermo-catalytic subsystems similar to those of Case 2. The self-pressurization being the most interesting characteristic (see Section 3.3.2.2) for it allows a smaller structural mass fractions and better mass performance. Nitrous Oxide can self-decompose exothermically like HTP, this propriety allows the same pressurization and control subsystems used with HTP.

Case 3 employs the simple blowdown scheme explained in Chapter 3 (Section 3.3.2.2); this scheme is expected to significantly reduce the dry mass by the elimination of much of the dry mass associated with the pressurization subsystem. Unfortunately, the density of Nitrous Oxide is very small and this characteristic is especially harmful for larger tanks used in blowdown systems.

4.1.4 Case 4: Aluminum Trihydride additive on LOX/paraffin

Specific impulse is the most important performance parameter in a rocket motor and any increase in its value leads to a considerable reduction in the system's mass for a given mission Delta v. More recently the usage of Aluminum Trihydride (AlH₃) was proposed for increase of specific impulse (Karabeyoglu, 2011).

Traditionally metallic additives are used in solid rocket propulsion and are the chief factor responsible for its actual status as competitive technological alternative, metal additives have elevated their specific impulse from 230s (Double Base) to 295s (Composite). Although common oxidizers used in solid rocket propulsion are inefficient (Nongaseous products) and toxic (contain Chlorine). On the other hand, the oxidizers usually employed in liquid rocket propulsion are much safer and deliver a significantly higher performance (LOX, NTO). Notwithstanding the fuels employed in liquid rocket propulsion are less energetic and less dense than metallic fuels, impacting on both the specific impulse and impulse density. Solid metallic additives cannot be used in liquid propulsion systems, as they would decant on the propellant tanks. Hybrid rockets show a unique opportunity to combine the advantages of both high energy metallic fuels and high efficiency liquid oxidizers.

The addition of AlH₃ has two benefic effects on the propulsion system: increase of the reaction energy, due to addition of high energy metallic components (Aluminum), and lowering of the product's average mass by adding hydrogen content. The introduction of this additive also shifts the OF Ratio to smaller values, which might increase the combustion chamber, but can reduce the overall mass by reducing the size of the pressurization tanks and gas.

Up to this date there is no experimental work done in paraffin+AlH₃ and special dynamics and the regression rate mechanisms can impact negatively on the possible usage of this additive.

4.1.5 Case 5: Turbopump feed system

Turbopumps feed systems are used in almost every liquid propulsion systems, as they allow for low pressure lighter propellant tanks and turbopump systems in themselves are much lighter than the balloons and gas used in pressure fed systems. In Liquid rocket propulsion, turbopumps have a huge impact when both propellants are stored in low pressure tanks. In hybrid propulsion this impact is undermined for the usage of turbopumps, as they have no impact on the combustion chamber's pressures where the solid fuel is located.

Turbopumps can potentially have a great impact on the structural mass fraction of each stage and eventually in the overall mass of the rocket. Although it is argued the complexity added by turbopumps will eventually kill the low cost characteristics of hybrid propulsion.

The low weight of the oxidizer tank and the independence of the chamber pressure from the tank pressure might cause a convergence to a much higher chamber pressure and a slightly higher OF ratios.

As described in Chapter 4 the material employed on the oxidizer tank's construction of a pump fed system will not be Carbon-epoxy composite but weldable Aluminum AMG6M. The low tank pressures in this kind of propellant tank would result in tank walls too thin to be fabricated if a high strength material such as Carbon composite or high strength steel were to be used

4.1.6 Case 6: Hydrogen Peroxide with Paraffin+ALH3 grain

Case 6 is a combination of both cases 2 and 4, although it can potentially output a much better result allowing of a nontoxic storable high energy system with various applications.

The increase in specific impulse when using AlH₃/paraffin with HTP is considerable, for this additive directly affects the most significant disadvantage of using HTP: the low combustion temperature. The currently employed percentage of AlH₃, 40%, shows slightly increase in specific impulse, although if the optimal percentage of 80% would be used the specific impulse can reach levels of 369s, similar to LOX/Paraffin or LOX/RP-1 without the inconveniences of dealing with cryogenic propellants such as liquid Oxygen. The lower concentration of additive was chosen as a safety precaution since it was not

experimentally shown that paraffin's high regression rates will be kept when operating with this kind of grain.

A high energy storable hybrid rocket such as the proposed here has a Game Changing potential specially on deep space mission and attitude control where propellant boil-off deny the use of cryogenic material such as liquid oxygen. Currently the most advanced storable propellant pair UDMH/NTO has a specific impulse of 335s not much superior to the suboptimal HTP/40% AlH₃+Paraffin grain with a specific impulse of 331s and without the toxicity and corrosion hazards of associated with UDMH and NTO.

The addition of AlH₃ reduces the optimal OF ratio of HTP/Paraffin from ~7.5 to ~5 which is similar to the described for the LOX/AlH₃+Paraffin. this reduction has a double effect on the structural mass fraction. On the one side, it increases the size of the heavy combustion chamber; on the other hand, it reduces the volume of the oxidizer tank reducing the pressurization subsystem's mass. The many useful subsystems employing decomposition of peroxide are still possible under this configuration.

4.1.7 Case 7: Steel Tanks

This case is by definition a suboptimal design, although the reductions in cost and the ease of fabrication of steel tanks might result in an interesting design.

Unlike the other cases (to the exception of Case 3) the oxidizer tank is not made of carbon composite but of high strength steel. The usage of steel in cryogenic temperatures might problematic due to increased brittleness although there are special cryogenic steels suitable for this kind of application. The best cryogenic steel found has a slightly lower yield and ultimate strengths than the previous considered steel (Section 4.2.2).

4.2 OPTIMIZATION RUNS AND DISCUSSIONS

The various cases were run and their results are shown here, further discussion follows. Peculiarity and changes in the optimization procedure needed for each of the cases are also discussed and explained.

4.2.1 Case 1

The initial tries on the optimization presented no convergence problems, though the resulting designs converged to inconvenient solutions with unusually large thrust to weight values. The larger thrusts might result from an attempt to reduce gravitational losses and

were more pronounced on the third stage where there is no aerodynamic drag. Following that it was found the longitudinal accelerations or overloads had unfeasible values ($\sim 25g$). Normally launch vehicles have values of longitudinal acceleration inferior to $6g$ and accordingly the satellites are designed to withstand such loads. Consequently a set of constraints was introduced to limit the maximum overloads to values inferior to 6 . These extra constraints were adopted in all the following cases.

In the initial runs, it was also noticed a convergence to very large aspect ratios, some on the order of 80 . The aspect ratio of a rocket affects how it handles transverse forces, such as caused by wind, the control system and the aerodynamic torque. The code does not account for such forces and as a rule of thumb the smaller the aspect ratio the less vulnerable the vehicle is to transverse forces. A maximum value of 25 was imposed on the aspect ratio, which corresponds to the Scout rocket.

The overall characteristics of the resulting optimal individual were very satisfactory. The converging design variables are presented below (the values were not rounded):

First Stage

- $D_{ext1}=0.7192000000000001$;
- $D_{r1}=0.9166666666666667$;
- $L_{g1}=3.8304347826086955$;
- $m_{dot_oxi1}=41.163043478260875$;
- $R_{t1}=0.14385714285714285$;
- $D_{int1}=0.324$; (not a design variable, although very important geometry wise)

Second Stage

- $D_{ext2}=0.5144000000000001$;
- $D_{r2}=0.85$;
- $L_{g2}=1.7652173913043478$;
- $m_{dot_oxi2}=10.521739130434783$;
- $R_{t2}=0.05142857142857142$;
- $D_{int1}=0.164$; (not a design variable, although very important geometry wise)

Third Stage

- $D_{ext3}=0.385$;
- $D_{r3}=0.33333333333333337$;
- $L_{g3}=0.9420000000000001$;
- $m_{dot_oxi3}=1.7608695652173916$;
- $R_{t3}=0.027142857142857142$;
- $D_{int1}=0.067$; (not a design variable, although very important geometry wise)

The general shape of the rocket is well within the expected. Each of the stage roughly appears to be proportional in a reasonable decrease from the first to the third. The only exception is the external diameter do the third stage which is smaller than the grain diameter, although very close.

The most significant output variables are presented below (Table 4.1):

Variable	Stage1	Stage2	Stage3
Thrust [kN]	158.09	45.58	8.11
Specific Impulse [s]	272.51	320.49	325.33
Nozzle Length [m]	0.619	0.983	0.591
Propellant mass [kg]	3832.56	1140.87	334.88
Oxidizer tank length [m]	3.65	1.29	1.85
Dry Mass [kg]	804.47	293.34	157.91
OF Ratio [NA]	2.30	2.66	2.28
Nozzle exit radius [m]	0.310	0.315	0.185
Expansion ratio [NA]	9.23	36.6	32.5
Structural mass Fraction [%]*	17.34	20.45	23.82
Gross mass, stage [kg]	4637.03	1434.21	489.59
Axial overload [g]	5.90	5.93	5.35
Combustion chamber pressure [Bar]	16.24	30.78	19.51
Burn time [s]	64.87	78.96	133.26
Mass Ratio (m0/mf) [NA]	2.40	2.45	3.12
Delta V [m/s]	2343.9	2818.9	3632.1
Total aerodynamic loss [m/s]	393.52		
Total gravitational loss[m/s]	950.01		
Total velocity loss[m/s]	1.343		
Total Rocket's mass [kg]	6.564		
Total Length [m]	21.13		
Length over Diameter Ratio	23.05		

***includes extra propellant loading, ignition, spare and unusable propellant**
Table 4.1: Geometric and performance characteristics of Case 1 Launcher

A preview of the general shape of the stages can be seen in the sketch below (Figure 4.3):

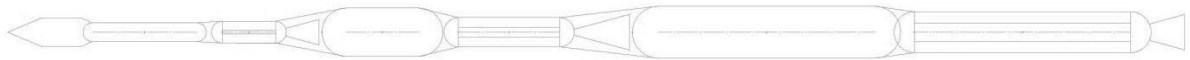
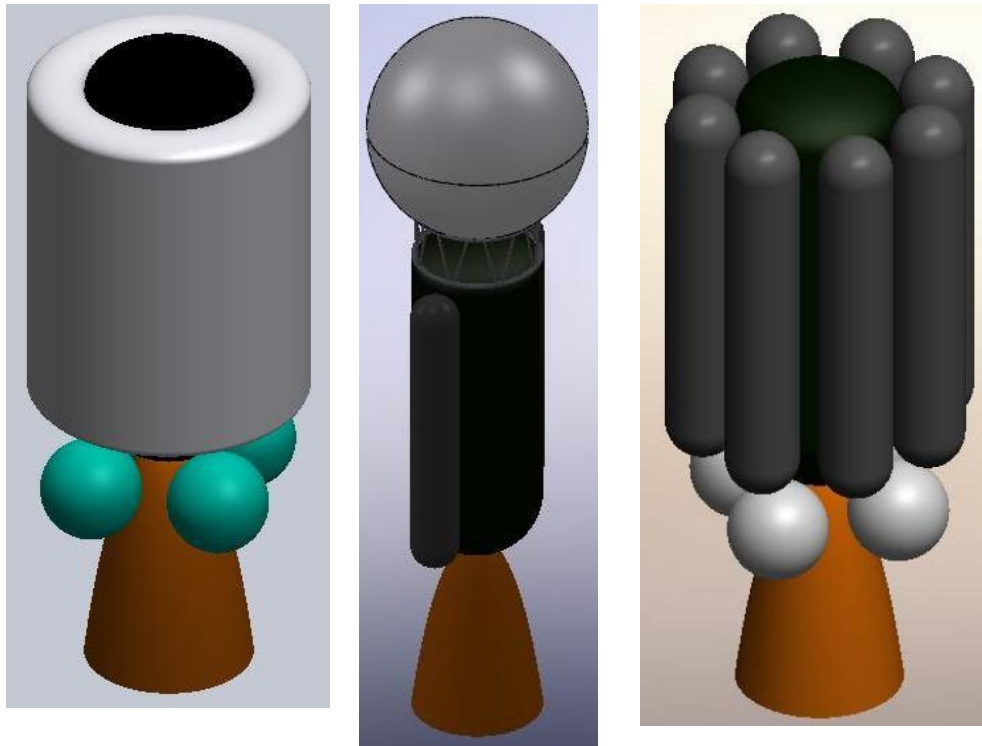


Figure 4.3: Layout of Case 1 rocket.

In the post processing of the results the tank shape can be improved using toroidal tanks or multiple side tanks. The final length of the rocket could be further reduced by the usage of multiple tanks in the third stage. The usage of the same D_r in all stages will also reduce the length of the rocket and costs, as it introduces standardization. Similar arrangements were also proposed in literature (Lynnyk, 2008; Karabeyoglu, 2011). The pressurizing gas tanks are not shown in the Figure 4.4, but the can be arranged in several different places (Figure 4.4).



Toroidal tank Larger diameter tank Multiple side tanks
Figure 4.4: Different layout alternatives, (Karabeyoglu, 2011)

The mass fraction for the first and second stages are almost identical resulting in a very similar Δv , indicating effective work of the optimization code. The larger mass ratio of the third stage is due to effective usage of the high specific impulse possible for a third stage. As abovementioned, the exhaust pressure were fixed and can be improved with better flight trajectory calculations in project detailing phase.

Other noticeable discrepancy was the relative small tank pressure of the first stage (16 bar), which probably results from a tendency to reduce structural mass fraction. The structural mass fraction of the first stage is indeed small, 16% rivals with some turbopump fed stages and solid stages, which is very impressive for a pressure fed rocket with 13% of extra propellant loading.

The specific impulse and OF behavior and other dynamic characteristics of the rocket showed expected result as can be seen below:

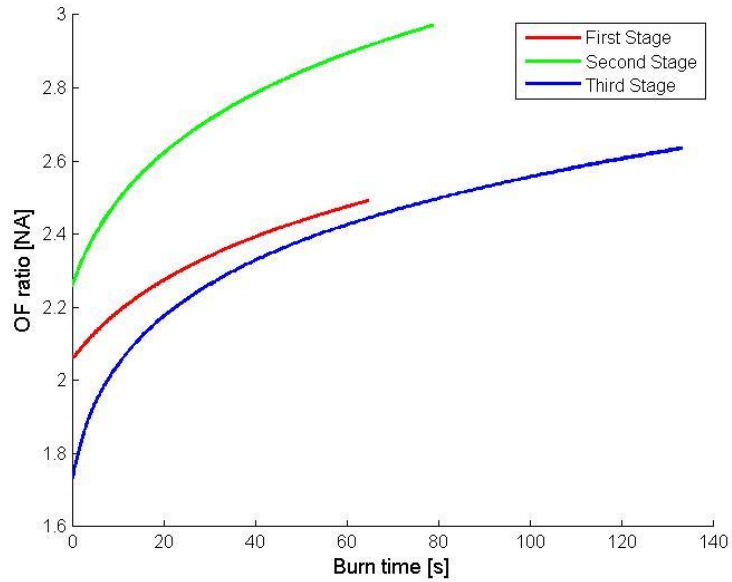


Figure 4.5: OF shift in Case 1

The OF ratios of both third and first stages have converged to a similar behavior, the OF ratio of the second however has a higher average value.

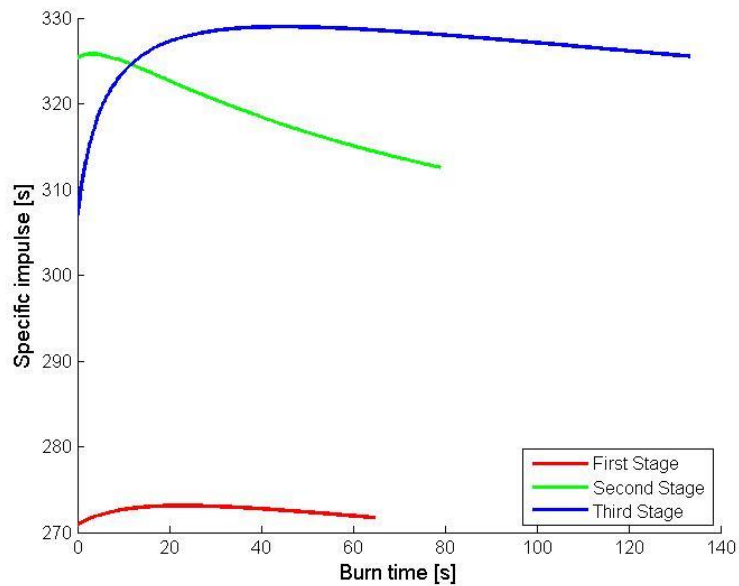


Figure 4.6: Specific impulse shift in Case 1

The behavior of the specific impulse for the first and second stages show signals of effective optimization with a strong increase culminating in a stable plateau, contributing to a stable working of the of those stages. The second stage presents a different behavior

with a steep decay during all its operation. The different behavior of the second stage's specific impulse is due the different OF profile. Both the OF profile and the resulting specific impulse profile can be easily improved by changes in the grain's length; and it can be done in project detailing.

4.2.2 Case 2

Case 2 contemplates the usage of Hydrogen Peroxide or HTP as oxidizer. This optimization required a new set of design variable's range because of the different regression rate law and optimal OF ratio.

The experimental regression law associated with hydrogen peroxide presents an extremely steep behavior caused by the very high regression coefficient. As explained in Chapter 3, the closer the regression coefficient is from 0.5 the less vulnerable the OF ratio is to changes in combustion port geometry. The very high regression coefficient of HTP/paraffin (0.96) resulted in strong coupling between the regression rate and the OF ratio, that easily resulted on OF ratio breaching the ballistic model's boundaries. The solution found was re-interpolate the polynomials until OF ratios of 16 to avoid breaking the polynomial coherence during optimization. Breaking of the polynomials' coherency was observed in preliminary optimization runs resulting in unrealistic performance predictions.

In order to correctly and impartially set the design variable's ranges the following procedure was implemented:

1. A design optimization run was made with the following objectives:
 - Maximize Delta v
 - Minimize System's mass
2. From the resulting Pareto set, it was then selected the individual with the Delta v closest to and superior to 7.454 m/s (delta v constraint for a 850km circular orbit).
3. The design variables' values from the individual selected in step #2 were set as the average values for the Design Variable.

Ideally the optimization described in step 1 of the procedure above would result in a Pareto set containing the lowest mass individual for any given Delta v limitation. This procedure

showed a good potential for exploring the design space and it was therefore used; and all of the following cases where new variable's ranges needed to be selected.

The overall characteristics of the resulting optimal individual were very satisfactory. The converging design variables are shown below:

First Stage

- $D_{ext1}=0.715$;
- $D_{r1}=1.2000000000000002$;
- $L_{g1}=6.0$;
- $m_{dot_oxi1}=129.88888888888889$;
- $R_{t1}=0.15428571428571428$;
- $D_{int1}=0.5751$; (not a design variable, although very important geometry wise)

Second Stage

- $D_{ext2}=0.3993333333333333$;
- $D_{r2}=0.9388888888888889$;
- $L_{g2}=4.5600000000000005$;
- $m_{dot_oxi2}=23.333333333333332$;
- $R_{t2}=0.07385714285714286$;
- $D_{int2}=0.2438$; (not a design variable, although very important geometry wise)

Third Stage

- $D_{ext3}=0.22800000000000004$;
- $D_{r3}=0.4141693025015564$;
- $L_{g3}=2.1021333333333333$;
- $m_{dot_oxi3}=3.066666666666667$;
- $R_{t3}=0.027600000000059997$;
- $D_{int3}=0.0884$; (not a design variable, although very important geometry wise)

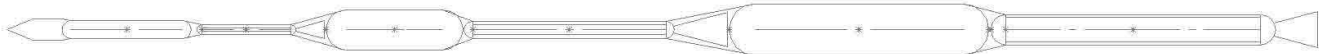


Figure 4.7: Layout of Case 2 rocket

From previous studies large aspect ratio grains were expected (Kaled Da Cás, 2012), also was the large internal diameter in relation to the grain's external diameter, both caused by the steep OF shifts and the high mass flow rates. The effect of OF shift is less pronounced in motors with low thrust and long burn time having a mild effect on the third stage's geometry and with a very small impact on very small thrusters, like the SARA de-boost motor (Kaled Da Cás, 2012). The large oxidizer mass flow rates are coherent with the large ideal OF ratios (~7.5).

The most significant output variables are presented below:

Variable	Stage1	Stage2	Stage3
Thrust [kN]	360.10	79.06	10.62
Specific Impulse [s]	256.45	297.87	304.43
Nozzle Length [m]	1.011	1.253	0.667
Propellant mass [kg]	8602.07	2502.23	545.86
Propellant Tank's length	2.147	2.284	2.1021
Dry Mass [kg]	2108.4	606.05	221.67
OF Ratio [NA]	9.84	6.37	6.62
Nozzle exit radius [m]	0.425	0.409	0.206
Expansion ratio [NA]	7.60	30.74	55.8
Structural mass Fraction [%]*	19.69	19.5	23.9
Gross mass, stage [kg]	10710	3108	767.5
Axial overload [g]	6.13	5.87	4.88
Combustion chamber pressure [Bar]	29.9	25.7	24.0
Burn time [s]	60.0	92.8	155.0
Mass Ratio (m0/mf) [NA]	2.4	2.8	3.4
Delta V [m/s]	2241.4	3031.2	3709.1
Total aerodynamic loss [m/s]	316.9		
Total gravitational loss[m/s]	1004.3		
Total velocity loss[m/s]	1321.2		
Total Rocket's mass [kg]	14586.0		
Ttal Length [m]	30.3		
Length over Diameter Ratio	25.2		

***includes extra propellant loading, ignition, spare and unusable propellant**
Table 4.2: Geometric and performance characteristics of Case 2 Launcher

Despite of the OF shift, Case 2 resulted in a considerably well design launcher, as it can be seen by: similar chamber pressure in all stages, low structural mas fraction in all stages, coherent mass ratio in all stages and moderated aerodynamic and gravitational losses. The good structural mass fraction characteristics could be explained by the large mass of the stage and also by high impulse density possible with peroxide. Additionally, the mean OF ratio and its transient behavior for the second and third stages are very similar, denoting a tendency toward OF ratios slightly below the optimum values. The specific impulse behavior of the second and third stages show signals of satisfactory working of the optimization as well, presenting a quick rise followed by a plateau, although a less stable than Case1's plateau due to OF shift.

In post processing, both the second and third stages could be redesigned with multiple side tanks or a toroidal tank. The first stage however is considerably difficult to be refined in any way. It can be seen form Figure 4.8 that it converged to a very thin propellant grain with a considerably large combustion port, possibly to mimeses the harmful effects of OF shift. It is argued that the thrust level and burn time of the first stage are in the threshold of possibly stable design; and any higher thrust level would requires much longer grains with

thinner propellant grains making the layout design of a feasible launch vehicle much difficult or impossible. An alternative to solve the layout problem of the first stage would be the utilization of multiple propellant grains fed by the same central oxidizer tanks. For example, if four of the second stage's grain and combustion chamber were to be used the final assemble would result in very close thrust level and propellant loading, the structural mass fraction could be even better than the current level, this can be seen in the image below (Figure 5.8):

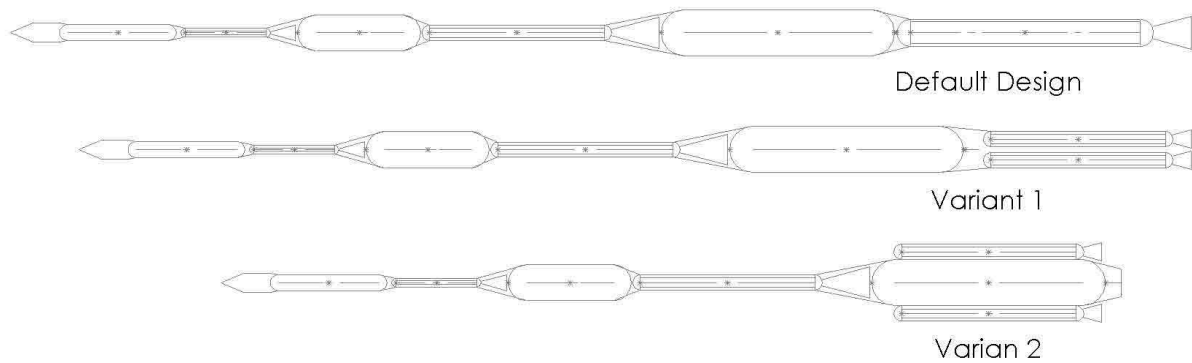


Figure 4.8: Exploratory layout study for multiple core construction

Multiple core design could allow for differential thrust steering, considerably simplifying the trust vector control system. This is but an exploratory study to envision possibilities for future development, and a proper tradeoff of those layout variants can only be properly made on the design detailing phase.

The time dependent behavior of Case 2's stages can be seen below:

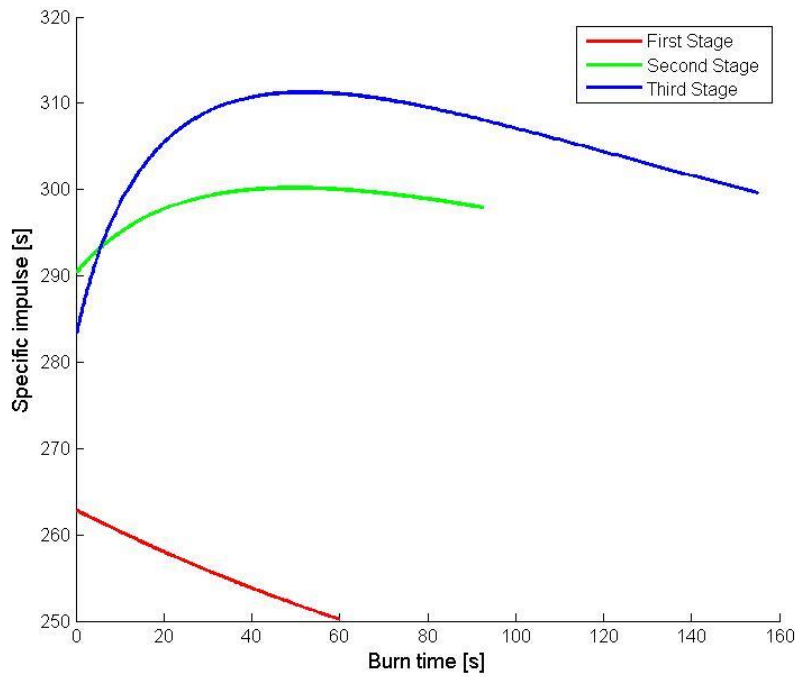


Figure 4.9: Specific impulse shift in Case 2

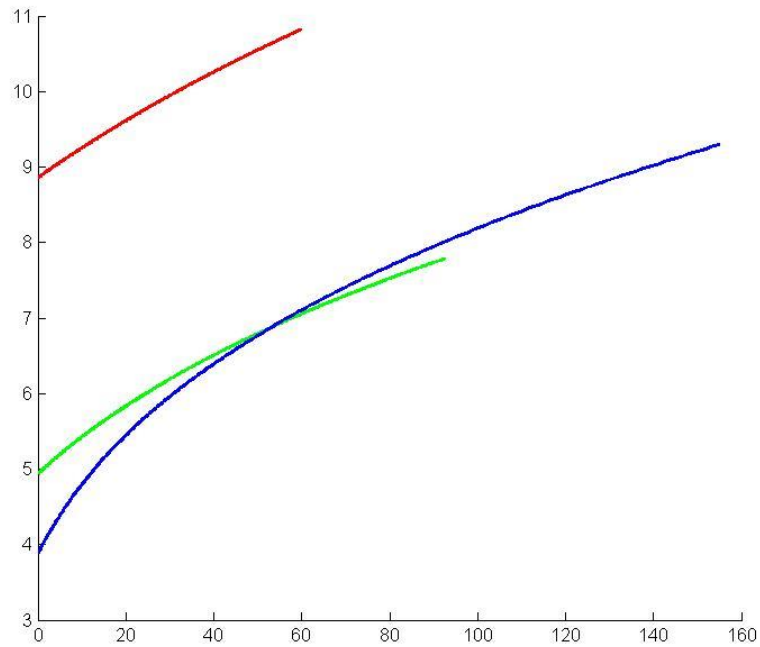


Figure 4.10: OF shift in Case 2

Case 2 showed promising results for the use of peroxide as oxidizer for a hybrid propulsion launcher, although the OF shift problems imposed seriously difficulties for its practical application. A possible way around the OF shift problem could be an active mass

flow rate control that could stabilize the OF at a desired level. The high density and the possibility of thermo-catalytic subsystems possible by peroxide still maintain this oxidizer as a viable alternative despite of the moderate specific impulse of its OF shift problems.

4.2.3 Case 3

Case 3 resulted in a failure to achieve the minimum mission requirements. The technique employed in Case 2 to select an adequate range for the design variables (Maximize Delta_v and Minimize systems mass) could not generate a single individual capable of generating the required 7454 m/s final velocity required for the 850km polar orbit, even without the design constraints of aspect ratio and overload. Although such result was not unexpected, considering that N2O/paraffin generates a specific impulse even lower than commercial solid propellant motors with a structural mass fraction far superior to solid motors. Notwithstanding the apparent failure, this optimization case showed the efficacy of the blowdown injection scheme.

The most significant output variables are presented below:

Variable	Stage1	Stage2	Stage3
Thrust [kN]	231.2	47.3	65.8
Specific Impulse [s]	217.20	272.76	286.26
Nozzle Length [m]	0.927	1.015	1.696
Propellant mass [kg]	7015.01	1254.41	163.51
Propellant Tank's length	10.24	6.27	5.17
Dry Mass	1238.49	290.01	55.49
OF Ratio [NA]	3.86	7.93	9.51
Nozzle exit radius [m]	0.361	0.324	0.498
Expansion ratio [NA]	10.23	38.23	129.38
Structural mass Fraction [%]*	15.0	18.7	25.3
Gross mass, stage [kg]	8253.50	1544.42	219
Axial overload [g]	7.72	8.62	63.70
Combustion chamber pressure [Bar]	38.56	32.11	60.2
Burn time [s]	65.24	71.03	6.96
Mass Ratio (m0/mf) [NA]	3.33	3.46	3.94
Delta V [m/s]	2543.0	3148.9	2628.8
Total aerodynamic loss [m/s]	349.8		
Total gravitational loss[m/s]	685.7		
Total velocity loss[m/s]	1035.6		
Total Rocket's mass [kg]			
Total Length [m]			
Length over Diameter Ratio			

***includes extra propellant loading, ignition, spare and unusable propellant**
Table 4.3: Geometric and performance characteristics of Case 3 Launcher

The most relevant aspect to be noted from the output variables (Table 5.4) are the structural mass fraction; they possess very small values comparable even to the ones displayed in Case 5 (LOX/Paraffin turbopump), although employing a much more affordable technological solution.

There is not much usable conclusion to be extracted from the other variables as a satisfactory convergence was not achieved.

4.2.4 Case 4

The convergence for Case 4 was achieved without much problems and the resulting design is somewhat similar to Case 1. Despite of the apparent well defined a design variables' range, the pre-optimization proposed in Case 2 was also applied.

First Stage

- $D_{ext1}=0.585$;
- $D_{r1}=1.005$;
- $L_{g1}=6.524000000000001$;
- $m_{dot_oxi1}=20.0$;
- $R_{t1}=0.11457142857142857$;
- $D_{int1}=0.226$; (not a design variable, although very important geometry wise)

Second Stage

- $D_{ext2}=0.44500000000000006$;
- $D_{r2}=0.867$
- $L_{g2}=2.0759999999999996$;
- $m_{dot_oxi2}=7.4$;
- $R_{t2}=0.04285714285714286$;
- $D_{int2}=0.1373$; (not a design variable, although very important geometry wise)

Third Stage

- $D_{ext3}=0.361$;
- $D_{r3}=0.276$;
- $L_{g3}=1.56$;
- $m_{dot_oxi3}=1.2466666666666668$;
- $R_{t3}=0.038$;
- $D_{int3}=0.0563$; (not a design variable, although very important geometry wise)

The only discrepancy visible in the design variables is the third stage's tank diameter which is smaller than the combustion chamber's. This discrepancy can be easily corrected by an increase in the tank's diameter. Also the low OF ratio of this propellant pair resulted in very long and thin fuel grains and consequently high diameter oxidizer tanks to accommodate the required oxidizer volume while maintaining the aspect ratio constraint.

The long thin propellant tanks suggest improvement in case the option for a toroidal oxidizer tank wrapped around the combustion chamber or the option for several cylindrical tanks positioned around the combustion chamber.

The most significant output variable are presented below:

Variable	Stage1	Stage2	Stage3
Thrust [kN]	133.24	41.21	8.51
Specific Impulse [s]	296.05	343.26	337.16
Nozzle Length [m]	0.625	0.941	0.625
Propellant mass [kg]	3079.3	870.52	358.58
Oxidizer Tank's length	1.113	0.866	2.851
Dry Mass	806.46	259.09	151.25
OF Ratio [NA]	0.776	1.540	0.952
Nozzle exit radius [m]	0.282	0.295	0.205
Expansion ratio [NA]	6.06	47.39	29.25
Structural mass Fraction [%]*	20.75	22.94	22.02
Gross mass, stage [kg]	3885.84	1129.62	509.83
Axial overload [g]	5.55	5.46	5.75
Combustion chamber pressure [Bar]	20.98	39.44	10.69
Burn time [s]	67.60	71.77	142.60
Mass Ratio (m0/mf) [NA]	2.25	2.13	3.37
Delta V [m/s]	2336.8	2549.6	4019.1
Total aerodynamic loss [m/s]	526.5523		
Total gravitational loss[m/s]	953.6802		
Total velocity loss[m/s]	1480.2		
Total Rocket's mass [kg]	5525.3		
Total Length [m]	21.68		
Length over Diameter Ratio	21.68		

*includes extra propellant loading, ignition, spare and unusable propellant
Table 4.4: Geometric and performance characteristics of Case 4 Launcher

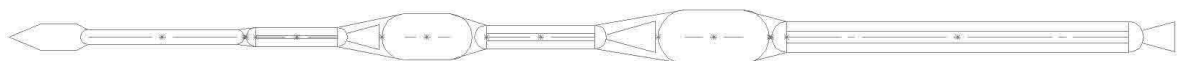


Figure 4.11: Layout of Case 4 rocket

The optimization showed signals of efficient working, this is evidenced by the Mass Ratios and OF ratios, both parameters presented values close to the expected for both a 3 stage LEO launcher and for the given propellant pair. The propellant mass fraction also converged to similar values, although high, but expected for pressure fed hybrids.

From the output variables, the most noticeable features are introduced by the smaller OF ratios, those resulted in the longer grains observed in the Design Variables and also in: short tank lengths, higher structural mass fractions, smaller combustion chamber pressures.

The discussion introduced in Section 5.1.4 of Chapter 5 regarding the impact of OF ratio reduction on the resulting structural mass fraction was partially answered by the results of this case - OF reduction increase structural mass fraction.

From the layout of Case 4 (Figure 4.11), it can be seen: a very long fuel grains and a short oxidizer tanks in the first and second stages. The long propellant tanks in the third stage can be easily corrected by a more efficient internal distribution of propellant tanks and grain.

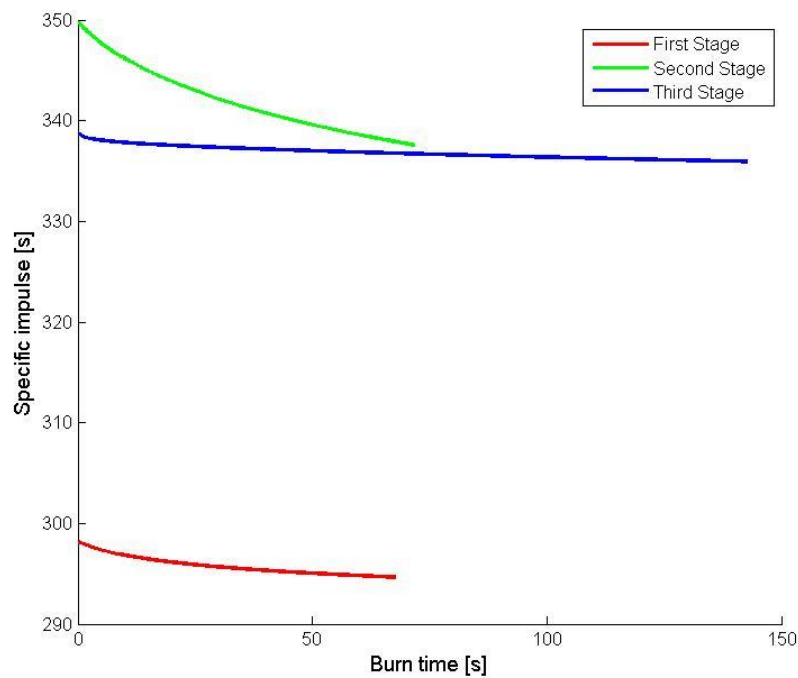


Figure 4.12: Specific impulse shift in Case 4

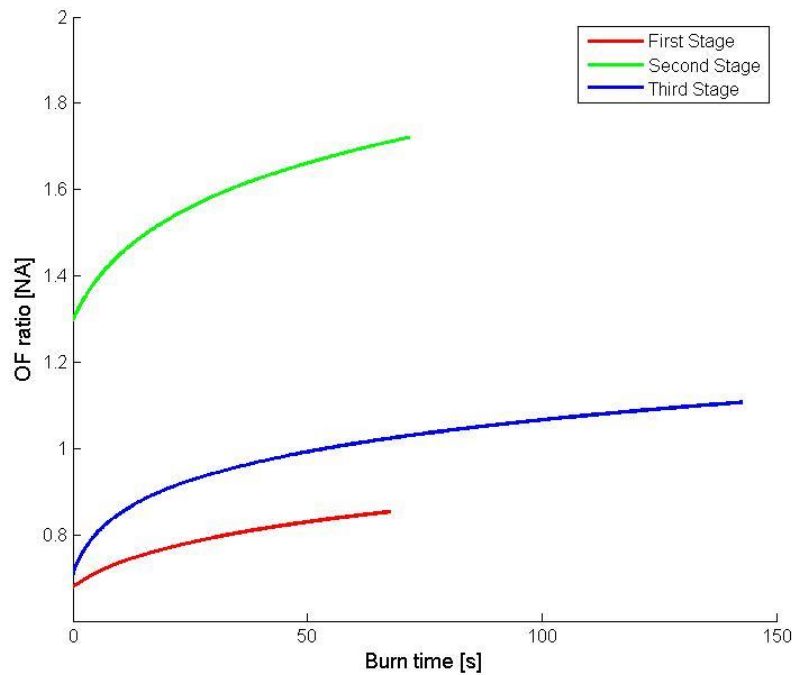


Figure 4.13: OF shift in Case 4

Despite of the higher mass fraction and its influence in other variables, the increase in specific impulse payoff and the resulting rocket is 15% less massive than Case 1. Although the proponents of AlH₃ added to the paraffin might be considerably expensive, preliminary research by the author also showed that AlH₃ is also not a common chemical reactant, hence hard to come by in the large quantities required (Karabeyoglu, 2011).

The usage of AlH₃ additive is promising, although more research is necessary mainly on regression rate behavior, grain casting and low cost synthesizing of AlH₃.

4.2.5 Case 5

The convergence for Case 5 was achieved without much problems and the resulting design is somewhat similar to Case 1. Despite of the apparent well defined a design variables' range the pre-optimization proposed in Case 2 was also applied.

First Stage

- D_ext1=0.6839999999999999;
- D_r1=0.972
- L_g1=3.6620000000000004;
- m_dot_oxi1=43.0;
- R_t1=0.087142857142857137;
- D_int1=0.331; (not a design variable, although very important geometry wise)

Second Stage

- $D_{ext2}=0.455$;
- $D_{r2}=1.055$
- $L_{g2}=2.008$;
- $m_{dot_{oxi2}}=11.988888888888889$;
- $R_{t2}=0.08171428571428571$;
- $D_{int2}=0.147$; (not a design variable, although very important geometry wise)

Third Stage

- $D_{ext3}=0.39166666666666666$;
- $D_{r3}=0.311$
- $L_{g3}=0.9159999999999998$;
- $m_{dot_{oxi3}}=2.2666666666666666$;
- $R_{t3}=0.02128571428571429$;
- $D_{int3}=0.076$; (not a design variable, although very important geometry wise)

Two discrepancies can be seen in the Design Variable: the third and second stage's tank diameters. The third stage's tank diameter is smaller than the combustion chamber, a larger diameter could reduce the rocket's length and also generate a lighter tank, once the more spherical the lighter the tank is. The second stage tank's diameter is slightly larger than the first stage's, once this does not pose as great problem, having a standard diameter could reduce fabrication costs.

The most significant output variables are presented below:

Variable	Stage1	Stage2	Stage3
Thrust [kN]	131.99	37.89	8.27
Specific Impulse [s]	291.2	300.5	325.3
Nozzle Length [m]	0.794	1.001	0.674
Propellant mass [kg]	3307.12	899.29	365.52
Oxidizer Tank's length [m]	3.010	0.458	3.55
Dry Mass	791.5	179.5	148.5
OF Ratio [NA]	2.43	2.42	2.60
Nozzle exit radius [m]	0.300	0.350	0.202
Expansion ratio [NA]	11.85	18.34	89.98
Structural mass Fraction [%]*	19.31	16.64	20.58
Gross mass, stage [kg]	4098.65	1078.87	510.25
Axial overload [g]	5.65	5.60	5.83
Combustion chamber pressure [Bar]	45.42	14.40	39.05
Burn time [s]	54.46	53.22	117.05
Mass Ratio (m0/mf) [NA]	2.38	2.30	3.46
Delta V [m/s]	2486.2	2451.3	3962.1
Total aerodynamic loss [m/s]		448.54	
Total gravitational loss[m/s]		981.76	
Total velocity loss[m/s]		1430.3	

Total Rocket's mass [kg]	5691.6
Total Length [m]	20.84
Length over Diameter Ratio	21.45

***includes extra propellant loading, ignition, spare and unusable propellant**
Table 4.5: Geometric and performance characteristics of Case 5 Launcher

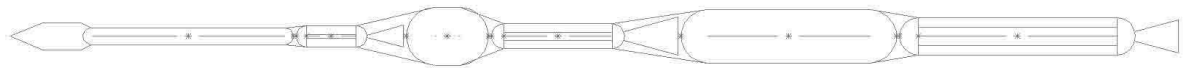


Figure 4.14: Layout of Case 5 rocket

The long length and smaller diameter of the third stage demotes that possibly the aspect ratio constraint of 25 is over dimensioned for Case 5. A smaller aspect ratio constraint would be possible.

From Table 4.5, it is noticeable the comparatively lower pressure in the second stage, while we cannot volunteer the cause of the phenomena, it resulted in a considerably lower structural mass fraction of 16.4, which is competitive with many liquid propulsion systems (Isarowitz, 2004). Also unusual was he Delta v and the Mass Ratio of the second stage, both smaller than the first's even with the possibility for higher specific impulse values on higher stages. The second stage's specific impulse is not much higher than the first's, corresponding to only 9.3s.

It can also be noticed from the data in Table 4.5 and figures 4.15 and 4.16 that Case 5 achieved a high degree of project refinement; the OF ratios of each of the stages achieved the exactly theoretical value for maximum specific impulse, and it also shows a very coherent transient behavior in each stage. The specific impulse behavior in time also represented the best signals of optimization among all cases, as each specific impulse grows, it achieves a plateau and slowly decays and this behavior is mimicked in every stage.

This Case shows the optimization code can design engines with high exact (equal to theoretical values) OF ratios and that the lower OF ratios, presented by the first and third stages on Cases 1 and 4. It probably reflects an evolutionary pressure and not a inefficiency in the optimization.

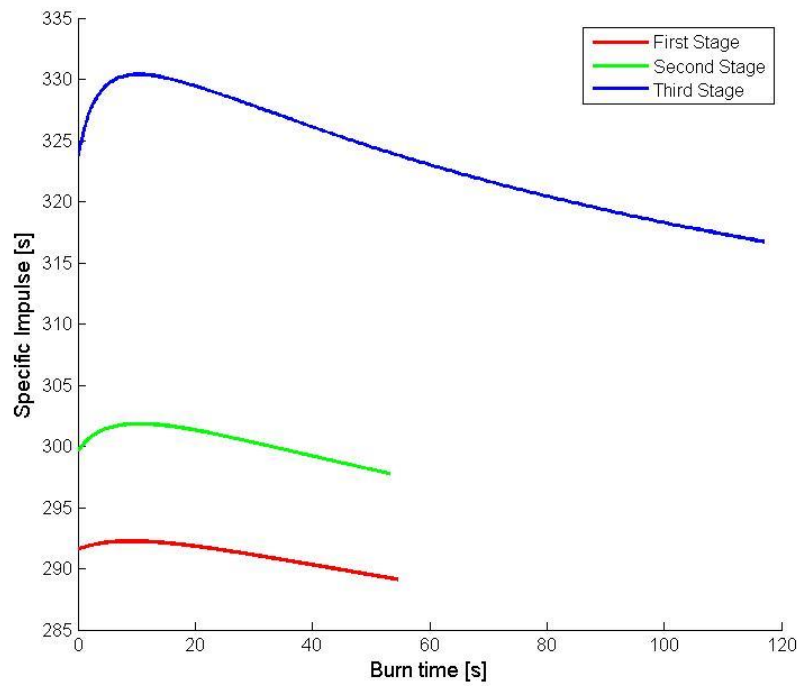


Figure 4.15: Specific impulse shift in Case 5

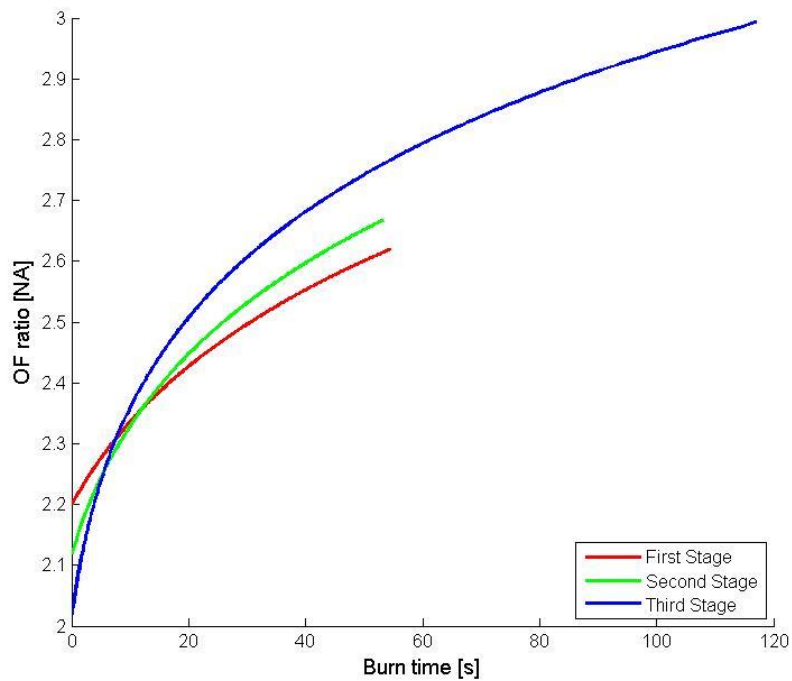


Figure 4.16: OF shift in Case 5

As it can be seen by the rocket's gross mass, Case 5 has the second best performance of all cases (behind Case 4), although the performance increase comes on the cost of simplicity. The turbopump pressurization system for a hybrid rocket although simpler than the ones

used on liquid bipropellant engines is still considerably complex and might render this alternative unattractive. The mass reduction enabled by turbopump usage was also smaller than predicted, around 15% less than Case 1, and it was even larger than the achieved by Case 4 with a much simpler technological alternative; AIH3 addition.

4.2.6 Case 6

The convergence for Case 6 was achieved without much problems and the resulting design is somewhat similar to Case 2. Despite of the apparent well defined design variables' range (from Case2's data), the pre-optimization proposed in Case 2 was also applied. Several optimization runs, with different initial populations were attempted to improve this case's design although they resulted in very similar designs. The best of those designs are presented below:

First Stage

- $D_{ext1}=0.596$;
- $D_{r1}=1.2779571888961507$;
- $L_{g1}=5.42$;
- $m_{dot_oxi1}=75.77777777777777$;
- $R_{t1}=0.14$;
- $D_{int1}=0.469$; (not a design variable, although very important geometry wise)

Second Stage

- $D_{ext2}=0.364$;
- $D_{r2}=1.1333333333333333$;
- $L_{g2}=4.4$;
- $m_{dot_oxi2}=24.555555555555557$;
- $R_{t2}=0.0692857142857143$;
- $D_{int3}=0.250$; (not a design variable, although very important geometry wise)

Third Stage

- $D_{ext3}=0.2596666666666667$;
- $D_{r3}=0.3833333333333333$;
- $L_{g3}=2.5$;
- $m_{dot_oxi3}=4.033333333333334$;
- $R_{t3}=0.04280000000005999$;
- $D_{int3}=0.101$; (not a design variable, although very important geometry wise)

The resulting design from Case6 is much similar to Case2 with long propellant grains with thin paraffin layers to minimize OF shift. This design is basically a smaller version of Case 2.

Variable	Stage1	Stage2	Stage3
Thrust [kN]	222.33	91.00	14.85
Specific Impulse [s]	261.52	315.38	310.73
Nozzle Length [m]	0.751	1.340	0.802
Propellant mass [kg]	6427.18	1718.86	830.63
Oxidizer Tank's length [m]	2.77	0.675	4.72
Dry Mass	1476.0	463.7	258.14
OF Ratio [NA]	7.018	5.109	5.118
Nozzle exit radius [m]	0.341	0.428	0.258
Expansion ratio [NA]	5.94	39.2	36.3
Structural mass Fraction [%]*	18.67	21.24	20.0
Gross mass, stage [kg]	7903.14	2182.55	1088.77
Axial overload [g]	4.77	5.97	5.87
Combustion chamber pressure [Bar]	22.95	32.96	14.25
Burn time [s]	74.15	58.50	172.91
Mass Ratio (m0/mf) [NA]	2.354	2.107	4.218
Delta V [m/s]	2196.3	2306.1	4387.4
Total aerodynamic loss [m/s]	419.2		
Total gravitational loss[m/s]	1009.2		
Total velocity loss[m/s]	1425.4		
Total Rocket's mass [kg]	11174.0		
Total Length [m]	28.14		
Length over Diameter Ratio	22.02		

***includes extra propellant loading, ignition, spare and unusable propellant**
Table 4.6: Geometric and performance characteristics of Case 6 Launcher

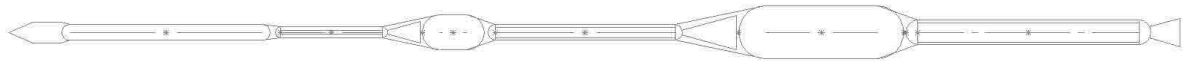


Figure 4.17: Layout of Case 6 rocket

The expected specific impulse increase happened and its impact on the rocket's gross mass was as expected, resulting in a 23% mass reduction in relation to Case 2, more than the 15% reduction found between Cases 1 and 4. Unfortunately is also noticeable that the usual signs of good optimization design are not present in this design the OF ratio, for the first stage was much larger than the theoretical optimum of 7.5. The propellant Mass Ratio of the second stage was smaller than the first's even with a higher specific impulse and chamber pressure on the second stage. It could be argued that the code opted for saving mass making a larger first stage and a low mass second stage with smaller chamber pressure, although the onsite was observed.

In a similar manner than proposed for Case 2, Case 6's resulting design would benefit from multiple motors fed by a single oxidizer tank in the first stage and/or on the second.

Although unlike Case 2 the use of a cluster of second stage's core on the first stage is unadvisable due to the poor design (low pressure) of the second stage motor. As in almost all cases, the use of multiple oxidizer tanks on the third stage will probably benefit the rocket's design.

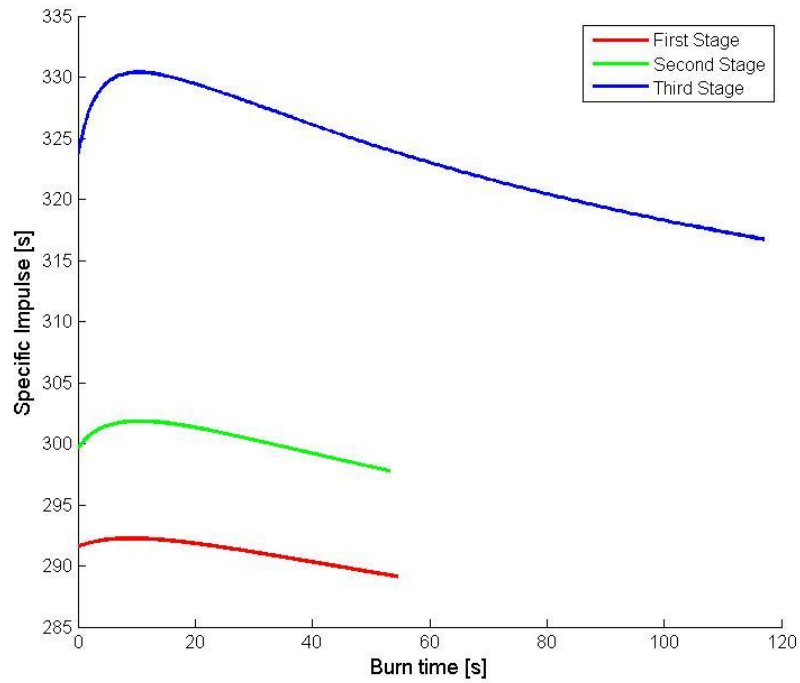


Figure 4.18: Specific impulse shift in Case 6

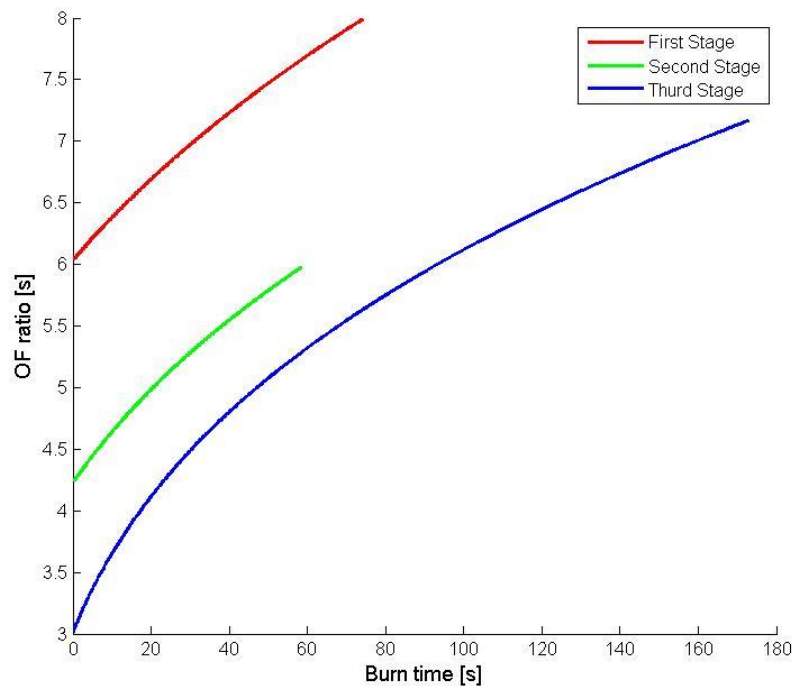


Figure: 4.19 OF shift in Case 6

Unfortunately it can also be seen from the transient behavior of the motor the poor degree of optimization achieved, with very large OF ratio on the first stage.

The use of AlH₃ still shows great potential to generate a high energy storable propellant combination, which is impossible in solid or liquid propulsion systems, although the steep OF ratio change problem needs to be addressed and corrected. Also it is necessary to evaluate both the availability of AlH₃ and its impact on grain casting and, most importantly, on the regression rate behavior. It is possible that the high mass fraction of AlH₃ needed to achieve optimal specific impulse with HTP (80% of AlH₃) results in a low regression rate grain less vulnerable to OF shift, thus more research is required to address those questions.

4.2.7 Case 7

The convergence for Case 7 was achieved without much problems and the resulting design is somewhat similar to Case 1. Despite of the apparent well defined a design variables' range the pre-optimization proposed in Case 2 was also applied. Case 7 is basically a larger version of Case1's Design.

First Stage;

- $D_{ext1}=0.7650000000000001$;
- $D_{r1}=0.9222222222222223$;
- $L_{g1}=3.7920000000000003$;
- $m_{dot_oxi1}=43.96111111111111$;
- $R_{t1}=0.11714285714285715$;
- $D_{int1}=0.335$; (not a design variable, although very important geometry wise)

Second Stage

- $D_{ext2}=0.525$;
- $D_{r2}=0.8777777777777778$;
- $L_{g2}=1.884$;
- $m_{dot_oxi2}=10.555555555555555$;
- $R_{t2}=0.04285714285714286$;
- $D_{int2}=164$; (not a design variable, although very important geometry wise)

Third Stage

- $D_{ext3}=0.375$;
- $D_{r3}=0.3555555555555557$;
- $L_{g3}=0.9586666666666667$;
- $m_{dot_oxi3}=1.9933333333333334$;
- $R_{t3}=0.04200000000000001$;
- $D_{int3}=0.071$; (not a design variable, although very important geometry wise)

As said before Case 7 is very similar to case Case1 with a larger mass. The geometrical differences are mainly in larger fuel grains and oxidizer tanks.

Variable	Stage1	Stage2	Stage3
Thrust [kN]	174.34	47.78	8.75
Specific Impulse [s]	285.39	329.38	312.40
Nozzle Length [m]	0.725	1.010	0.603
Propellant mass [kg]	4504.13	1224.46	325.64
Oxidizer Tank's length [m]	4.400	1.288	2.182
Dry Mass	1239.6	345.58	160.28
OF Ratio [NA]	2.41	2.51	2.34
Nozzle exit radius [m]	0.311	0.313	0.203
Expansion ratio [NA]	7.07	53.51	23.50
Structural mass Fraction [%]*	21.58	22.01	25.3
Gross mass, stage [kg]	5743.7	1570.0	485.92
Axial overload [g]	5.392	5.857	5.568
Combustion chamber pressure [Bar]	25.77	45.52	9.15
Burn time [s]	72.4	83.2	115.12
Mass Ratio (m0/mf) [NA]	2.37	2.47	3.03
Delta V [m/s]	2411.9	2925.1	3399.2
Total aerodynamic loss [m/s]	284.0		
Total gravitational loss[m/s]	989.7		
Total velocity loss[m/s]	1273.7		
Total Rocket's mass [kg]	7799.7		

Total Length [m]	21.81
Length over Diameter Ratio	23.65

***includes extra propellant loading, ignition, spare and unusable propellant**
Table 4.7: Geometric and performance characteristics of Case 7 Launcher

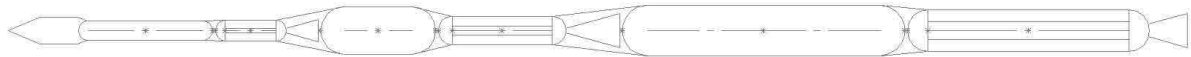


Figure 4.20: Layout of Case 7 rocket

The use of more standard materials like high strength steel instead of carbon fiber in the tanks and frames was expected to generate an increase in the rockets final gross mass, Case 7 was 18% heavier than Case 1, a smaller increase when compared to the possible cost reductions and ease of manufacturing.

The very small pressure on the third stage is somewhat unusual and possibly the performance of the launcher might be increased with a higher chamber pressure

The majority of high strength steels are weldable greatly simplifying the fabrication process and reducing the requirement for fixture devices (bolts and rivets) and complex metal-composite interfaces.

As it happened in all cases, Case 7 would greatly beneficiate from the use of a toroidal tank on state 3, which would reduce the rocket's length and possible the dry mass of that stage. Although stages 1 and 2 seem to have converged to an acceptable layout, the pressurization subsystem will have to be added in the layout blueprint.

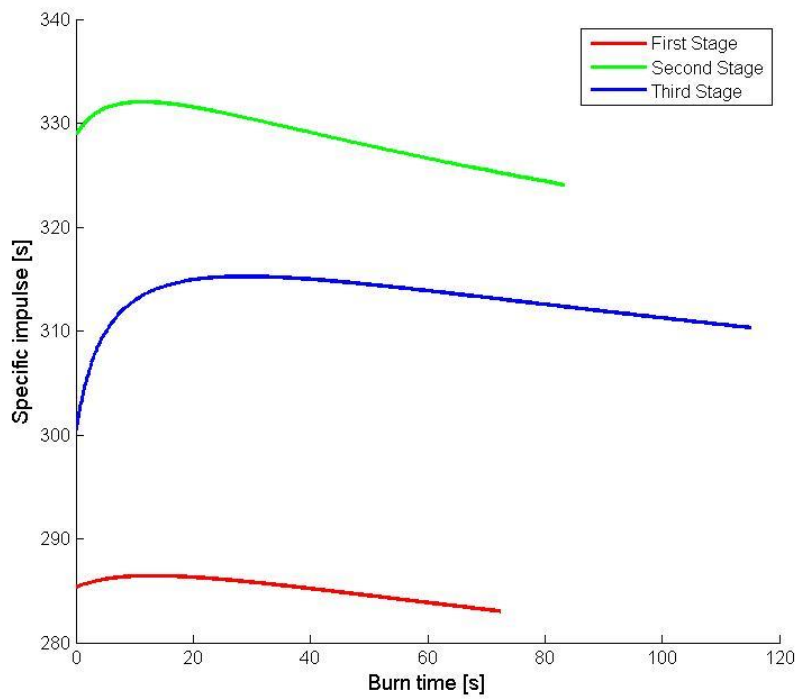


Figure 4.21: Specific Impulse shift in Case 7

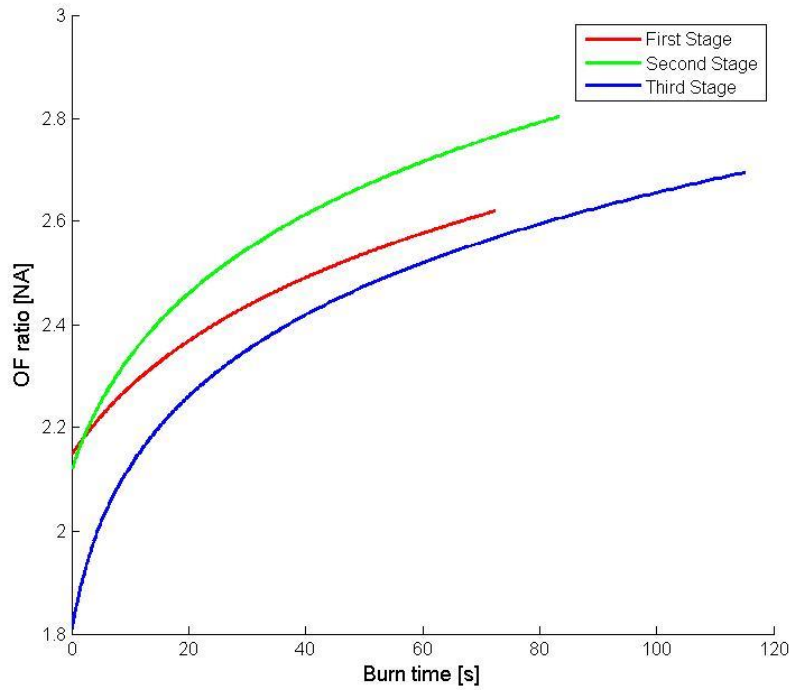


Figure 4.22: OF shift in Case 7

Case 7 has the highest industrial potential of all cases for it reduces fabrication cost by employing materials and techniques usual to a common industrial park. The usage of a welded tank instead of a composite one greatly simplifies the integration of intra-tank components (baffles and internal plumbing) and external connections (flanges, valves, and others).

Alternately possessing a working launch system based on Case7 could allow for simple payload improvement by fabrication of composite oxidizer tanks. Exploratory studies showed that if composite tanks were used in Case7 launcher its payload could be of 70kg, corresponding to a 40% increase.

In Case 7, both tanks and combustion chamber are fabricated with the same processes and tooling, therefore it is even more important to employ standardized diameters for the compartments. First, second stage's oxidizer tanks and the first stage combustion chamber could be made to match diameters. This could be done through MDO by setting D_{r1} and D_{r2} equal to D_{ext1} ; and letting D_{int1} become a design variable.

4.3 COMPARISON AND CONCLUSION

The most important parameter in the selection of the best case for design detailing is convenience. A convenient design possesses a combination of several important factors:

- Cost
 - Low cost through reduced mass
 - Low cost through cheaper materials, processes and/or technologies
- Few limiting factors, like:
 - Hard to find/toxic propellants
 - Complex technologies required.
- General Design concerns
 - Cryogenic/toxic propellants

This design decision is very subjective requiring large practical design experience and practical experience (Lynnyk, 2008). An attempt to quantify each of the relevant factors for this selection was made. A decision matrix was constructed from the quantification of the convenience parameters and the best solution could be visualized more easily (the weight system is explained better in Annex I).

	Cost Concerns		Limiting Factors		Design Concerns		Final Score
	Mass	Material	Propellants	Technology	Launch Logistics	Fabrication	
Case 1	1	1	1	1	1	1	6
Case 2	2.2	1	0.5	0.5	0.5	1	5.7
Case 4	0.8	1	1.5	1	1	1	6.3
Case 5	0.9	1	1	1.4	1.1	1	6.3
Case 6	1.7	1	1	0.5	0.5	1	5.7
Case 7	1.2	0.6	1	1	1	0.8	5.5

Table 4.8: Decision matrix comparing the 7 design Cases

From the decision matrix above the most convenient solution engineering wise is Case 7, mainly due to its reasonable mass, cheap materials and fabrication process. Case 7 will be selected for further detailing and will provide the base technological guidelines for further research.

4.4 CASE 8

As it was said in previous sections, all designs would benefit from a lateral placement of the propellant tanks of the third stage (Figure 4.24), as this measure would greatly reduce the launcher's length and aspect ratio and up to some extent reduce the launchers mass. It was also observed (Section 4.2.7) that the first stage's combustion chamber and the first and second stage's oxidizer tanks could be made to share the same diameter, for increased standardization and cost reduction.

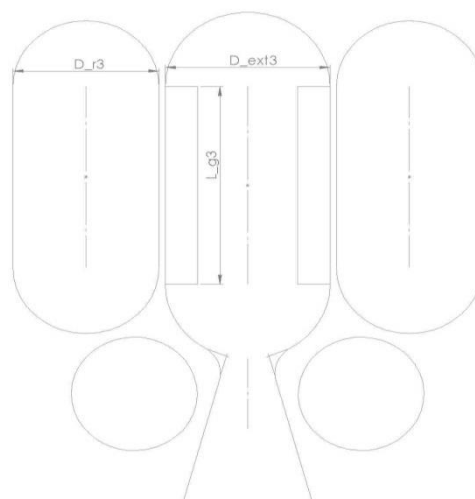


Figure 4.23: Third Stage general scheme

The optimization was made to equal the standard diameters and to use 4 parallel tanks on the 3rd stage following the layout in Figure 4.24. Equaling the diameter reduced the number of variables by 2 and the internal diameters of both 1st and 2nd were included as design variables. Aspect ratio constraint was also reduced from 25 to 23. The Fairing diameter was fixed on 570mm to avoid the small fairings found on Chapter 4. The results are presented below:

First Stage

- D_ext1=0.895;
- **D_r1=0.895;**
- L_g1=3.6960000000000006;
- m_dot_oxi1=49.35;
- R_t1=0.13657142857142857;
- D_int1=0.6095652173913043;

Second Stage

- D_ext2=0.5592857142857144;
- **D_r2=895;**
- L_g2=1.7719999999999998;
- m_dot_oxi2=9.888888888888889;
- R_t2=0.04971428571428572;
- D_int2=0.14220951321402805;

Third Stage

- D_ext3=0.35500000000000004;
- D_r3=0.28888888888888886;
- L_g3=0.9026666666666667;
- m_dot_oxi3=2.046666666666667;
- R_t3=0.02600000000000001;
- **D_int3=0.0722;**

Variable	Stage1	Stage2	Stage3
Thrust [kN]	179.93	43.24	9.29
Specific Impulse [s]	273.67	321.29	329.29
Nozzle Length [m]	0.683	0.963	0.636
Propellant mass [kg]	4420.75	1393.48	286.21
Oxidizer Tank's length [m]	4.851	1.430	0.627
Dry Mass	1129.1	347.0	161.9
OF Ratio [NA]	2.795	2.606	2.489
Nozzle exit radius [m]	0.320	0.308	0.196
Expansion ratio [NA]	5.48	38.32	57.13
Structural mass Fraction [%]*	20.34	19.94	28.10
Gross mass, stage [kg]	5549.84	1740.46	448.10
Axial overload [g]	5.528	5.544	5.861
Combustion chamber pressure [Bar]	20.05	31.23	24.03

Burn time [s]	65.98	102.13	100.39
Mass Ratio (m0/mf) [NA]	2.332	2.753	2.768
Delta V [m/s]	2273.8	3191.5	3289.0
Total aerodynamic loss [m/s]	304.3		
Total gravitational loss[m/s]	989.3		
Total velocity loss[m/s]	1287.6		
Total Rocket's mass [kg]	7738.4		
Total Length [m]	19.71		
Length over Diameter Ratio	22.02		

***includes extra propellant loading, ignition, spare and unusable propellant**
Table 4.9: Geometric and performance characteristics of Case 8 Launcher

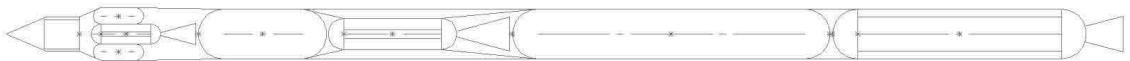


Figure 4.24: Layout of Case 8 rocket

Figure 4.25 shows that the general layout of the rocket is very similar to the general shape expected from a three stage launch vehicle. The same is backed by data from Table 4.9.

4.4.1 Detailed Performance analysis

As advanced on previous sections, a more advanced trajectory program could be used for trajectory prediction. For the new trajectory prediction the DBallistic Manual (2003) was used. The software allowed for different trajectory profiles and pitch angle optimization. The orbital profile for the Case 8 is shown below:

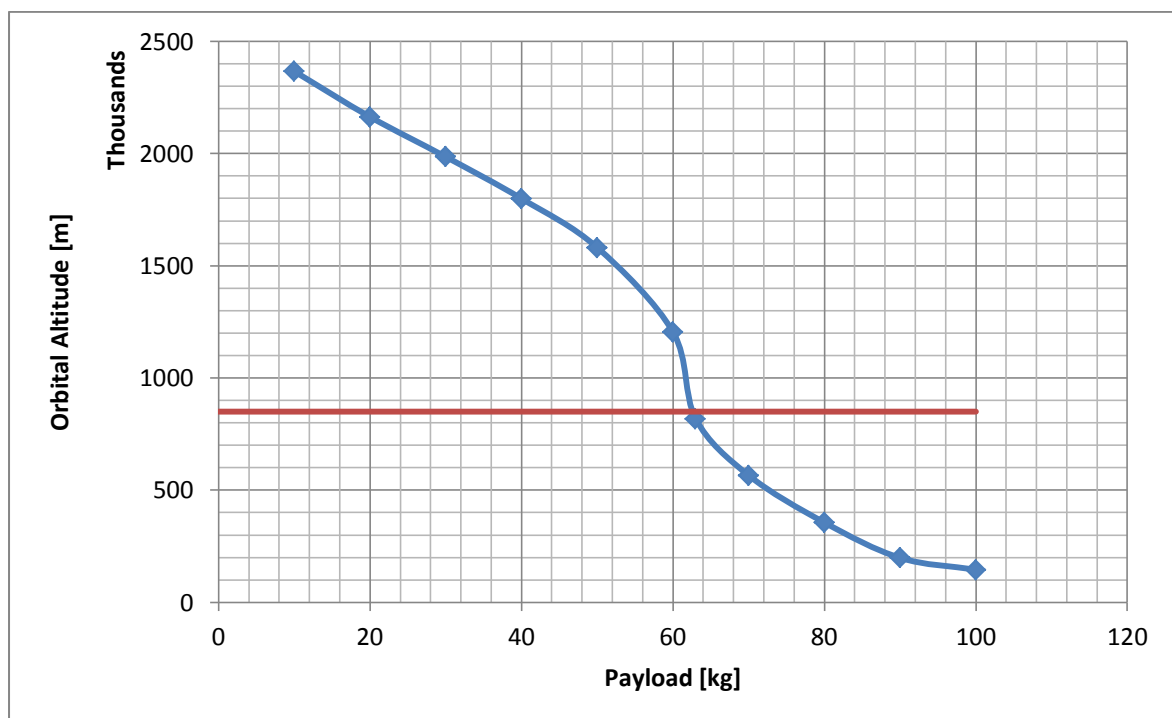


Figure 5.25: Payload profile

The resulting profile showed a performance slightly above the intended and the specified 850km orbit was achieved with a payload of 63kg. This is a result of the primitive Velocity Module when compared with DBallistic software. Figure 5.3 shows the possible payloads from 10kg to 100kg.

This chapter outlined the preliminary project of an optimized launcher; the next phase would be the Design Detailing, including the analysis and design of all subsystems and posterior fabrication. It is of the author's opinion that this can be done in Brazil with modest investment. In Design Detailing various new alternatives could be considered, though they cannot be properly evaluated now; e.g. which thrust vector control system to use, air launch alternatives, innovative pressurization systems, lighter command and control devices, and others.

Despite of the relative importance of those subsystems, their advantages and disadvantages can only be properly evaluated on a multidisciplinary design environment. For example, jet vanes are considered an older suboptimal solution, although on a low cost environment they can outperform a much more expensive Flexible Nozzle solution.

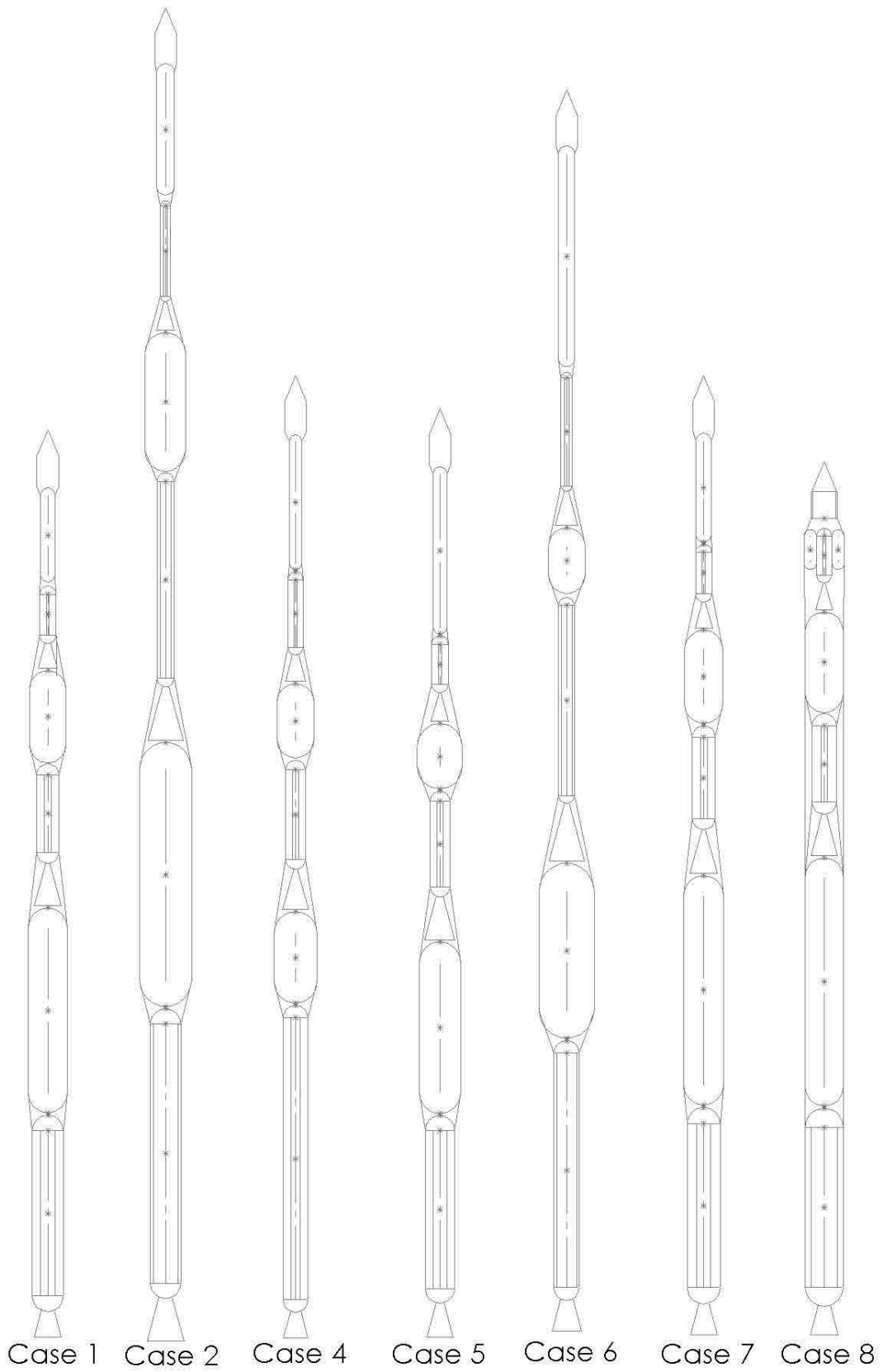


Figure 4.26: Layout comparison of all the eight cases

5- CONCLUSION

As advanced in the previous section (4.4.1), this dissertation is a discussion on preliminary design of a low cost micro satellite launch vehicle. Although this work does not present the complete design of such vehicle, it presented that the vehicle is possible and moreover that it is feasible with simple technologies and therefore it is possible to be done in Brazil with low cost.

Within a limited scope, this work also presented the real possibility of applying evolutionary and multidisciplinary techniques to solve complex design problems. With simple mathematical tools, i.e. zero dimensional model, an accurate design prediction was possible and a comparison showing the real impact of different technologies by the means of comparing optimal solutions instead of subjectively comparing the merits of each technological alternative. For example, the utilization of a suboptimal low cost material like steel proved to have a small impact on the launcher's design and in the end proved itself as the best possible alternative.

Case 8 also showed that it is possible to insert in an optimization environment real design insights, e.g.. standard tubing and different 3rd stage layout, and that new design insights can be included in the optimization as they are found and as they become quantifiable. For example, when a more accurate guidance and trajectory program becomes available, it will substitute the Velocity Module, with a guidance routine, the thrust vector control systems can be evaluated and should be included on the mass predictions.

5.1 SUGGESTION FOR FUTURE STUDIES

The design of a system is an upward spiral of further detailing and optimization with feedbacks at each circle (Figure 5.1). In the course of this dissertation, we achieved the second step, Preliminary Design, the next step is the Final Design and posteriorly the Construction. For the Final Design of this rocket to be possible, considerable testing and IR&D are necessary. Many of the central subsystems are not closed, for example the thrust vector control system can only be properly evaluated after the guidance calculations are made, the pressurization subsystem - one the heaviest component of the stages - shows possibility for different design alternatives that can only be evaluated through testing.

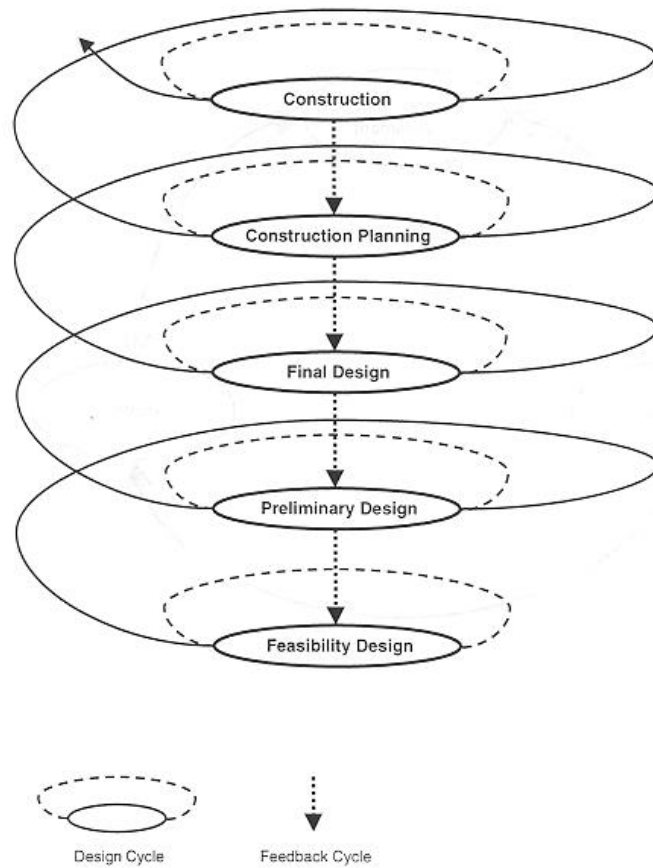


Figure 5.1: The upward spiral of Engineering Design

5.1.1 Thrust Vector Control

As abovementioned, for a correct dimensioning of the Thrust vector control (TVC) systems, it is of central importance to know the required control force, from the guidance calculations. In the current state of the project, this data is not available. More importantly for a decision on which system to employ, a concise figure on the cost and availability of such system is needed. Brazil retains the technology for Flexible Nozzle, from the VLS program, and the technology for Side Injection, from the Sonda Program, also jet vanes can be developed for they are relatively simple (Table 5.1). The decision on which system to employ is, on the other hand, based on costs of fabrication, availability of the materials and process and performance of the system, and cannot be properly done in this stage of development.

System type	Pros	Cons	Image

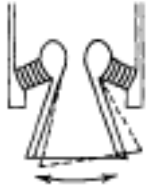


Flexible nozzle	Proven technology, no sliding or moving seal. Up to $\pm 12^\circ$	High actuation forces; high torques at low temperatures; variable actuation force	
Jet vanes	Proven technology; low actuation power; high slew rate; compact; roll control with single nozzle $\pm 9^\circ$	Thrust loss of 0.5% to 3% erosion of jet vanes limited duration; extend rocket's length	
Side injection	Proven technology, specific impulse from injectant nearly offsets the weight penalty; high slew rate, easy to adapt to different motors;	Toxic liquids are required for high performance; excessive maintenance; risk of spills	

Table 5.1: Comparison of different TVC schemes

It is recommended that more research is made on TVC systems for small, low cost hybrid rockets. This is already being done in many research centers in Brazil. It is worth saying that there currently is an initiative at UnB on the direction of developing low cost jet vanes that could be scaled up to suit the BR MSL proposed here.

5.1.2 Pressurization system

The single most massive subsystem of a pressure fed propulsion system is the pressurization system. However using the traditional high pressure bottle and valve being cost effective and simple, it generates an unnecessarily massive system. An alternative system was proposed for usage on Scorpious LV (Chakroborty, 2004). This system consists in using a hot gas generator instead of the tradition cold gas system for pressurization. Hot gas pressurization was used in several soviet launchers and ICBM and constitutes a viable alternative (Lynnyk, 2008). Hot gas pressurization can be done on a hybrid rocket by the means of a small thermocatalytic gas generator, using for example a small hydrogen peroxide dedicated tank and a catalytic bed.

Another advantage from such system is that it might possibly scale well. If the system is designed for a larger motor, it could be applied to a small with only the use of a smaller peroxide tank; the small engine would demand a smaller peroxide flow which possibly the larger catalytic bed is capable of.

A system such as described could service not only the proposed hybrid rocket family of motors, but also a liquid pressure fed system such as being proposed for the L5 motor currently being developed at IAE. Since the scale of this project is also small, it could be easily be developed by a small company or a University in Brazil.

5.1.3- Liquid Propellant Brazilian Micro Satellite Launcher

As discussed on Chapter 1, a liquid propellant pressure fed system could possibly fight for the same market niche as the proposed hybrid propellant launch vehicle, with slightly more complexity, cost and performance. The main advantage of such system will be the on the launcher's internal layout, without the defined shape of the combustion chamber it is possible to arrange the tanks' shape to a more optimized mass and aerodynamic behavior.

The fixed OF behavior of liquid propellant rockets generate a better result for the hydrogen peroxide case. Liquid rocket motors can be much easily arranged in parallel allowing for a single engine model to be used in more than one of the stages.

It is advisable that a study similar to the one done in this work for hybrids be done for a liquid propellant pressure fed alternative in the future.

BIBLIOGRAPHY

- United States Federal Aviation Administration (FAA). 2010. 2010 Commercial Space Transportation Forecasts., http://www.faa.gov/about/office_org/headquarters_offices/ast/media/2010_launch_fo_recast_report.pdf. Accessed September 1, 2012.
- Mr. Ian Christensen, Mr. David Vaccaro, Mr. Dustin Kaiser MARKET CHARACTERIZATION: LAUNCH OF VERY-SMALL AND NANO SIZED PAYLOADS ENABLED BY NEW LAUNCH VEHICLES, 10th International Aeronautical Congress
- Dr. Shyama Chakroborty* and Dr. Thomas P. Bauer†Microcosm, Inc., El Segundo, Using Pressure-Fed PROPULSION TECHNOLOGY TO LOWER SPACE TRANSPORTATION COSTS, 40th AIAA/ASME/SAE/ASEE Joint Propulsion Conference and Exhibit AIAA-2004-3358 11-14 July, 2004, Fort Lauderdale, Florida
- DePasquale1, Dominic; Charania, A.C; Kanayama, Hideki; Matsuda, Seiji; Analysis of the Earth-to-Orbit Launch Market for Nano and Microsatellites, AIAA-2010-8602
- Agência Espacial Brasileira, Programa Nacional de Atividades Espaciais, 2012-2021. Programa Nacional de Atividades Espaciais : PNAE : 2012 - 2021 / Agência Espacial Brasileira. Brasília : Ministério da Ciência, Tecnologia e Inovação, Agência Espacia Brasileira, 2012.
- Mr. Dominic DePasquale, Mr. A.C. Charania NANO/MICROSATELLITE LAUNCH DEMAND ASSESSMENT, Space Works Corporation, external source for educational proposes
- Fultron Corporation, FULTRON'S 2010 SPACE COMPETITIVENESS INDEX - A COMPARATIVE ANALYSIS OF HOW COUNTRIES INVEST IN AND BENEFITFROM SPACE INDUSTRY, Executive Summary.
- Latin Hypercube Sampling: McKay M.D., Conover W. J. and Beckman, R. J. (1979), A Comparison of Three Methods for Selecting Values of Input Variables in the Analysis of Output from a Computer Code, Technometrics 21(2), pp. 239-245

- Iman R.L. and Conover W. J. (1982), Restricted Pairing Algorithm: “A Distribution-Free Approach to Inducing Rank Correlation Among Input Variables”, *Commun. Stat.*, B11(3), pp. 311-334
- Dandekar R. A. (1993), Iterative Refinement: Performance Improvement of Restricted Pairing Algorithm for Latin Hypercube Sampling, ASA Summer conference
- K. Deb “Multi-Objective optimization using Genetic algorithms”, 7th edition, New York, USA, John Wiley & Sons,
- Kaled Da Cás, Pedro L.; Vilanova, Cristiano Q.; Barcelos, Manuel N. D. Jr.*; Veras, CarlosAlberto G. An Optimized Hybrid Rocket Motor for the SARA Platform Reentry System, *J. Aerospace Technology and Management*, São José dos Campos, Vol.4, No 3, pp. 317-330, Jul.-Sep., 2012
- Sasaki and S. Obayashi, 2005. “Efficient Search for Trade-offs by Adaptive Range Multi-Objective Genetic Algorithms”, *J. Aerospace, Computing, Information and Communication*, Vol. 2, pp. 44-64.
- Lynnyk A. K.; *Основи Конструювання Ракет-носіїв (Principles for the Design of Launch Vehicles)*, Dnepropetrovsk-2008
- Casalino, L. and Pastrone, D., 2005, ““Oxidizer Control and Optimal Design of Hybrid Rockets for Small Satellites.”” *Journal of Propulsion and Power*, Vol. 21, pp. 230-238.
- Casalino, L.; Letiziay, F.; Pastronez, D. ; “Design Trade-offs for Hybrid Rocket Motors” 48th AIAA/ASME/SAE/ASEE Joint Propulsion Conference & Exhibit 30 July - 01 August 2012, Atlanta, Georgia
- Brown, T. R. and Lydon, M. C., 2005, ““Testing of Paraffin-Based Hybrid Rocket Fuel Using Hydrogen Peroxide Oxidizer””, AIAA Region 5 Student Conference, Wichita, USA.
- Karabeyoglu, M. A. et al., 2004, ““Scale-up Tests of High Regression Rate Paraffin-Based Hybrid Rocket Fuels.”””, *Journal of Propulsion and Power*, Vol. 20, No. 6, pp. 1037-1045.

- M. A. Karabeyoglu, J. Stevens, D. Geyzel, B. J Cantwell and D. Micheletti, High Performance Hybrid Upper Stage Motor 47th AIAA/ASME/SAE/ASEE Joint Propulsion Conference and Exhibit, 2011
- Sutton, G. P., 2001, ““Rocket propulsion elements: an introduction to the engineering of rockets””, 7th edition, New York, USA, John Wiley & Sons,
- Veras, C. A. G.; Neto, D. B.; Silva, L. F. F; Lacava, P. T. “Aplicação da Parafina como Combustível de Alto Desempenho em Foguetes Híbridos” December - 2003
- Scorpius Space Launch Company, “PRESSUREMAXX- The Sapphire 77 series”, cryogenic pressure vessel catalog, Hawthorne CA
- Anderson, M.B., 2002, ““Genetic Algorithms In Aerospace Design: Substantial Progress Tremendous Potential.” Paper presented at the RTO AVT Course on ““Intelligent Systems for Aeronautics””, held in Rhode-Saint-Genèse, Belgium, 13-17 May 2002, and published in RTO-EN-022.
- Whitmore, S. A; Chandler S. N, “Engineering Model for Self-Pressurizing Saturated-N₂O-Propellant Feed Systems”, JOURNAL OF PROPULSION AND POWER, Vol. 26, No. 4, July–August 2010
- HPR Altman, D. and Holzman, A., 2007, “Overview and History of Hybrid Rocket Propulsion.” In Chiaverini, M.J., Kuo, K.K. (ed.), Fundamentals of Hybrid Rocket Combustion and Propulsion, American Institute of Aeronautics and Astronautics, Inc., Reston, Virginia, Vol. 218, Chapter 1, pp. 01-36.
- Almeida, L. A. R. and Santos, L. M. C., 2005, ““Design, fabrication and launch of a hybrid rocket with paraffin and N₂□ propellants□ ” (In Portuguese), Graduation Project, Mechanical Engineering Department, University of Brasília, Brasília, D. F., Brazil, 83p.
- Space Exploration Technologies (SpaceX), “SpaceX Update 9 May 2003”, <http://www.spaceref.com/news/viewstr.html?pid=9113>, Accessed on 3/11/2013
- Key to Metals, “Steels for Cryogenic and Low-Temperature Service”, <http://steel.keytometals.com/Articles/Art61.htm>, Accessed on 3/11/2013

Matweb, AISI E4340 Steel, oil quenched 845°C, 425°C (800°F) temper,
<http://www.matweb.com/search/DataSheet.aspx?MatGUID=b2151261135d4025b7a64f6b123f8f45> Accessed on 4/30/2013

Isarowitz, S. J.; Hopkins J. B.; Hopkins Jr., J. P.; “International Reference Guide to Space Launch Systems” 4th edition, Reston Virginia USA, American Institute of Aeronautics and Astronautics,

Software package «DBallistic» Program Manual Version 1.0.3.0, Программный комплекс «DBallistic» Методическое пособие Версия программы 1.0.3.0сг. Днепропетровск 2003

Latin Hypercube Sampling: McKay M.D., Conover W. J. and Beckman, R. J. (1979), A Comparison of Three Methods for Selecting Values of Input Variables in the Analysis of Output from a Computer Code, *Technometrics* 21(2), pp. 239-245

Iterative Refinement: Dandekar R. A. (1993), Performance Improvement of Restricted Pairing Algorithm for Latin Hypercube Sampling, ASA Summer conference

George, P.; Krishnan, S.; Varkey, P.M.; Ravindran M.; Ramachandran L., “Fuel Regression in Hydroxyl-Terminated-Polybutadiene/Gaseous Oxygen Hybrid Rocket Motor” *Journal of Propulsion and Power*, Vol. 17 No. 1 January-February 2001

Hill, C. N.; “Black Arrow. A Vertical Empire: The History of the UK Rocket and Space Programme”, 1950-1971 (2006 ed.). London: Imperial College Press. pp. 155–188. ISBN 1-86094-268-7.

M. A. Karabeyoglu, D. Altman and D. Bershader, Transient Combustion in Hybrid Rockets, AIAA-95-2691, 31st AIAA/ASME/SAE/ASEE Joint Propulsion Conference and Exhibit, San Diego, California, July 1995.

Viegas, F. L. and Salemi, L. C., 2000, “Design and assembling of a static test bench for hybrid rocket engines”, Graduation Project, Mechanical Engineering Department, University of Brasília, Brasília, D.F.

- Costa F. S.; Vieira, R.; “Preliminary Analysis of Hybrid Rockets for Launching Nanosats intoLEO”, J. of the Brazilian. Society. of Mechanical. Sciences. & Engineering. October-December 2010, Vol. XXXII, No. 4
- Gouvêa, L. H., “Análise de Desempenho de um Motor Híbrido Utilizando Parafina e Peróxido de Hidrogênio Como Propelentes”, National Institute of Space Reserch INPE, São José dos Campos 2008
- Oiknine, C., 2006, “New perspectives for hybrid propulsion”, Proceedings of the AIAA paper 2006-4674, 42nd AIAA/ASME/SAE/ASEE Joint Propulsion Conference and Exhibit, Sacramento, California.
- Dyer, J.; Doran, E.; Dunn, Z.; Lohner, K.; Bayard, C.; Sadhwani, A.; Zilliac, G.; Cantwell, B. and Karabeyoglu, A.: “Design and Development of a 100 km NitrousOxide/Paraffin Hybrid Rocket Vehicle”, AIAA 2007-5362, 43rd AIAA/ASME/SAE/ASEE Joint Propulsion Conference & Exhibit; Cincinnati, Ohio, 8-11 July 2007.
- McConnaughey, P. K.; Femminineo, M. G.; Kroelfgen, S. J.; Lepsch R. A.; Ryan, R. M. Taylor, S. A.; “DRAFT Launch Propulsion Systems Roadmap – Technology Area 1” National Aeronautcs and Space Administration NASA, Novenber 2010
- Zubrin, R; Wagner, R.; Clarke A. C., “The Case for Mars, The Plan to Settle the Red Planet and Why We Must”, 1st edition, New York, USA, Touchstone, 1996
- HARTFIELD, R. J., JENKINS, R. M., BURKHALTER J. E. : Optimizing a solid rocket motor boosted ramjet powered missile using a genetic algorithm. Applied Mathematics and Computation, 2006.

ANEXES

ANEXE I: WEIGHT FOR COMPARISON OF DESIGN CASES

- Case 1: Base line reference, pressure fed LOX-Paraffin and standard materials.
- Case 2: Hydrogen Peroxide is used as oxidizer, instead of LOX.
- Case 3: Nitrous Oxide is used as oxidizer, blowdown injection is used.
- Case 4: Aluminum Hydride (AlH₃) is used as additive in the paraffin grain with LOX.
- Case 5: Turbopump feed system is used instead of pressure fed.
- Case 6: Hydrogen Peroxide is used with paraffin grain doped with AlH₃.
- Case 7: Low cost alternative with steel tanks instead of carbon composite.
- Case 8: Post Optimization based on the output from the first 7 cases.

	Cost Concerns		Limiting Factors		Design Concerns		Final Score
	Mass	Material	Propellants	Technology	Launch Logistics	Fabrication	
Case1	1	1	1	1	1	1	6
Case2	2.2	1	0.5	0.5	0.5	1	5.7
Case4	0.8	1	1.5	1	1	1	6.3
Case5	0.9	0.7	1	1.4	1.1	0.8	5.9
Case6	1.7	1	1	0.5	0.5	1	5.7
Case7	1.2	0.6	1	1	1	0.8	5.6

This appendix explains the decisions behind the decision matrix presented on Section 4.3. The values and methodologies presented here are a suggestion and different weights and values can be used depending on the designer's discretion. Any changes on the weights and values directly impact the conclusion extracted from the design matrix.

As explained before, the Case 1 is the baseline and all of its characteristics have the neutral value of one. If a Design possesses some characteristic which is "better" (meaning lighter, cheaper, etc...), the design's value for that characteristic is subtracted a correspondent value, the opposite happens when a Case has a characteristic which is worst than Case 1.

COST CONCERNS

The Cost concerns refer to an estimation of the launch vehicle's development and launch costs; this attribute is divided on two subcategories: mass and materials.

The mass characteristic represents the cost increase by size of the launcher. All other characteristics remaining equal, a heavier launcher will cost more to be developed and fabricated. Non-scalable or weakly-scalable costs such as ground equipment test facilities and fabrication plants are considerable equal for all cases and are not included on this characteristic. The value of Mass Cost Concern MCC is calculated by the following equation (Equation A1):

$$MCC_x = \frac{m_{tx}}{m_{t1}}, \quad (A1)$$

Where MCC_x is the Mass Cost Concern of Case X and m_{tx} and m_{t1} are the total gross mass of Case X and Case 1.

The material cost concern (MtCC) refers to the cost increase due to from more expensive materials. All other characteristics remaining equal, a launcher made of more expensive material will cost more. The value used for the MtCC is shown below:

- MtCC=1 if the launcher has composite tanks and Steel combustion chambers (CC)
- MtCC=0.7 if the launcher has AMG6M Aluminum tanks and steel CC
- MtCC=0.6 if the launcher has steel tanks and CC

LIMITING FACTORS

The Limiting Factors refer to an estimation of the availability and conveniences of the technologies used on the launch vehicle; this attribute is divided on two subcategories: propellant and technology.

The propellant limiting factors (PLF) refer to the ease of handling, availability and cost of the propellants used.

As explained before, the Case 1 has the Baseline value of one and so its propellants. The High test Peroxide and the Nitrous Oxide are storable propellants and the concerns regarding cryogenic operation are absent. Preliminary research showed that ALH3 additive

is hard to acquire and expensive (100\$/kg), therefore the cases using this kind of additive were penalized. The calculation of the PLF is shown below:

- PLF=1 if propellants are LOX/Paraffin
- PLF=0.5 if oxidizers are storable HTP or NOX
- PLF=1.5 if propellants are LOX/Paraffin with ALH3 additive (1+0.5)
- PLF=1 if oxidizers are storable HTP or NOX with ALH3 additive (1+0.5-0.5)

The technology limiting factors (TLF) represent the impact of crucial technologies that are not yet available in Brazil. The most critical technologies that are not fully developed in Brazil are the use of cryogenic propellant and the design and fabrication of turbopumps feed systems. The criteria for the evaluation of the TLF are shown below:

- TLF=1 for cryogenic pressure fed systems
- TLF=1.4 for pump fed cryogenic systems
- TLF=0.5 for storable propellant pressure fed systems.

DESIGN CONCERNS

Design concerns refer to more systemic and subjective concerns the designer should take in consideration when choosing a technology, this attribute is divided on two subcategories: launch logistic and fabrication.

The launch logistics design concerns (LLDC) refer to inconveniences introduced by the different technologies to the launch operations. Cryogenic components require special operation such as cooling and purging of the injection lines prior to launch, such propellants also require special short term storing close to the launch pad due to boil losses. In the cases of isolated launch center in situ propellant production might be necessary. Turbopump fed system also requires slightly more complicated launch procedures, due to startup of the turbines. The criteria for the evaluation of the LLDC are shown below:

- LLDC=1 for cryogenic pressure fed systems
- LLDC=1.1 for pump fed cryogenic systems
- TLF=0.5 for storable propellant pressure fed systems.

The fabrication design concerns (FDC) refer to inconveniences caused by employing fabrication techniques that are not common in the industry. The systems using carbon composite tanks are penalized due to utilization of uncommon winding machines instead of more common welding and forging processes. Although unusual the winding machines can be easily applied to small fabrication plants (Section 3.2.1), therefore the penalization was small. The criteria for the evaluation of the FDC are shown below:

- FDC=1 if the launcher has composite tanks and Steel combustion chambers (CC)
- FDC=0.8 if the launcher has AMG6M Aluminum tanks and steel CC
- FDC=0.8 if the launcher has steel tanks and CC